Wildfire suppression technology: Exploration for a directed energy beam (DEB) attenuating electron transfer by cyclical vacuum subduction of dioxygen dication species, O_2^{2+}

Richard L Amoroso[1,2], Salvatore Giandinoto[1,3] and Sabah E Karam[4,5]

[1]Noetic Advanced Studies Institute, Hogan's Wash, Escalante Desert UT 84714 USA
[2]amoroso@noeticadvancedstudies.us
[3]salgino20@yahoo.com
[4]Morgan State University, 1700 E Cold Spring Ln, Baltimore, MD 21251 USA
[5]sabah.karam@morgan.edu

Abstract. Modeling wildfire suppression technology, inspired by Einstein's long quest for a final theory, is based on a Unified Field Mechanical (UFM) Ontological-Phase Topological Field Theory (OPTFT) derived from modified M-theory, parameters of the Wheeler-Feynman-Cramer Transactional Interpretation, with combined extensions of a de Broglie-Bohm Implicate Order super-quantum potential as a unified field *force of coherence* control factor. The device is multiphasic. Operationally, O_2 electron transfer attenuation occurs by nonlocal matter-wave phase adduction/subduction interference nodes in dynamic-static Casimir-Polder resonant interactions pertinent to bumps and holes within a covariant polarized Dirac vacuum as the most salient feature of dioxygen dication, O_2^{2+} coupling to mirror symmetric *nonlocal antispace* (vacuum), rather than neutral molecular species in local 3-space as demonstrated in experimental studies of dioxygen dication, O_2^{2+}. Additionally, beam emission requires a new dual class of nonlocal OCHRE (Oscillation Coupled Helicoid Resonance Emission) in tandem with localized OCRET (Optically Controlled Resonance Energy Transfer) to produce ballistic-like conduction of vacuum energy by the summation of cyclical resonant incursive oscillations within the structure of cellular Least Units tessellating spacetime as a means of mediating the additional dimensionality (XD) of brane topological phase transitions in the *Bulk*. Finally, device operation requires an M-theoretic form of scalable universal quantum computing (UQC), a paradigm shift beyond confines of the locality-unitarity basis of presently standard Copenhagen quantum theory.

1. Introduction

When he [Fermi] *speculates ... you know it is based already on concrete thought, therefore his words carry authority, because you know, that these are not the random 'off the top of one's hat' kind of remarks*. Nobelist C.N. Yang – Stoney Brook Masters Series [1].

The US Department of Forestry and Fire Protection, now states that Wildfire Seasons no longer exist! Instead, the scenario has become a state of Perpetual Fire, with literally dozens of wildfires always burning. The average annual cost of fire suppression has risen in excess of US$ 4 billion; not inclusive of property loss. Dozens of nations suffer wildfires [2]; in 2018, there were 55,911 wildfires, and 64,610 wildfires in 2017 [3]. For this reason, liberty is taken to speculate on the design path such a complex directed energy beam (DEB) technology able to suppress the ability of dioxygen to transfer its oxidizing electrons will take, with effort for maintaining correspondence to numerous existing physical theories.

Conferences are arenas for announcing discovery and testing hypotheses not as easily introduced elsewhere. This challenging work, requires reaching far into the mist of the imminent paradigm shift beyond the standard model (SM). This scenario is acutely confabulated, because as recently promulgated by the US Department of Forestry and Fire Protection, *there is no longer a fire season, but constant fire*. Under this panoply of urgency, a DEB generator technology, a radical design for attenuation of wildfires by suppressing dioxygen dication, O_2^{2+} is outlined with the best of the authors current understanding.

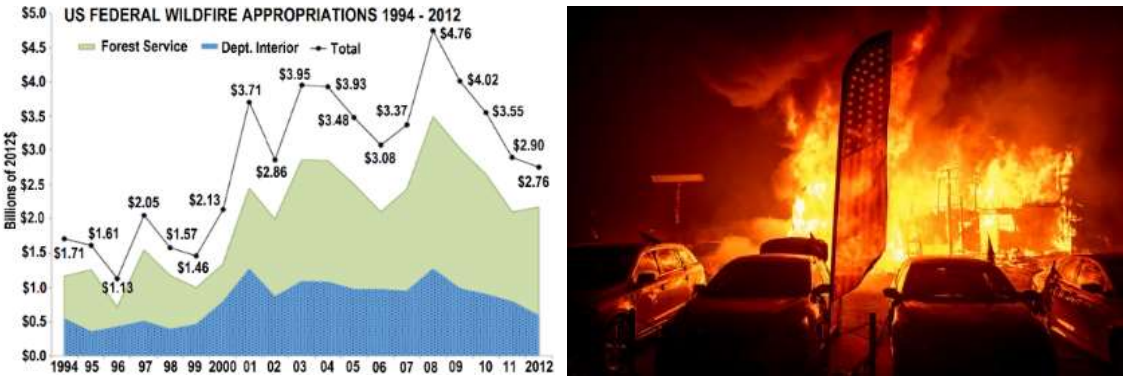

Figure 1. a) US federal wildfire control-management funds; source: Congressional Research Service Report RL33990, now increased to > 4 Billion per year. b) Paradise, CA USA fire 9 November 2018 burned so fast neighborhoods were destroyed well before fire services arrived.

2. Overview

Implementing the DEB wildfire suppression technology requires a significant number of new concepts. Gauge theories are the basis for much of modern physics; but gauge conditions are approximations, suggesting additional theory is required to complete the Standard Model (SM). Recently, QED a main pillar of modern physical theory, has been violated at the $\sigma 5$ level [4,5], suggesting proximity of additional physics beyond the SM. Experiments have been designed with programs underway to perform required empirical tests [6,7], primarily to access putative M-theoretic additional dimensionality (XD).

There are over 2-dozen forthcoming DEB technologies (Tbl 1) all necessitating the utility of Unified Field Mechanics (UFM) [8-11]. A concatenation of new parameters related to the looming paradigm shift must be addressed:

- All require Universal Quantum Computing (UQC), implementing a realistic form of 6D M-theoretic r-qubit a in a geometric-topological form allowing the uncertainty principle to be supervened [12].
- The key fundamental UFM element: A dual structured Least Cosmological Unit (LCU) tessellating localized-spacetime and embedded in the nonlocal-brane backcloth [12-14].
- An operationally complete form of quantum mechanics making correspondence to an M-theoretic Einsteinian Unified Field Theory (UFT) that incorporates key aspects of the Wheeler-Feynman-Cramer Transactional Interpretation (TI) [15] and de Broglie-Bohm superimplicate coherence [16].
- A unique 12D UFM iteration of string/M-theory with a cyclical *continuous-state* parallel transport spin-exchange dimensional reduction compactification process [12,17,18].
- A technologically surmountable finite radius semi-quantum manifold of uncertainty [12].
- Duality of localized OCRET (Optically Controlled Resonance Energy Transfer**)** [19] in tandem with nonlocal OCHRE (Oscillation Coupled Helicoid Resonance Emission).
- Utility of Extended Electromagnetic Theory [20-22] for static-dynamic Casimir-Polder interactions [23-25] in a covariant polarized Dirac vacuum for applying Dirac Hole-Theory [26,27].
- Extension of the electron conduction model of a Ballistic Mean-Free-Path to an unrestricted generalized M-theoretic instantaneous path for evanescence of directed vacuum energy [28].

Directed Energy-Beam Technologies
The Imminent New Age of Vacuum Engineering

1. Aerospace
1.1 Resonant Cavity Thruster
   A. Fuel-less interplanetary rockets
   B. Space Cruisers
   C. Supersonic Airplanes
1.2 FTL Warp Drive
1.3 Geometrodynamic gravity suppression
2. Artificial protein
3. Astrophysics
   A. Q-Telescope
4. Coherence - quantum
   A. Fusion power generation
   B. Quantum computation microlithography
5. Communication
   A. Focused narrow beam sound
   B. Instantaneous quantum signaling
6. Environmental
   A. Fire prevention
   B. Weather control
7. Gravity waves
   A. Archeology
   B. Mining
   C. Oil/gas/coal discovery
   D. Infrastructure testing
8. Infrastructure
   A. Autonomous vehicle
   B. VTOL tiered 'flying cars'
9. Medicine
   A. Ontological-phase holographic interferometry
   B. 'Star Trek' class medical tricorder
      a. Diagnostic
      b. Therapeutic
10. Military
   A. Defense shield
      a. Missile
      b. Bunker
      c. Personal
   B. Phaser
   C. Invisibility

Table 1. Some of the more than two-dozen forthcoming DEB technologies.

3. Tiered concatenation of directed energy-beam (DEB) design elements

In this section we briefly summarize the three main design components of DEB technology proposed for suppressing wildfires. The DEB beam generator alone could suppress the wildfire; but it would not be as efficient. For space limitations, components 1 & 3 are only briefly outlined, with intent to provide sufficient insight to grasp the path design will take from extension of current technology.

1. Photographic grid, patterned to encompass the topology and circumference of the wildfire (Fig.2).
2. Programmed vacuum energy beam generator design elements.
3. Fire grid cooling based on enhancing existing laser cooling techniques.

3.1 Quantum holographic transduction of fire grid pattern dynamics

An infrared digital camera with a programmed grid, transduces images of the wildfire domain both in 3D terrain contour and heat range. The image is processed holographically (similar to MRI) in order to dynamically correlate the suppression beam with the 3-space grid area supplied by the camera and integrate it with vacuum tessellation. Cells in the camera grid are designed to overlap with the cellular automata tessellating the vacuum. A buffer zone beyond the wildfire circumference is added to the suppression beam's coverage array (Fig. 2).

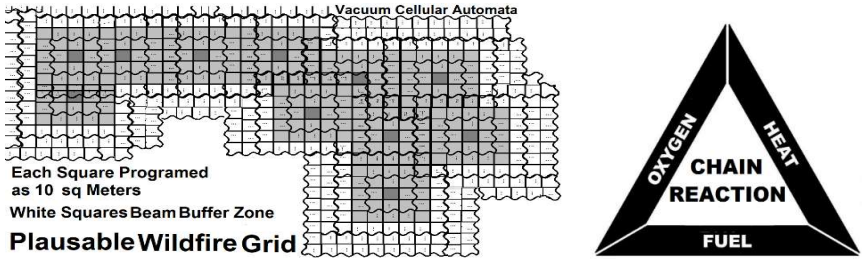

Figure 2. a) Generalized wildfire grid. Suppression beam programmed to cover area/terrain of fire (filled cells) with added Buffer Zone (white cells) to facilitate containment within the periphery of the wildfire circumference. b) Fire tetrahedron - 4 requirements for combustion.

An infrared digital camera with a programmable 3D fiducial grid, images the wildfire domain both in area and heat range. The suppression beam is correlated with the pattern of the camera grid and vacuum tessellation in order to cover the wildfires area with 3D altitude and heat range included. A buffer zone beyond the wildfire circumference is added to the suppression beam's coverage array.

This imaging system is readily described by the theory of quantum holography as applied to clinical Magnetic Resonance Imaging (MRI). Coherent wavelets form a unified basis for multichannel reconstruction in high resolution MRI into real 3D holographic projective space governing design of coils inside the MRI scanner system. Aligning the fire area pattern array with resonating cellular automaton properties of the Dirac polarized spacetime vacuum is achieved by UFM based quantum computing [29,30] which aids transducing the grid information into the DEB with dynamic precision.

Creating a precisely correlated wildfire grid enables the DEB to focus suppression energy efficiently on the area of the fire, it's 3D contours and also adapt to the thermodynamics of hot-spots.

Ideally, by geosynchronous orbit satellite imaging; or alternatively, with some diagnostic time cost, the DEB generator could be flown to the wildfire location by helicopter (replacing the Bambi bucket).

3.2 DEB generator wildfire suppression technology – programmed vacuum energy resonator

The US Department of Defense has developed reasonably mature ever more powerful electromagnetic femtosecond terawatt laser pulsed directed energy weapon (DEW) technologies [31]. In terms of UFM these are trailing-edge em-devices limited to 4D SM quantum physics without technical access to large-scale additional dimension (LSXD) M-theoretic UFM vacuum energy programming [17,18,32,33].

We briefly mention here some of the DEB parameters listed in Sec. 2, then concentrate on why we believe it is possible to develop a DEB technology based on a modified 12D M-theory, not as accorded to current thinking (search for a unique compactification producing the SM); but where compactification is a continuous process occurring cyclically through all 12D [12-14], before deeper analysis in Sec. 4 as the core of the paper.

Operationally, M-theoretic UFM DEB techs have commonality with lasing (generation of coherent energy emission) principles. But instead of the prototypical gain medium with mirrors confined in cylindrical 3-space plasma tubes or semiconductor materials; DEB emission occurs by the energetics within vacuum antispace static-dynamic Casimir-Polder resonant cavities [23-25] utilizing tessellated LCUs instead of excited atoms. This requires a detailed discussion of how we define space-antispace and the nature of brane XD-LSXD topological phase transitions.

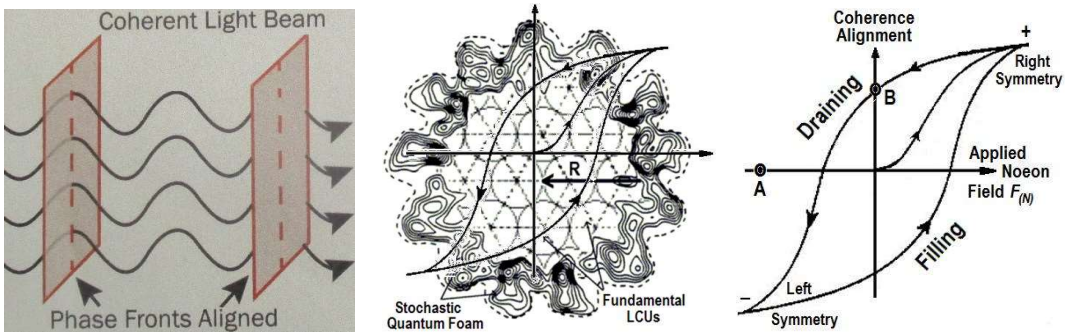

Figure 3. a) Laser operation, phase fronts align multiplicatively at mirror surface. b) Symbolic vacuum antispace hyperspherical *Casimirror* Calabi-Yau resonant LCU cavities with hysteresis coherence length R. c) Cyclic hysteresis oscillation alignment with UF coherence.

We have assumed spacetime is tessellated by a cellular automata-like array of Least Units (LCU) with a structured duality. Dimensionality up to this semi-quantum limit is a finite radius XD manifold of uncertainty. Beyond which lies LSXD M-theoretic brane topological transitions. Matter in that regime takes the form of dynamic highly symmetric Calabi-Yau florets. In the same manner quantum fields are manipulated by em-fields in 3-space; LSXD topological phase transitions may be operated on by cyclically interfering/modulating the UF to adduct/subduct antispace electron dications on D-branes.

Dications, general form 2+, made by removing two electrons, form neutral species. Diatomic dications corresponding to stable neutral species decay into two singly charged particles, due to the loss

of electrons in bonding molecular orbitals. Energy levels of diatomic dications (general formula X^{2+}) are studied with good resolution by measuring the yield of pairs of zero-kinetic-energy electrons from double photoionization of a molecule as a function of the photoionizing wavelength as in Fig. 4.

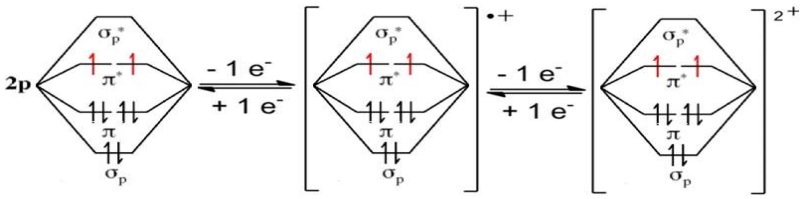

Figure 4. Usual format for producing a dioxygen, O_2 dication, O_2^{2+} made by stripping two electrons off dioxygen molecule species used for double-charge-transfer spectrometry.

Wildfire creating redox reactions involve the transfer of electrons between chemical species (fire tetrahedron, Fig. 2b). In order for a UFM M-theoretic DEB device to suppress a wildfire by interfering with electron transfer, the O_2 dication, O_2^{2+} must undergo cyclic spin-spin, spin-brane proton-adduction, electron-subduction Dirac n-spinor spherical rotation fusion resonance with LCU automata. Trapping the proton (adduction to position) to capture the electron (subduction) by topological charge is set up to occur by interference with the topological mass-charge transitions in Calabi-Yau brane bouquets.

Physics at the fundamental level reduces to fermions appearing as singularities rather than extended objects, difficult to describe in the 3D space of observation. However, the algebra of the Dirac equation suggests that fermions require a double, rather than a single, vector space, which seems confirmed by the double rotation (720º not 360º) required by spin ½ objects, effects of *zitterbewegung* and Berry phase shift. The 2nd space is, in effect, an antispace, containing the same information as real 3-space but less accessible. The two spaces cancel producing a norm 0 (nilpotent) object with exactly the mathematical structure required for a fermionic singularity [17].

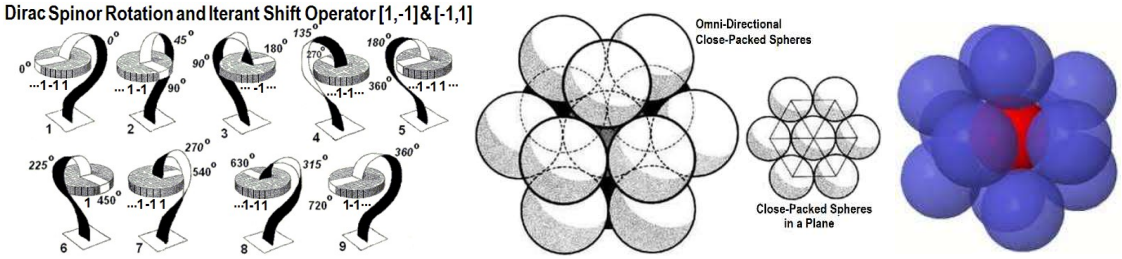

Figure 5. a) Illustrating the 360º – 720º Dirac spinor rotation. b) System of close-packed spheres (12) which represent a single LCU. c) Revealing hexagonal property of the LC U with a 3-cube center, collapsed into a 2D hexagon. d) Another view of the LCU. There is enough space inside, whether cubic or hexagonally close-packed so that the 13th sphere in the center may pass through; which has importance in transformations.

There are several putative theoretical parameters in acute contrast to conventional wisdom; saliently, our UFM formulation of M-theory does not seek a unique XD compactification to the 4D SM, reverts to the original Hadronic form of string theory with variable tension, adds a 12th dimension to complete a de Broglie-Bohm superimplicate order coherence principle to complete the UF, gravity is not quantized – integration occurs with the UF. Most importantly, XD are not professed to be unobserved because they are curled up at the Planck-scale, this is not the only interpretation. They are not (as yet) observed because of an inherent subtractive interferometry in the *continuous* compactification process through all dimensionality [13]. This, and additional constructs will be sorted out soon by experiment [6,7].

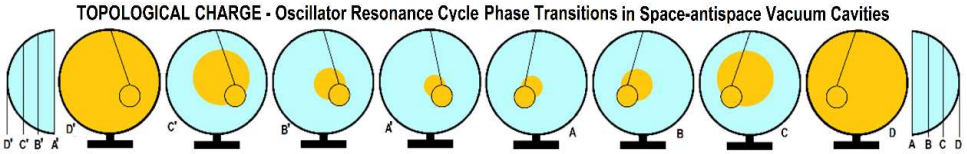

Figure 6. Simplified model of cavity wave-particle dual spinor oscillation modes. The antispace proton mode (nucleus) is subducted from the center of the LCU cavity periodically in its cycle toward the topologically charged wall (median rotational axis); the optimal moment in the oscillation beat frequency to subduct the electron as a cellular automata dication, O_2^{2+}.

Loosely considering aspects of Fig. 6 as dual mirror symmetric static-dynamic Casimir-Polder antispace LCU cavities; the orange ball (electron), coupled by the string (topological charge) to the cavity (nucleus) undergoes UF driven pumping cycles with periodic emission at full charge. The additional dication cycle is not pictured.

In Fig. 7, consider the spinning green ball as added degrees of freedom to the orange electron in Fig.6. Not shown in Fig. 6 or 7, is the fact that, as hidden by the uncertainty principle, the Dirac double rotation (360^o-720^o) has additional complexity beyond what has so far been claimed for the space-antispace transform - the topology takes the form of a trefoil (3^{rd} tongue not shown). Multiply connectivity through parallel transport allows topological raising and lowering boosts and compactification cycles.

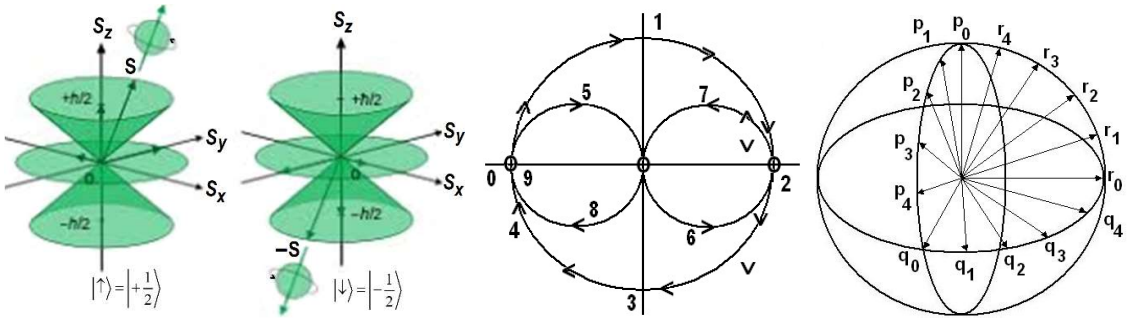

Figure 7. a) Spin-1/2 angular momentum cones; basis of Pauli exclusion principle and 720^o return cycle. Compare to suggested parameters within Figs. 5a & c, 6b) 2D simplistic view of 4D Dirac 360^o-720^o rotation map. c) 2D rendition of an additional 5D view of Dirac hyperspherical rotation for raising and lowering the topological annihilation-creation vectors to order polarization of induced magnetic dipole moments by applied electric currents with the proper frequency.

The origin of the magnetic moments responsible for magnetization can be either microscopic electric currents resulting from the motion of electrons in atoms, or the spin of the electrons or the nuclei. Net magnetization results from the response of a material to an external magnetic field, together with any unbalanced magnetic dipole moments that may be inherent in the material itself. By definition, the magnetization field, M-field is described with *dm* the magnetic moment and *d*V the volume element, $dV = \rho(u_1,u_2,u_3)\,du_1du_2du_3$ as distributed over the region considered, $\mathrm{M} = \dfrac{dm}{dV}$, $m = \iiint \mathrm{M}dV$ or analogously to $\mathrm{P} = \dfrac{dp}{dV}$, $\mathrm{p} = \iiint \mathrm{P}dV$, electric polarization field, P-field determining the dipole moment, p for r-dependent spin-orbit couplings. For our UFM utility of the polarized Dirac vacuum, the vibrational structures of singlet states, when coupling occurs between intrinsically repulsive states of different asymptotic degeneracy aide in the Double-charge-transfer of O_2^{2+}. This will operationally

occur when Spin-spin coupling is the interaction between the spin magnetic moments of different electrons and/or nuclei. Additionally, spin-transfer torque is an effect in which the orientation of a magnetic layer in a magnetic tunnel junction or spin valve can be modified using a spin-polarized current. Charge carriers have a property known as spin which is a small quantity of angular momentum intrinsic to the UF brane topological charge carrier.

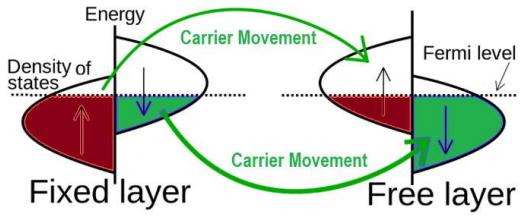

Figure 8. Spin-transfer torque. A simple model of spin-transfer torque for two anti-aligned layers. Current flowing out of the fixed layer is spin-polarized. When it reaches the free layer the majority spins relax into lower-energy states of opposite spin, applying a torque to the free layer in the process.

By passing a current through a thick magnetic layer (fixed layer), one can produce a spin-polarized current. If this spin-polarized current is directed into a second, thinner magnetic layer (free layer), the angular momentum can be transferred to this layer, changing its orientation. This can be used to excite oscillations or even flip the orientation of the magnetic field. The electron donating power of a donor molecule is measured by its ionization potential, which is the energy required to remove an electron from the highest occupied molecular orbital. The electron accepting power of the electron acceptor is determined by its electron affinity, which is the energy released when filling the lowest unoccupied molecular orbital.

The overall energy balance (ΔE) is the energy gained in a spontaneous charge transfer. It is determined by the difference between the acceptor's electron affinity (E_A) and the donor's ionization potential (E_I), adjusted by the resulting electrostatic attraction (J) between donor and acceptor: $\Delta E = E_A - E_I + J$. The positioning of the characteristic CT bands in the electromagnetic spectrum is directly related to this energy difference and the balance of resonance contributions of non-bonded and dative states in the resonance equilibrium.

We choose to call our reconfiguration of M-theory as correlated with putative parameters of an Einsteinian Unified Field Theory as Noetic Theory, mainly because it is designed to include aspects of reality related to the Observer. It is not easy to proceed this far afield of current thinking; and hope experimental validation will imminently occur.

De Broglie matter waves, of quantum wave/particle duality, describes two kinds of fields, the force field mediating bosons like photons and the mass/energy field for fermions such as the electron. The electron field is the mass energy waves surrounding a nucleus. Electrons are spherical standing waves (ideally) created by the constructive interference of these waves. The electron field is theoretically the harmonic resonance of the nucleus', as center of mass, and therefore relatively greater energy density than the electron field. Thinking of an atom as spherical with valence layers, starting with the core as the zero-point field, moving out to the quark/qluon field, the proton field, and finally, furthest from the center, the last layer is the electron field. These inherent parameters, when incorporated into M-theory, will allow manipulation of the HD brane topology of the matter field to act in ways similar to NMR and underlying operating principles of lasers, will allow formation of a new branch of UFM physical chemistry with the tools to construct a DEB device.

Operation of DEB devises require access to XD by surmounting the uncertainty principle and programming spacetime with a UF-basis UQC. Recently, we have shown that Yang-Mills Kaluza-Klein equivalence [34] provides an empirical path extending standard 4D model of particle physics to include

3rd Unified Field Mechanical (UFM) regime for a noetic (observer) science of mind-body [6,35,36]. We begin with Einstein's 1905 realization that Maxwell's equations obey the special relativity principle - The laws of physics are the same for all observers in uniform relative motion, with coordinate metric

$$x^{\mu} = \left(x^0, x^1, x^2, x^3\right) = \left(t, x, y, z\right); \tag{1}$$

which he continued in 1916, with the principle of general relativity where the laws of physics are the same for *all* observers, described by a gravitational field with two indices, $g_{\mu\nu}(x)$, where the infinitesimal line element *ds* between two 4D points is,

$$ds^2 = g_{\mu\nu}(x)dx^{\mu}dx^{\nu}. \tag{2}$$

In 1919, Kaluza made his attempt to combine electromagnetism and general relativity by postulating a 5th dimension with the new coordinate, θ denoted collectively as

$$x^M = (x^0, x^1, x^2, x^3, x^4) = (t, x, y, z, \theta). \tag{3}$$

Kaluza's 5D Riemann metric tensor line element, $d\hat{s}$ was

$$d\hat{s}^2 = \hat{g}_{MN}(x)dx^M dx^N \tag{4}$$

where he then made a 4D + 1D split

$$\hat{g}_{MN} = \begin{pmatrix} g_{\mu\nu} + \Phi A_{\mu}A_{\nu} & \Phi A_{\mu} \\ \Phi A_{\nu} & \Phi \end{pmatrix} \tag{5}$$

identifying $g_{\mu\nu}(x)$ with Einstein's G-field and $A_{\mu}(x)$ with Maxwell's em-field; at the time Maxwell's em-theory was seen to be a consequence of general relativity in 5D [37].

The problems associated with Kaluza's work were solved in 1926 by Klein [38,39] by assuming the 5th dimension had circular topology so that the coordinate, θ (eq. 3) is periodic, $0 \le \theta \le 2\pi$. It is this *circular* topology that is embraced and extended in a modified original hadronic version of M-Theory compatible with 12D UFM [40-42]. The periodicity in θ means that the fields $\hat{g}_{MN}(x,\theta)$ may be expanded [37], which we do with additional coordinates some of which are infinite size [41,43]. The UFM M-Theoretic requirements for a unified field theory are: 1) Mirror/Supersymmetry, 2) Topological bane dynamics, 3) Semi-quantum Manifold of Uncertainty (MOU) of finite radius, 4) Additional dimensions, 5) Extended material objects (brane bouquet) and, 6) a cyclic UFM force of coherence.

Resonantly aligned DEBs utilize an array of tessellated cellular automaton QED Dirac polarized LCU vacuum cavities. When the antispace *Casimirrors* are cyclically aligned, beam emission into 3-space is spontaneous. The power can be calculated, and correlates with what is called coherence length, ξ [44,45]; the greater number of cavities aligned the greater the power. For simplicity the 1D equation, $\xi = \sqrt{\hbar^2/2m|\alpha|}$ where $|\psi|^2 = \alpha\left(T_c - T\right)/\beta$ and *m* is the Cooper pair mass. In temperature dependent superconducting, the mean-free-path must be set for ballistic conduction to be maintained [46].

DEBs are temperature independent so that only a Bessel function aligned resonance oscillator is required to synchronize the beat frequency. The explanation is a little messy temporarily. The semiclassical limit, the boundary (limit of taking $\hbar \to 0$) is the transition regime from classical mechanics to the domain where quantum mechanics applies. Now we define a semi-quantum limit as the boundary where local quantization (phenomenology of mediated quantum fields) ends and nonlocal

UFM ontology (energyless topological transitions) begins [12]. The semi-quantum limit is not trivial; it entails a cyclical uncertainty manifold of finite radius. The structure is a duality; best described as a Randall-Sundrum D-brane throat [47,48], a cyclic (in our model) wormhole-like XD manifold acting as a gateway to LSXD. Because of the continuously transforming topological-charge (Fig. 6) of the Calabi-Yau brane bouquet, UFM-basis UQC can be programmed to format dioxygen, O_2 dication, O_2^{2+} adduction-subduction coupling cycles to tune with the inherent synchronization backbone of spacetime.

Reasoning for this machination is esoteric, best cast as beyond the limitations of this paper. One key however, is the mirror *image of the mirror image of the antispace image* of the 3D cavity-QED *particle in the box* is causally free of the local quantum state, and: mirror-symmetric duality increases the number of topological phase transitions required to access that cycle. This abominable snowman is what allows supervening the uncertainty principle and the spontaneous evanescence/emission of vacuum energy for DEB technology. Essentially, an additional set of UFM transformations beyond the Galilean-Lorentz-Poincairé must be defined. We pause the brief outline here and continue delineation in Sec. 4 below.

3.3 Cooling the Wildfire grid by combining/enhancing existing laser cooling techniques

It is not enough to extinguish a wildfire. Smoldering embers can remain inflammatory for days; deep cooling techniques can eliminate this aspect of wildfire control. Laser Cooling of atoms and molecules to ultracold temperatures evolved in the 1970s and 80s, with a variety of experimental techniques leading to improvements in atomic clock frequency standards by high-resolution spectroscopic measurements, a new ultracold state of matter - the Bose condensate, and lithography with cold atomic beams to form very accurate controlled structures [49-52]. Several of the techniques or a combination thereof can be extended to antispace UFM operation modes for utility with DEB wildfire prevention technologies [53-56]. Extending laser cooling techniques to extinguish embers will be straight forward when engineering access to XD occurs [6,7].

Meanwhile, the role of quantum interference in atomic physics has been experimentally demonstrated [57-59]; Since the 1970s, it was shown that quantum interference can prevent absorption in the presence of resonant light [60]. When considering a $\Lambda-\text{shape}$ configuration of internal states (two ground and one excited state), there exists a coherent superposition of the two ground states, for which the two excitation amplitudes to the excited state interfere destructively. For counter propagating laser beams, such a dark state is velocity sensitive, and it can thus be used for cooling processes going below the single photon recoil energy. An experimental proof of such *velocity selective coherent population trapping* (VSCPT) was first demonstrated in 1988 [50].

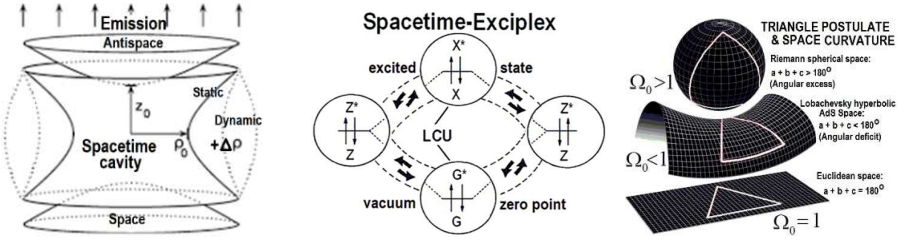

Figure 9. Exciplex UFM spacetime properties. a) Simplistic idealization of a Penning laser trap extended to an antispace static-dynamic oscillating Casimir-Polder cavity incorporating DEB required exciplex energy dynamics. b) Illustrating the energetics of LCU exciplex excitation dynamics in remaining above ground state (eq. 6), putatively allowing UFM energy to continuously summate with ballistically conductive DEB superradiance. c) Casimirror-Polder cavity oscillations also curve space. Fig. 9a) adapted to DEB form from [61].

The $\pm 1\ \Omega_0$ oscillation of antispace brane topology is important in the parallel transport cycle [12].

General equation for exciplex energetics,

$$
\begin{aligned}
&G^* + G^* \Leftrightarrow Z^*; \quad Z^* + m_\gamma \Leftrightarrow X^* \\
&X^* - m_\gamma \xrightarrow{\text{emission}} Z^* \quad \text{or} \quad G^* \\
&X^* + m_\gamma \rightarrow Z^* \quad \text{or} \quad G^*
\end{aligned} \tag{6}
$$

where *G* is the ZPF ground (not reached in excimer cycles), *Z* DEB UFM cavity excited states and *X,* the spacetime C-QED exciplex coupling. UFM Exciplex Properties hidden behind the veil of uncertainty in antispace entail existence of a harmonic *beat frequency* as part of the synchronization backbone inherent in the XD-LSXD duality of UFM brane topology. The exciplex complex as illustrated in Fig. 9b and eq. (6) is the programmable mechanism related LCU structure with an inherent KK cyclicality oscillating from an asymptotic virtual Planck-scale to the Larmor radius of the hydrogen atom [62,63].

Lasers provide a source of highly concentrated energy at near zero entropy, very effective for cooling close to absolute zero. In addition, laser generated traps are considered to have zero temperature walls, with oscillators able to reach the quantum ground state. Recent generations of experiments have additionally allowed cryogenic temperatures of macroscopic objects [56].

Efficiency cycles per background (antispace) absorption can be tremendously increased using exciplex states which have the particular property of exhibiting transitory bound excited states. Following Sommer et al., the mechanism is based on the particular property of exciplexes which exhibit a transitory bound excited state. During the short time window of exciplex formation, a laser of energy, $\hbar\omega_{\mathrm{L}}$ energetically matched around the instantaneous binding energy can be absorbed. In subsequent dynamics, the exciplex becomes unbound and up-converted photons at energy, $\hbar\omega_0$, corresponding to the transition can be spontaneously emitted. An overall energy loss occurs at $\hbar\Omega$ leading to a kinetic energy reduction and correspondingly a drop in the gas temperature [56].

It is proposed that cavity-mediated laser cooling will enable DEB technology to cool large samples of atomic particles collectively and non-destructively to very low temperatures [55]. The theory of cavity-mediated laser cooling can be analyzed in detail by utilizing a well-known Master Equation. Considering an idealized version of the proposed collective cooling mechanism, taking *N* non-interacting particles so strongly confined that their motion becomes quantized. Then following Kim [61], assuming that the atomic gas is placed inside an optical cavity and that its system Hamiltonian equals

$$
H_{\text{ideal}} = \sum_{i=1}^{N} \hbar J \left[b_i c^\dagger + b_i^\dagger c \right]. \tag{7}
$$

In the chosen cavity picture. b_i with $\left[b_i, b_j^\dagger \right] = \delta_{i,j}$ and *c* with $\left[c, c^\dagger \right] = 1$ are the bosonic annihilation operators of a solitary phonon for motion of particle *i*, and a photon inside the resonator, with *J* a photon-phonon coupling rate; and assuming a spontaneous decay rate, κ. Thus, the density matrix $\rho\mathrm{I}$ of phonons and cavity photons evolves in the corresponding interaction picture according to a master equation,

$$
\dot{\rho}\mathrm{I} = -\frac{i}{\hbar}\left[H_{\text{ideal}}, \rho\mathrm{I} \right] + \frac{\kappa}{2}\left(2c\rho\mathrm{I}c^\dagger - c^\dagger c\rho\mathrm{I} - \rho\mathrm{I}c^\dagger c \right). \tag{8}
$$

This master equation can predict expectation value dynamics; of significance are the two expectation values

$$
m \equiv \frac{1}{N}\sum_{i=1}^{N} \left\langle b_i^\dagger b_i \right\rangle, \quad \zeta \equiv \frac{1}{N(N-1)} \sum_{i=1}^{N} \sum_{j \neq i} \left\langle b_i^\dagger b_j \right\rangle. \tag{8}
$$

Normalizing the variables to be independent of N in the infinite many-particle limit, one finds that $\dot{m} = \dot{\zeta} = -\left(4NJ^2/\kappa\right)\zeta$. In a large cavity of decay rate κ with sufficient N, $\kappa \ll J$ and $N \gg 1$. This suggests cooling when m is an approximation of the vibrational energy of the trapped particles.

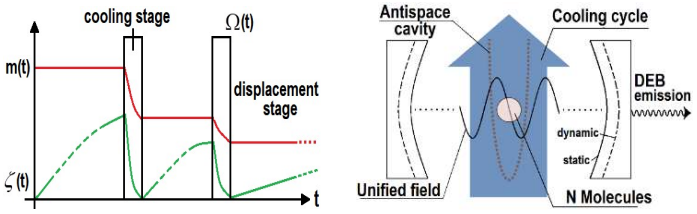

Figure 10. a) Schema for dynamics of the mean phonon number m and mean phonon expectation value ζ. The proposed cooling process consists of cooling stages interspersed with displacement stages. During each cooling stage, a cooling laser with Rabi frequency Ω is turned on which returns the atoms to the center of the trap, thereby returning ζ to zero while reducing m with a collectively-enhanced cooling rate. b) Modeling antispace static-dynamic Casimir-Polder cavity emission dynamics. Figs. redrawn/adapted from [61].

In summary, regarding our speculative wildfire ember cooling scenario based on an extension of the wide variety of extant laser cooling principles to M-theoretic UFM Casimir-Polder cavity dynamics, we postulate a combination of the cavity and exciplex models are most likely to lead to eventual use as DEB design elements. Kim [61] has proposed a cyclic two-stage cavity cooling scheme to transfer of a non-interacting atomic gas to very low temperatures. His experimental setup confines the atoms to an asymmetric trapping potential inside an optical (UFM modified) resonator (Fig. 10b). The role of the cavity and the external laser field is to remove vibrational energy from the atoms and to release it in the form of photons into the environment. Sommer [57] illustrated the prospects towards macroscopic scale for exciplex-mediated resonance cooling.

4. More detailed analysis of putative UFM M-theoretic DEB generation

A DEB device requires production of a charge-transfer complex (donor-acceptor) O_2^{2+} dication to be formed between D-brane topological charge and a dioxygen antispace electron $\overline{D}$-brane by spin coupling. Double charge transfer (DCT) for O_2 bombardment by protons (H^+) producing O_2^{2+} has been well studied in order to understand the selection rules governing DCT. Calculations found the O_2^{2+} ground state $X^1\sum_g^+$ to be a bound state with a well depth of 4.7 eV with an equilibrium radius r_e of 1.010 Å. The first O_2^{2+} excited state $A^3\sum_\mu^+$ was found to be 4.16 eV above the ground state, bound with an r_e of 1.285 Å [64,65] and references therein.

This exploration for a directed energy beam (DEB) wildfire attenuator is introduced in a seminal albeit highly speculative theoretical framework utilizing a 3rd regime Unified Field Mechanical (UFM) approach with some correspondence to existing theory (primarily a modified M-theory; also, saliently to de Broglie-Bohm super-implicate order and Cramer's transactional interpretation). The core of DEB wildfire suppression technology design is the attenuation of dioxygen, O_2 electron transfer by cyclical vacuum coupling of the species dication, O_2^{2+} by generating a holophote (rotating lighthouse beacon) *Least-Unit dual OCRET-OCHRE* resonance field. This resonant coupling is achieved by amplified matter-wave space-antispace annihilation-creation phase oscillation cycles of alternating spacetime electron Tight Bound State (TBS) [66] adduction (pulls toward) antispace subduction (at convergent brane boundary edges cyclically trapped) zero modes. In order to make that concatenation intelligible, a

new understanding of matter must be introduced. The explanation includes how a UFM M-theoretic reality of an inherent synchronization backbone is utilized in space-antispace constructive-destructive interference of this cyclic KK beat frequency of the Dirac polarized vacuum to implement the quantum computer (QC) programmed *Least-Unit dual OCRET-OCHRE* resonance field for adduction-subduction of brane bouquet topology. Of absolute utility is that the QC operate UFM-based r-qubits requiring an XD-LSXD [12,67-69] duality able to surmount the uncertainty principle [12].

4.1 Introduction to the Dimensional Conundrum

Protocols utilizing Yang-Mills Kaluza-Klein (YM-KK) equivalence as a path to verifying XD-LSXD) is suggested [6,7,34,41,43,67,68]. Riemannian KK manifolds, M with horizontal and vertical subspaces in the tangent bundle (M = X x G) defined by the YM connection are orthogonal with respect to the KK metric, where X is a 4D spacetime and G an arbitrary gauge Lie group; the corresponding YM theory, M is a trivial principle G-bundle [34,69]. This suggests orthogonal XD, changing the meaning of the concept of dimensionality [12,17]. This method validates M-Theory by tabletop-low energy UFM *cross section* alternatives for *viewing* putative brane topologies in a trans-dimensional 'slice' rather than supercollider cross section particle spray techniques.

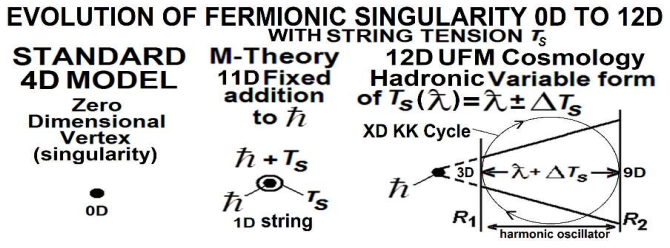

Figure 11. a) Usual 4D SM consideration of a fermion, the fundamental object of physics, as a 0D singularity. b) The current 1D basis of string theory, a fixed length, string tension T_S added to the Planck length, $\hbar + T_S$. c) UFM M-theoretic model reverting to the original hadronic form of string theory with variable T_S, for continuous-state cyclical compactification.

Two special processes emerge for modelling XD: 1) Duality, where dimensions are fundamentally different in character, and 2) Anti-commutativity, where they are fundamentally the same [17,70]. Rather than the current iteration of String/M-Theory this work is based on a radical extension of the original, hadronic form of the theory because of corresponding key elements such as virtual tachyon/tardon interactions (allowing more than one temporal dimension [7,71,72) and a variable concept of string/brane tension, T_S yielding experimental design parameters for accessing additional dimensionality (XD) [73,74,7].

It is generally known that KK modeling makes correspondence to the SM through YM Gauge Theory [72,75-77**];** now extended to an 11D M-Theory with Calabi-Yau mirror symmetric brane topology [78]. M-Theory has been severely criticized until now by the inability to perform experimental tests [79].

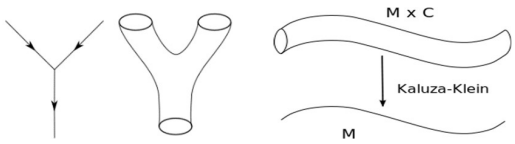

Figure 12. a) Interacting 0D fermionic point particle world line. b) M-Theory world sheet 1D string; extended to $M_{12} = M_4$ x C_8 brane topology in our model where $(C_8 = \pm C_4)$. c) KK space, M x C compactified over set C; KK decomposition produces a field theory over M. The tangent bundle of M (M = X x G) defined by the YM connection orthogonal for to the KK metric.

A salient feature of YM-KK correspondence as a path for extending the SM is the utility of the additional degrees of freedom allowed by dimensionality beyond the 4D of the SM. That a mathematical YM-KK correspondence exists is reasonably obvious [75-83] and not under overt dispute; what is questioned is whether or not extended real physical correlations exist. We list formulations briefly here:

A correspondence path to unified theory began in 1919, but not until the 1940's was KK theory completed. Kaluza's 1921 invariant 5D line element is $ds^2 \equiv \tilde{g}_{ab}dx^a dx^b = g_{\mu\nu}dx^\mu dx^\nu + \phi^2\left(A_\nu dx^\nu + dx^5\right)^2$ where $\tilde{g}_{ab}$ is the 5D metric and $g_{\mu\nu}$ the 4D spacetime metric; ϕ is the associated scalar field at a 5th diagonal, and A the Electromagnetic (em) vector potential from which the equations of both General Relativity (GR) and em can be derived [38,39,84].

It is possible to have supersymmetry in alternate dimensions because spinor properties change dramatically with dimensionality. For example, in d dimensions, spinor size is ~ $2^{d/2}$ or $2^{(d-1)/2}$. The maximum supersymmetries, is said to be 32; thus, the greatest number of dimensions in which a supersymmetric theory can exist is 11D. An SU(3) x SU(2) x U(1) gauge symmetry group can describe all known particle interactions. Following Witten, [78,83] the minimum number of dimensions of a manifold with this symmetry is 7D. Gauge fields arise in SU(3) x SU(2) x U(1) group symmetry in a gravitational field as components of more than 4D. This forms a reality of at least four non-compact and seven compact spacetime dimensions, $M^4 \times S^7 = 11\text{D}$, which Witten [78] calls a '*remarkable numerical coincidence*' because this 11D supergravity maximum is the minimum for SU(3) x SU(2) x U(1) symmetry which for symmetry reasons observed in nature is in practicality the largest group one could obtain from KK theories in seven XD.

Following Sundrum, [85] for 5D GR the Einstein action is $\ni \partial_\mu$ or $\partial_5 Gr^0_{MN}(x) \to 0$ for XD fluctuations $ds^2 \ni Gr_{55}\left(dx^5\right)^2 = Gr_{55}R^2 d\theta^2 \Rightarrow Gr^{(0)}_{55}(x) \equiv$ dynamical XD radius. Randall and Sundrum [47,48] found an HD method for solving the hierarchy problem utilizing 3-branes with opposite tensions, $\pm\sigma$ residing at the orbifold fixed points which together with a finely tuned cosmological constant form a source for 5D gravity.

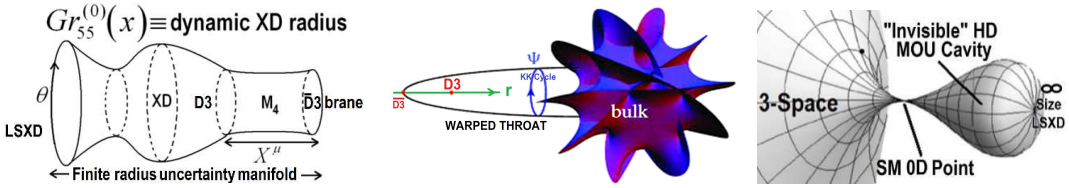

Figure 13. a) Randall-Sundrum model of dynamic GR radius for LSXD fluctuations, where X^μ are the Lorentz coordinates. Redrawn from [85]. b,c) Additional XD throat models.

The various Randall-Sundrum models utilize a 5D warped geometry to describe reality as an anti-de Sitter (AdS^5) space with elementary particles residing on a localized 3 + 1 4D brane (D3 Planck brane) and an additional separated gravity brane. The Randall-Sundrum warped AdS^5 XD postulate aligns sufficiently with our finite radius manifold of uncertainty [12] to give a semblance of credibility to each. Technological access to XD-LSXD requires a new group of transformations beyond the Galilean-Lorentz-Poincairé.

As a reminder, a Galilean transformation occurs between the absolute space and time coordinates of two Newtonian (non-relativistic) reference frames, (*x, y, z, t*) and (x', y', z', t') equated as $x' = x - vt$, $y' = y, z' = z, t' = t$ The common form of the Lorentz transformation for special relativity, is a velocity confined to the *x*-direction, with $t' = \gamma\left(t - \left(vx/c^2\right)\right)$, $x' = \gamma\left(x - vt\right)$, $y' = y$, $z' = z$, where γ is the

Lorentz factor, $\left(\sqrt{1-\left(v^2/c^2\right)}\right)^{-1}$ and (x, y, z, t) and (x', y', z', t') are the coordinates for an event in two reference frames.

We have all the pieces to formulate a new UF transform group, but are not yet sufficiently aware of topological restrictions to make a formal attempt; it is not clear in this case, whether experiment or theory will drive discovery. Because of the importance of this looming condition, we take liberty to speculate, hypothetically outlining the plethora of required components. As noted above our version of UFM M-theory reverts to an original hadronic form of string-theory having a tachyon (considered nonphysical) and variable string tension. Both these concepts become relevant in the UFM scenario where the present instant is a standing-wave of the future-past. Indeed the 1945, Wheeler-Feynman absorber theory, $T_{\mathrm{tot}}\left(\mathrm{X},t\right)=\sum_n\left(E_n^{\mathrm{ret}}\left(\mathrm{X},t\right)+E_n^{\mathrm{adv}}\left(\mathrm{X},t\right)\right)/2+\sum_n\left(E_n^{\mathrm{ret}}\left(\mathrm{X},t\right)-E_n^{\mathrm{adv}}\left(\mathrm{X},t\right)\right)/2=\sum_n E_n^{\mathrm{ret}}\left(\mathrm{X},t\right)$ describes radiation as a standing wave [86].

Cramer's transactional interpretation (TI) of quantum mechanics [15] (based on Wheeler–Feynman absorber theory), also describes quantum interactions as standing waves formed by retarded (forward-in-time) and advanced (backward-in-time) waves. Many consider Cramer's TI standing-waves too primitive; but a 1D oscillating string is only the basic concept. In reality, when extended to Calabi-Yau mirror symmetric dual 3-tori, a 6D hyperspherical standing wave M-theoretic topological interaction; the model can be made to work (Fig. 13d).

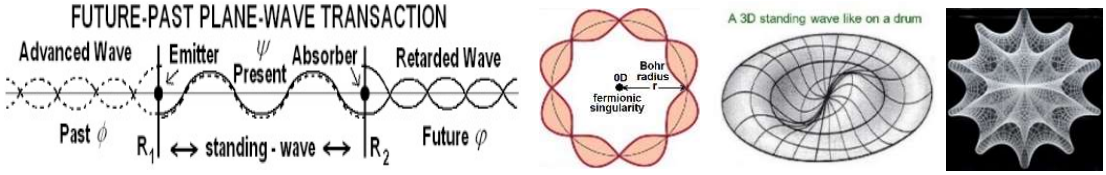

Figure 14. Cramer's Transactional Interpretation showing 1D, 2D, 3D and 6D standing waves.

Additional complexity appears in continuous-state spin-exchange parallel transport dimensional reduction compactification process. Because there must be holophote entry of the UF force of coherence (cannot be continuous) UF generator of 3D reality of the observer (flatlanders) [12].

A Lorentz boost is a Lorentz transform not involving rotation. Lorentz boosts are well-known; superluminal Lorentz boots (SLB) less so [87-89]. In a SLB a spatial dimension is transformed into a temporal dimension. This not a substance of space; we do not know what space is other than to name it extension (Einstein's term). We can consider it a substance of spacetime. Below we will consider additional boosting.

Lorentz boosts (no rotation) in x,y,z-directions respectively, for coordinates (t,x,y,z) and $\beta = v/c$:

$$\begin{bmatrix} \gamma & -\beta\gamma & 0 & 0 \\ -\beta\gamma & \gamma & 0 & 0 \\ 0 & 0 & 1 & 0 \\ 0 & 0 & 0 & 1 \end{bmatrix} \begin{bmatrix} \gamma & 0 & -\beta\gamma & 0 \\ 0 & 1 & 0 & 0 \\ -\beta\gamma & 0 & \gamma & 0 \\ 0 & 0 & 0 & 1 \end{bmatrix} \begin{bmatrix} \gamma & 0 & 0 & -\beta\gamma \\ 0 & \gamma & 0 & 0 \\ 0 & 0 & 1 & 0 \\ -\beta\gamma & 0 & 0 & 1 \end{bmatrix} \tag{9}$$

For boosts in any direction the values of γ and β change as follows

$$\gamma = 1/\sqrt{1-\left(v_x^2+v_y^2+v_z^2/c^2\right)};\quad \beta_x=\frac{v_x}{c},\beta_y=\frac{v_y}{c},\beta_x=\frac{v_y}{c} \tag{10}$$

and the boost matrix for $v=\left(v_x,v_y,v_z\right)$ is

$$\begin{bmatrix} L_{tt} & L_{tx} & L_{ty} & L_{tz} \\ L_{xt} & L_{xx} & L_{xy} & L_{xz} \\ L_{yt} & L_{yx} & L_{yy} & L_{yz} \\ L_{zt} & L_{zx} & L_{zy} & L_{zz} \end{bmatrix}. \tag{11}$$

$L_{tt}=\gamma;\ \ L_{ta}=L_{at}=-\beta_a\gamma;\ \ L_{ab}=L_{ba}=\left(\gamma-1\right)\left(\beta_a\beta_b/\beta_x^2+\beta_y^2+\beta_z^2\right)+\delta_{ab}=\left(\gamma-1\right)\left(v_a v_b/v^2\right)+\delta_{ab},$ and where *a* and *b* are *x,z* or *z*. δ_{ab}, the Kronecker delta [90,91], is a function of two variables (typically non-negative integers), where the function is 1 if *a,b* are equal and 0 if unequal:

$$\delta_{a,b}=\begin{cases}0 & \text{if } a\neq b,\\ 1 & \text{if } b=a,\end{cases} \tag{12}$$

where the Kronecker delta, δ_{ab} is a piecewise function of *a* and *b*; for example $\delta_{1\,2}=0,$ but $\delta_{3\,3}=1$ [90,91]. This is the stepping-stone, at the semi-quantum limit, in terms of making correspondence to a new UFM XD transform dynamics.

Again, we ill make no serious attempt at derivation here, only introducing simplistically some of the required tools necessary that relate to Kronecker stepping functions. We will later on, again only briefly, show how Kronecker products related to coquarternion and octonions will be a valuable tool in discovering the UFM M-theoretic transform.

Typically, the Kronecker delta is restricted to positive integers; for space-antispace, future-past annihilation-creation topological phase transitions we will also require negative integers to fully utilize the cyclical elements in quaternions and octonions. For example, $\delta_{(-1)(-5)}=0$ and $\delta_{(-3)(-3)}=1.$ The Kronecker delta is said to have (changing notation) a *sifting* property for $j\in\mathbb{Z}:\ \sum_{i=-\infty}^{\infty}a_i\delta_{ij}=a_j.$ If the integers are considered to be a counting measure space, this property is coincident with a defining property of Dirac's delta function, $\int_{-\infty}^{\infty}\delta\left(x-y\right)f\left(x\right)dx=f\left(y\right),$ important in some sequences [90].

Briefly, following [92], coquaternionic, *C* and quaternionic, *Q* Kronecker products are derived. The distinguishing difference is in the inverse of *C* and *Q* respectively,

$$C^{-1}:=\frac{1}{\left|w\right|^2-\left|z\right|^2}\begin{bmatrix}\overline{w} & -z\\ -\overline{z} & w\end{bmatrix};\ \ \mathrm{Q}^{-1}:=\frac{1}{\left|w\right|^2+\left|z\right|^2}\begin{bmatrix}\overline{w} & -z\\ \overline{z} & w\end{bmatrix}. \tag{13}$$

The inverse of *C* only exists if $\left|w\right|^2-\left|z\right|^2\neq 0,$ but Q has an inverse so long as $Q\neq 0.$ The salient difference regards which elements are noncommutative or commutative [92].

Leaving this for now, with the additional mention of combining these functions with relative work of Kauffman on the concept of iterant algebra to formation of basic Clifford algebras reconstructing the complex numbers in terms of a formalization of temporal process. Kauffman's iterant algebra includes all of matrix algebra and a representation of the SU(3) Lie algebra for the Standard Model and a construction of the Dirac Equation, making it clear how solutions arise from nilpotent elements in a Clifford algebra, and how Fermion algebra including the algebra of Majorana Fermions (Center Figs. 43,46b) emerges in this context. Kauffman continues a formulation of the original Majorana Dirac Equation in terms of Clifford algebra in the context of his iterants [93,94].

Why is the Kauffman Interant of interest? The simplest discrete system corresponds directly to $\sqrt{-1}$, when $\sqrt{-1}$ is seen as an oscillation between ± 1. Generally, starting with a discrete time series of positions, one immediately has a non-commutativity of observations which can be encapsulated in an iterant algebra which is used to formulate the Lie algebra *SU*(3) for the Standard Model for particle physics and Majorana Fermion Clifford algebra. This Majorana Dirac equation is $\left(\partial/\partial t + \hat{\eta}\eta\partial/\partial x + \varepsilon\partial/\partial y + \hat{\varepsilon}\eta\partial/\partial z - \hat{\varepsilon}\hat{\eta}\eta m\right)\psi = 0$, η and ε are the simplest generators of iterant algebra, $\eta^2 = \varepsilon^2 = 1$ and $\eta\varepsilon + \varepsilon\eta = 0$, and $\hat{\varepsilon}, \hat{\eta}$ forming a commuting copy of this algebra. This combination of the simplest Clifford algebra with itself underlies the structure of Majorana Fermions, forming the underlying structure of all Fermions! Kauffman also includes the Kronecker delta in his *SU*(3) and Gell-Mann matrices discussion [93,94].

As well-known Hamilton had to sacrifice commutativity in order to close the quaternion algebra. In finding the formalism for Noetic UFM group of transformations, closure must be periodically broken; this cyclical process is key to empirically accessing the brane bulk. A Kauffman-Kronecker continuous-discrete cycle iterant algebra (commutative-anticommutative) will aid discovering the topological phase.

In addition to the mentioned boosts, rotations, standing-wave future-past annihilation-creation and various topological phase transitions; the nature of dimensionality also undergoes transformation in the new UFM M-theoretic group. In our mindset we dwell too much on the concept of dimensionality as a spatial construct, and not its complete physical meaning. Here we review firstly, the well-known Superluminal Lorentz Transformations (SLT) that changes real quantities into imaginary; how a SLT transforms a spatial dimension into a temporal dimension.

Following Cole [88] & Rauscher [14,87] we illustrate the transformation of complex spatial dimensions into temporal dimensions by orthogonal superluminal boosts (SLB). For example an SLB in the x direction with velocity $v_x \pm \infty$ the SLT is $x' = \pm t,\ \ y' = -iy,\ \ z' = -iz,\ \ t' = x.$ To clarify the meaning of imaginary quantities in an SLT time is represented as a 3D vector; with t defined as $t = t_x\hat{x} + t_y\hat{y} + t_z\hat{z}$, in expanded form is $t_x = t_{x\mathrm{Re}} + it_{x\mathrm{Im}},\ \ t_y = t_{y\mathrm{Re}} + it_{y\mathrm{Im}},\ \ t_z = t_{z\mathrm{Re}} + it_{z\mathrm{Im}}$

Finally, for the SLB with velocity $v_x \pm \infty$ along x, the transformations are

$$\begin{aligned} &x'_{\mathrm{Re}} + ix'_{\mathrm{Im}} = t_{x\mathrm{Re}} + it_{x\mathrm{Im}},\ \ y'_{\mathrm{Re}} + iy'_{\mathrm{Im}} = y_{\mathrm{Im}} - iy_{\mathrm{Re}},\ \ z'_{\mathrm{Re}} + iz'_{\mathrm{Im}} = z_{\mathrm{Im}} - iz_{\mathrm{Re}} \\ &t'_{x\mathrm{Re}} + it'_{x\mathrm{Im}} = x_{\mathrm{Re}} + ix_{\mathrm{Im}},\ \ t'_{y\mathrm{Re}} + it'_{y\mathrm{Im}} = t_{y\mathrm{Im}} - it_{y\mathrm{Re}},\ \ t'_{z\mathrm{Re}} + it'_{z\mathrm{Im}} = t_{z\mathrm{Im}} - it_{z\mathrm{Re}} \end{aligned} \tag{14}$$

where the SLT in *x* of M_4 spacetime transforms real components into imaginary, and imaginary complex quantities into real quantities as one major property of the periodic nature of noetic anthropic multiverse spacetime [13,14,87].

UFM postulates how boundary conditions transform the dimensionality of space and time along with the energy covering (de Broglie-Bohm super-quantum potential) of the UF by $D_S \to D_t \to D_e$; i.e. space $\to$ time $\to$ energy (UFM) [13,14]. In complex Minkowski space the coordinates are $z^u = x^u_{\mathrm{Re}} + ix^u_{\mathrm{Im}}$ where z is complex and $X_{(\mathrm{Re})}$ and $X_{(\mathrm{Im})}$ are real and the index u runs over 0,1,2,3. Using classical notation for simplicity $t = t_{\mathrm{Re}} + it_{\mathrm{Im}},\ \ x = x_{\mathrm{Re}} + ix_{\mathrm{Im}},\ \ y = y_{\mathrm{Re}} + iy_{\mathrm{Im}},\ z = z_{\mathrm{Re}} + iz_{\mathrm{Im}}$.

4.2 Space-antispace

The nilpotent condition for the two vector spaces can be made from arbitrary scalar values and be represented by the 5 generator objects E, p_x, p_y, p_z, m to form the two commuting vector spaces by,

$$\left(\mathrm{K}E + i\mathrm{I}ip_x + i\mathrm{I}jp_y + i\mathrm{I}kp_z + i\mathrm{J}km\right)\left(\mathrm{K}E + i\mathrm{I}ip_x + i\mathrm{I}jp_y + i\mathrm{I}kp_z + i\mathrm{J}km\right) = 0\,. \tag{15}$$

Which becomes the nilpotent condition, $E^2 - p_x^2 - p_y^2 - p_z^2 - m^2 = 0.$ The bracketed object above has squared to zero, the duality is identical and defines the principle of a point in either space as a norm 0 crossover between them. Physics is mediated by the concept of space, requiring a dual space to ensure that the fundamental condition of the universe is a zero totality. The real space of observation is defined by quaternions as i, j, k [17,67]. The dual space, I,J,K not accessed as a physical quantity (until now) is called `vacuum space', or `antispace' because it combines with real space to produce a nilpotent zero totality. The creation of nilpotent structures zeroing all higher terms and the perfect group symmetry allowing a complete cancellation ensure that Nature exhibits zero totality in all of its aspects, material and conceptual, and it does this via a fundamental principle of duality [67-69].

Another way to look at this is to say the fermion always exists in the two spaces from which it is constructed, real space and vacuum space, and the non-classical *zitterbewegung* motion, Schrödinger found in the solution to the free-particle Dirac equation [95], represents the switching between these spaces which makes it possible to define the fermion as creating a point singularity through the intersection of two spaces. We can here apply a reverse argument from topology. The creation of a particle singularity using its `intersection' with a dual space can be seen as the creation of a multiply-connected space from a simply-connected space through the insertion of a topological singularity.

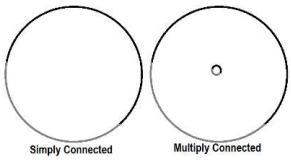

Figure 15. Simply and multiply-connected spaces effect parallel transport (One of our UFM generators of topological switching) differently.

According to a well-known argument, parallel transporting a vector round a complete circuit in a multiply-connected space will produce a phase shift of π or 180^o in the vector direction, whereas transporting it round a simply-connected space will not, and so, in the first case, the vector will be required to do a double circuit to return to its starting point [68,96]. This is exactly what happens with a spin ½ fermion, which, as a point-singularity, can be regarded as existing in its own multiply-connected space. We can interpret this as meaning that the fermion requires a double circuit because, just as in *zitterbewegung*, it spends only half of its time travelling in the real space of observation.

4.3 Matter as continuous-state Calabi-Yau brane bouquet transformations

M-theory currently remains silent in any attempt to configure a bouquet of resonant strings into a model of a fermion. The googolplex of possibilities, essentially 10^{∞} for deriving a single unique compact-ification of the 11D bulk producing the 4D Standard Model has remained elusive. While we have been able to derive a unique vacuum utilizing an alternative derivation of string tension in a continuous-state cosmology [13], our anthropic UFM model, provides feasibility of such modeling on the horizon; success would be elusive without the new noetic UFM group of transformations.

All matter appears to observation as a singularity. In wave-particle duality, the quantum field is like the clothing of the particle. Physical science has no idea of what the fundamental nature of a field is; we put a metric in its proximity and measure salient properties. Likewise, we do not know what space is, other than to apply Einstein's definition, that it is extension. Our observations of matter in Euclidean-Minkowski-Riemann space are considered geometric. The additional 8D of the M-theoretic bulk are considered topological, with attempts underway to provide topological field theories [8,12].

Wave-particle duality, yes, is a probabilistic Heisenberg potentia given either wave or particle depending on measurement conditions. This QM regime is only an oasis in the combinatorial hierarchy of reality [8-14]. However, in passing beyond the Copenhagen wall of QM exclusion/uncertainty, the inherent processes of existence are a continuous cycle of this duality and its extended mirror symmetric

partners. Anthropic reality depends on this. Assuming (not yet proven) Descartes is correct in his dualism postulate, the dynamic propagation of 3-space (observation) manifold embedded in the M-theoretic Bulk of the UF, must be, in terms of the *injected* (ontologically topologically switched) coherence force of the UF, holophotic, not continuous, otherwise, the *flatlander* cannot abide his 2D existence. His eyes, by subtractive interferometry, would see 12D and he would fall through the floor (pass through like the 3-sphere visitor to Flatland) out of temporal existence. However, many degrees of freedom we define SM temporality with, localized realism is limited. The UFM nonlocal holographic ∞ has all degrees of freedom. As well-known, Einstein claimed, if one put a saddle on a photon, one could circumnavigate the universe without the passage of time. This is not all; its observation pertains to the nonlocal instantaneity where temporal dimensions are transformed by annihilation. As a metaphorical SM mantra: if one assumes matter is a vector gluon, the leading lightcone singularity is modulated by a phase of the quark gluon field. We attempt upgrade to UFM: If one assumes that reality is a tensor psychon, the superimplicate order is an evanescent ontology of the UFM noeon field.

In this section, we attempt to provide some insight into the nature of topological brane dynamics in the bulk. It is radically different than the string communities current thinking, primarily because compactification is continuous. We will not argue this point now, other than to propose in passing, that the reason is anthropic. Einstein himself stated that his long sought UF could explain living systems.

Fermionic matter can no longer be considered 0D point particles (electrons) or as rigid Mass-charge quark microspheres (nucleons), as treated by vector algebra or quantum field theory, embedded in (3)4D (+,+,+,-) Minkowski-Riemann manifold; but must now be devised as a compactification of 6D D-brane mirror symmetric Calabi-Yau florets cyclically driven by de Broglie-Bohm-Cramer piloted matter-wave XD brane topology-phase transitions. The generator design's multiphasic concatenation requires utilization of a unique interpretation of M-Theory, the modified model of matter, albeit incorporating relevant *off-the-shelf*, parameters currently incorporated into the vast panoply of thinking comprising String Theoretic parameters; especially those related to T-Duality D-brane mirror symmetry, because as generally known, T-duality interrelates two theories with different spacetime geometries. Thus, allowing correspondence with usual notions of classical atomic geometry, quantum field theory or our radically different UFM formulation of T-duality.

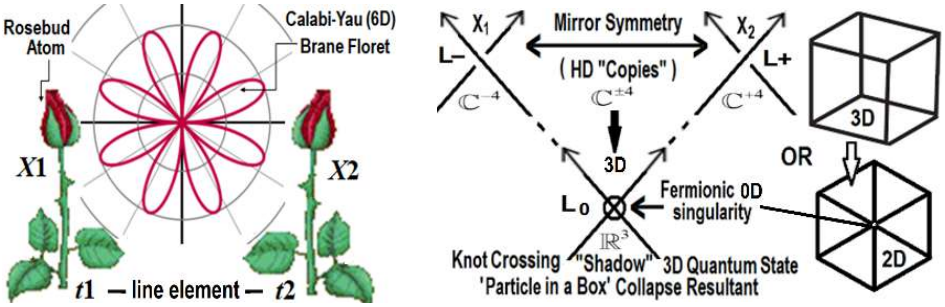

Figure 16. 12D UFM models of matter. a) Consider $X_1(t_1)$ and $X_2(t_2)$ as ends of a line element between two atoms depicted in 3-space as rosebuds. For a space-antispace configuration, X would only represent the knot shadow, fermionic singularity of observation in b) with Euclidean coordinates x,y,z. b) An oriented left-right (over-strand, under-strand) crossover link diagram; each component has a preferred direction as shown by the arrow. For a given crossing L_+, L_-, resultants L_0 and $\mathbb{R}^3$ change the diagram as proposed. Braid elements in the HD complex, $\mathbb{C}^{\pm 4}$ brane world become a knotted shadow when projected onto Euclidean space, $\mathbb{R}^3$. c) Illustrating how a crossing shadow reduces dimensionality.

Figure 16a is simplistic in that the rosebud is only illustrated for an x coordinate; whereas it is proposed that a quaternionic space-antispace mirror symmetric representation, $\pm\, i, j, k$ would entail six

buds continuously blooming (Calabi-Yau brane topology) and compactifying into the 3-space knotted shadows. A knot projected onto a plane casts a shadow. A small change in the angle of projection shows if it is one-to-one except at the crossings, where a 'shadow' of the knot crosses itself once transversely. Analogously, knotted surfaces in 4-space can be related to immersed surfaces in 3-space.

The knot crossing shadows in Fig, 16b in the next step are illustrated as trefoil knots. In work in progress, we show that the topology of the Dirac spinor is a trefoil in HD; a fact hidden from observation, until now, by the uncertainty principle.

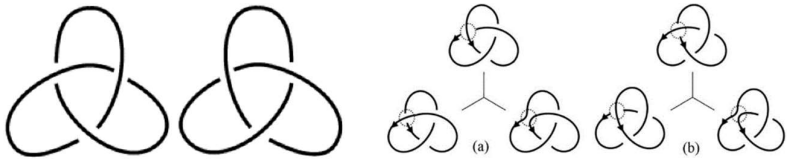

Figure 17. a) Left and right handed trefoil knots are mirror images of each other. b) Raising and lowering of trefoil over and under crossings allows a variety of topological moves.

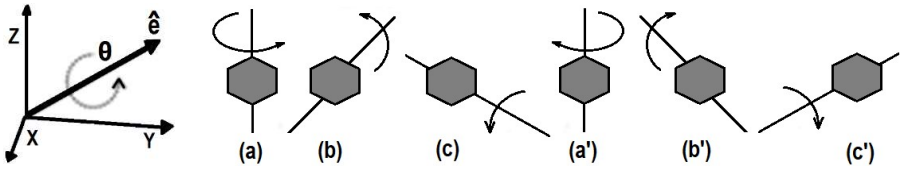

Figure 18. In regards to Fig, 17, unknotting the crossover links during parallel transport conditions allows rotations to be added to the topological phase transitions.

Topological moves (phase transitions) are richly endowed. We are attempting to illustrate the battery of parameters useful in describing the operation of the UFM transformation group. We will continue to briefly address these elements in an introductory manner in the subsections that follow primarily to give an overview of the requirements as seen at this point in time in the hopes of engendering interest in further development to address the dire and costly need to ameliorate *perpetual fire*.

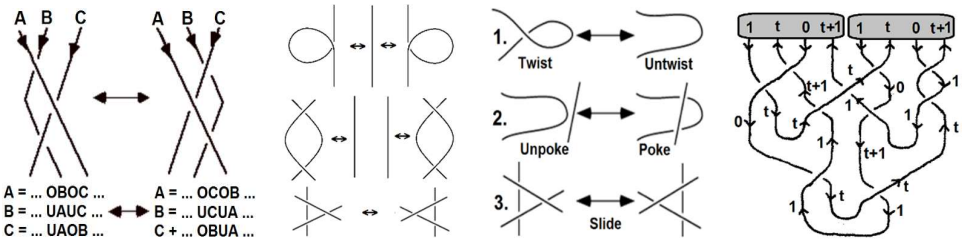

Figure 19. a,b,c) Varieties of Reidemeister moves. d) A roll spun knot.

The local SM component corresponds to 4D quantum Field Theory wherein Copenhagen aspects are replaced by resultant Cramer Transactional and extended de Broglie-Bohm piloted implicate order causality with a corresponding nonlocal duality of Large-Scale Additional Dimensionality (LSXD) in the bulk described by an Ontological-Phase Topological Field Theory developed as a 12D form of cyclic Kaluza-Klein theory initially introduced by Yang-Mills Kaluza-Klein correspondence to include a fundamental Least Cosmological Unit (LCU), the primary requirement for an Einsteinian Unified Field Theory as the tessellation of space/spacetime [7,73,74,77,97].

To fully represent matter up to and beyond space-antispace, three oriented rosebuds *X,Y,Z* would be

required mirror symmetrically designated with quaternion notation, $Y = i, j, k$ and $Z = -i, -j, -k$. In addition, the space-antispace configuration would be represented as in the center of a) as rose petals in bloom. *X,Y,Z* undergo Dirac spinor rotation, where a rotation through antispace takes 720° rather than the 360° needed for a 3-space rotation to return to the starting position. Because this only represents the penultimate compactification to 3-space, *X,Y,Z* are represented by a trefoil configuration of three sets of quaternions. This fact has been hidden from observation as an element of the Dirac spherical rotation by the quantum uncertainty principle. To complete the UFM line element cycle the rose petal symmetry (Calabi-Yau topological brane interactions), continues through a continuous 12D KK cycle. The mirror image of the space-antispace mirror image is causally free of the knot crossing shadow in 16b), which is realized or the collapsed resultant of the local 3(4)D Euclidean/Minkowski quantum *particle in a box*.

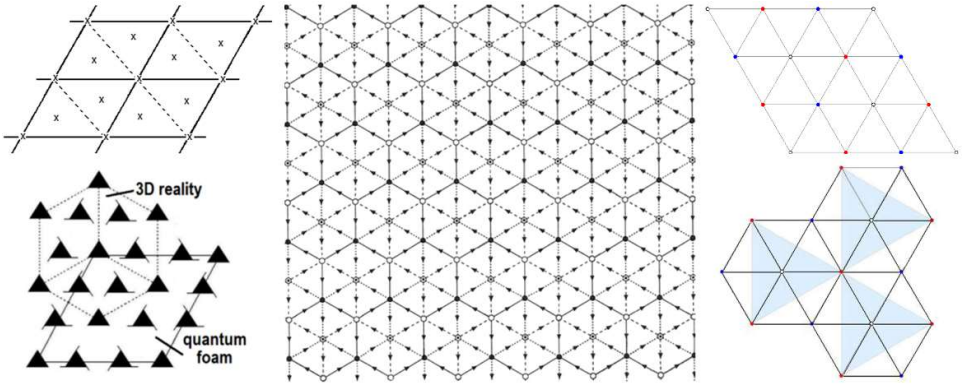

Figure 20. a) 2D and projected 3D view of LCU tiling, giving rise to higher dimensionality (1 sphere in Fig. 5b,c,d in spacetime backcloth. LCU spacetime loses its stochasticity at the semi-quantum limit; and becomes more ordered by coherent control at the upper (HD) limit of the *manifold of uncertainty* by coherence of the UF. b) Least-unit exciplex C-QED backcloth tessellating space, able to accommodate any geometry and any transform by topological switching. Fig. adapted from [98]. c-bottom) P and H domains of Dixon functions for sm z, Fig. adapted from [99].

In Fig. 19a-bottom, the triangles with tails represent the trefoil knots in Fig. 7 and the naked triangles the resultant cyclic point or fermionic vertex quantum state in 3-space (Spheres in Fig. 5b).

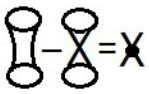

Figure 21. The Dirac mobius transforms to an HD trefoil to tunnel through the semi-quantum limit. Tunneling ≡ wormhole.

Our proposal that Dirac spherical (spinor) rotation (360°-720°) for SM particle physics in Minkowski/Riemann space 3(4) +,+,+, - includes hidden trefoil crossover topology in the semi-quantum interface requires further discussion on the parametrization of the trefoil surface in relation to the Dirac Mobius. Because of the existence of HD-LSXD duality, hidden (until now) from observation by the uncertainty principle, takes the form of a mirror symmetric trefoil with utility of its over/under crossings for parallel transport in both simply and multiply-connected topologies. This scenario is required to describe the UFM transform and operation of HD M-theoretic bulk reality.

Firstly, the Trefoil, $\mathcal{T}$ has polar equation $r^3 = 2A\cos(3\theta)$ and Cartesian coordinates $\left(x^2 + y^2\right)^3 = A\left(2x^3 - 6xy^2\right)$. Following Langer & Singer's [99] description of the trefoil as a sextic curve with exceptional properties, such as a genus-1 Platonic surface with 18 equilateral triangle faces that may be exchanged and rotated like the faces of an icosahedron (dual of dodecahedron).

Dixon elliptic functions, based on the curves $x^3 + y^3 - 3axy = 1$ and the trefoil make a perfect fit. Our interest is in the Fermat cubic, $x^3 + y^3 = 1$, for which when $a = 0$, the Dixon functions display a unique hexagonal symmetry; a simpler curve with the same projective symmetry group as τ. Especially as the Dixon sine sm z can be used to map a regular hexagon onto a Riemann sphere, where the hexagon interior is conformally mapped onto the complement of the three rays joining ∞ to a cube root of unity. In this sense, arc length parameterization provides the trefoil's structure as a genus-one Platonic surface, whose 18 equilateral-triangular faces may be arbitrarily exchanged and rotated, like the faces of an icosahedron [99].

The trefoil has many noted features. The Dixon sine equation $\mathrm{sm}\, z = \tan \frac{p}{2} e^{i\lambda}$ correlates the hexagon point with complex coordinate $z = x + iy$ with the point in the sphere of latitude $\pi/2 - p$ and longitude λ. The function $w = \mathrm{sm}\, z$ defines real z by $z = \int_0^w dx \Big/ \left(1 - x^3\right)^{2/3}$, and $\mathrm{cm}\, z$ by $\mathrm{sm}^3 z + \mathrm{cm}\, z = 1$. Then interestingly, sm (0) = 0, cm (0) -1, and $\frac{d}{dz}\mathrm{sm}\, z = \mathrm{cm}^2 z$, $\frac{d}{dz}\mathrm{cm}\, z = s\mathrm{m}^2 z$. In 1896, Caley finally paved the way for formalizing sm z and cm z as elliptic functions.

Since sm z and cm z have periods $p_1 = 3K$ and $p_2 = 3\omega K$, with $\omega = -1 + i\sqrt{3}/2$ as a cube root of unity: $\mathrm{sm}\left(z + 3\omega^j K\right) = \mathrm{sm}\, z$, $\mathrm{cm}\left(z + 3\omega^j K\right) = \mathrm{cm}\, z$, $j = 0,1,2$. As for any elliptic functions, one can describe the values of sm z and cm z, $z \in \mathbb{C}$, via a tiling of the plane by copies of a `period parallelogram' P with edges corresponding to the pair of periods. There is a corresponding triangulation of P by 18 equilateral triangles (Fig. 19c-top). One may also define rotational and quasiperiodic translational symmetries [99].

The tiling of sm z and cm z trefoil properties to the vacuum are an entry point for applying micromagnetics to the Dirac polarized vacuum. When a static electric dipole d is placed in front of an ideally conducting wall, it interacts with its mirror image. In historical terms, this Casimir–Polder (CP) result, gives the interaction potential between a ground state atom and a mirror as obtained within the cQED (cavity-QED) framework known to be valid for any separation z between the atom and the mirror and results from modification of vacuum fluctuations by the mirror. Recent experiments have given clear evidence for the existence of retardation terms in the atom-wall problem, in good agreement with Casimir-Polder predictions. We extend these parameters in our 3rd regime M-theoretic UFM approach in order to enable aspects of the Static-Dynamic (S-D) Casimir Effect in relation to topological charge inherent in cyclical (KK-like T-duality) brane interaction dynamics mediated by a super quantum potential of the unified field. The UFM interaction is an Ontological (energyless) transfer of information, not phenomenological (quantal) as in quantum field theory.

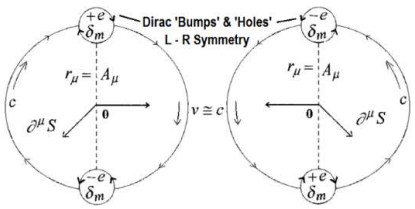

Figure 22. Oppositely charged sub-elements rotating at v$\cong c$ around center 0 behaving as dipole bumps and holes on the surface of a covariant polarized Dirac vacuum, allowing Sagnac interferometric rf-modulation.

The dynamics of micromagnetics becomes part of LCU vacuum programming by resonant pulsed external fields. The magnetic domains in Dirac LCU vacuums act as an aggregate of spins. There are four applicable magnetic forces, magnetostatic, exchange, anisotropic and external which can be

programmed to act on the other three. These phenomena work in conjunction with topological invariants such as winding, wrapping and linking numbers. Toffoli states, emergent structures of micromagnetics do not constitute a motley collection of features, rather, they are arranged in a dimensional hierarchy (respectfully 3, 2, 1, and 0 dimensions) interconnected with topological constraints [98].

Of extreme importance to the duality required to surmount the uncertainty principle for quantum computing is the application of topological phase transitions to the finite radius manifold of uncertainty beginning at the semi-quantum limit; this takes the form of topological switching between the regime of micromagnetics and HD brane topology. The LCU tessellated spacetime network of signals and nodes representing information transactions. The nodes are partitioned into triangular sublattices. The transition between lattice states entails the collapse of a hexagonal lattice into a triangular lattice which is a form of symmetry breaking. In the schema of topological switching, perfect symmetry is everywhere extant relative to the force of coherence mediating the UF, wherein the hexagonal lattice is a programmable metastable state which can be cyclically protected from decoherence [12,98,100,101].

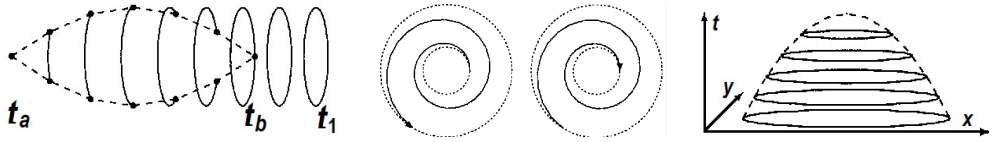

Figure 23. a) Two Bloch points created as a pair at $t > t_0$, move apart and subsequently come together (dashed), annihilating at $t < t_1$. Moving in space they leave a trail of twisted magnetization (solid) eventually closing on itself but still hovering in space even after the Bloch points disappear. b) Path described by a Vertical Bloch Wall (VBL) lying on the wall of an expanding bubble (left). Dotted lines indicate the bubble's initial and final sizes. As the wall slowly moves outwards, the VBL slides along it at a speed much larger than the wall itself (here ~10); compound VBL motion (radial and tangential) is a logarithmic spiral. When the magnetic field changes in opposite direction the wall retreats, the VBL spirals inwards (right). c) As a bubble is made to shrink until it disappears, its boundary (circles) generates a surface (paraboloid-like figure) having the topology of the disk. Figures modified from [98].

5. Universal quantum computing (QC) – M-theoretic r-qubits

Of late QC mathemagicians claim QCs already exist; but by what chimeric definition. Does flipping a few qubits in a single purpose logic gate without an algorithm qualify as quantum computing? In physics, theory bears little weight without rigorous experimental confirmation, less if new, radical or a paradigm shift. DEB Tek requires UQC based on '3rd regime' M-theoretic UFM physics. What distinguishes this work from a myriad of other avenues to UQC under study? Virtually all R&D paths struggle with technology and decoherence. If the currently highly favored room-sized cryogenically cooled quantum Hall anyon bilayer graphene QCs ever become successful, they would be reminiscent of the city block-sized Eniac computer of 1946. In 2017 quantum Hall techniques experimentally discovered additional synthetic dimensions. This scenario will not last long; the floodgates will open soon. Then we will have actual Bulk UQCs! The QC prototype proposed DEB Tek is room temperature and tabletop. It is dramatically different in that it is not confined to the limitations of quantum mechanics (locality & unitarity); since it is based on principles of UFM, the Uncertainty Principle and Decoherence no longer apply. Thus, this QC model could be implemented on any scalable r-qubit quantum platform.

To implement bulk UQC) [102-108] a new relativistic approach to quantum information processing (QIP) that includes a new physically real coordinate transformation beyond the current Riemann Block 2-sphere rendition in Hilbert space and a relativistic definition of the qubit (r-qubit). This is part of an end to the historical pillars of ‘unitarity and locality’. The Bloch 2-sphere representation of the qubit $|\Psi|^2 = \cos\frac{\theta}{2}|0\rangle + e^{i\phi}\sin\frac{\theta}{2}|1\rangle$ maps to the polar coordinates along the z axis as a linear combination of

$|0\rangle$ and $|1\rangle$ between $-\hat{z}$ and $\hat{z}$, and where $e^{i\phi}$ is a phase factor. In this regard we have $|\Psi(\theta=0,\phi=0)\rangle=|0\rangle$, and $|\Psi(\theta=\pi,\phi=0)\rangle=|1\rangle$ yielding $|\Psi(\theta,\phi)\rangle=\cos(\theta/2)|0\rangle+\sin(\theta/2)e^{i\phi}|0\rangle$ since $\cos(\theta/2)=0$ and $\sin(\theta/2)=1$. This scenario is very useful when applying π or $\pi/2$ pulses to basis states.

Note that angle $\theta/2$ [109] doubles when going from the Dirac ket

$$|\psi\rangle=\begin{bmatrix}\cos\dfrac{\theta}{2}\\ e^{i\phi}\sin\dfrac{\theta}{2}\end{bmatrix},\quad \|\psi\|=1,\quad \vec{r}=\begin{bmatrix}x\\y\\z\end{bmatrix}=\begin{bmatrix}r\cos\phi\sin\theta\\ r\sin\phi\sin\theta\\ r\cos\theta\end{bmatrix},\quad r=1, \tag{16a,b}$$

to the operator for the density matrix $\rho=|\psi\rangle\langle\psi|=\frac{1}{2}(1_{2\times2}+\vec{r}\cdot\vec{\sigma}),\quad \mathrm{tr}\rho=1$. From (16a) we get (16b), the vector for the radius in spherical coordinates, and with σ_i as the Pauli matrices.

For a spin ½ 2-state quantum system (qubit), the quantum state is $\psi=c_0|0\rangle+c_1|1\rangle$, c_0 and c_1 are complex numbers in Hilbert space and ψ is the norm:

$$\|\psi\|^2\equiv\psi^*\psi=|c_0|^2+|c_1|^2=1,\quad c_0,c_1\in\mathbb{C}. \tag{17}$$

A qubit state is considered a superposition of the two usual logical bit states, False, True or 0,1 with complex coefficients described by a ray in complex Hilbert space or as a complex projective space, $\mathbb{C}P\sim\mathbb{C}\cup\{\infty\}$. Every ray ($c_0$, c_1) is represented by the complex number, $\xi=c_0/c_1$ where the $|0\rangle$ corresponds to 0 and the $|1\rangle$ to ∞ on opposite poles of the Bloch sphere. The plane, ξ and the 2-sphere, S make correspondence because of stereographic projection, $\xi=(x-iy)/(1-z)$ [110].

Coordinates (x,y,z) are represented on the unit 2-sphere as:

$$x=\frac{2\,\mathrm{Re}\,\xi}{|\xi|^2+1}=\frac{c_0\overline{c_1}+c_1\overline{c_0}}{c_0\overline{c_0}+c_1\overline{c_1}},\quad -y=\frac{2\,\mathrm{Im}\,\xi}{|\xi|^2+1}=\frac{-i(c_0\overline{c_1}-c_1\overline{c_0})}{c_0\overline{c_0}+c_1\overline{c_1}},\quad z=\frac{|\xi|^2-1}{|\xi|^2+1}=\frac{c_0\overline{c_0}-c_1\overline{c_1}}{c_0\overline{c_0}+c_1\overline{c_1}} \tag{18}$$

Because of (17) this can be simplified to (X,Y,Z) instead:

$$X=c_0\overline{c_1}+c_1\overline{c_0},\ Y=i(c_0\overline{c_1}-c_1\overline{c_0}),\ Z=c_0\overline{c_0}-c_1\overline{c_1}. \tag{19}$$

In terms of group theory, the 2D complex Hilbert space, $H=\mathbb{C}^2$ for the qubit is a 2-spinor representation of the $G=SU(2)$ Lie group, a double cover of the 3D rotation group $SO(3)$ [109]. State transformation from spatial rotation of the coordinate system can be described by a unitary matrix

$$\psi'=\begin{bmatrix}a & b\\ c & d\end{bmatrix}\psi,\qquad \begin{matrix}\overline{a}=d,\ \overline{c}=-b\\ ad-bc=|a|^2+|b|^2=1.\end{matrix} \tag{20a,b}$$

This is the $SU(2)$ group of unitary 2 x 2 matrices corresponding to the principle that transformation of the wave vector is described by a group coordinate transformation. The $SU(2)$ group represents the $SO(3)$ group of spatial rotations in a 2D complex vector space, where due to 2-1 $SU(2)$ and $SO(3)$ isomorphism any rotation corresponds to a unitary matrix up to sign allowing transition to other coordinate systems [110]. The $SO(3)$ $SU(2)$ relationship is shown by (18). Applying a unitary transformation (19) gives $U:(c_0,c_1)\to(c'_0,c'_1)$ such that

$$X^2+Y^2+Z^2=\left(|c_0|^2+|c_1|^2\right)^2. \tag{21}$$

The angles between vectors do not change; These unitary qubit state transformations correspond to rotations of a sphere; and the two matrices U and $-U$ produce the same rotation because of (18) [110].

5.1 Case for Relativistic Information Processing – Relativistic R-Qubit

Here we describe steps for merging Relativistic Quantum Field Theory (RQFT) with the theory of computation. One must consider transformation of a qubit state due to rotation, boost and translation of the coordinate system. The $SL(2,\mathbb{C})$ Lorentz transformation is considered. New properties of this transform suggest the usual Riemann Bloch 2-sphere model of the qubit must be changed. For RQFT it is necessary to consider qubits in different coordinates. The simplest case may be 3D local rotations and SU(2) spinors. In considering temporal coordinates, it is necessary to use Lorentz transformations and 4D spinors. The best approach needs to include a full Poincairé group of transformations plus RQFT. Also, in order to meet the penultimate requirement of surmounting uncertainty and supervening decoherence, a new set of HD unified field mechanical (UFM) transformations is introduced. The UFM transform likewise obviates no-cloning and quantum erasure theorems.

Quantum theory, relativity and Shannon's information theory are inseparably connected [111,112]. The speed of transmission of information signals has been bounded by the velocity of light (standard model only). Because information requires a material carrier obeying the laws of physics, Landauer proposed that information is physical [113].

In the conventional consideration of quantum computing a quantum bit or qubit is any 2-state quantum system defined as a superposition of two logical states of a usual bit with complex coefficients that can be mapped to the Riemann Bloch sphere by stereographic projection. Geometrically, stereographic projection is a mapping projecting each point on a sphere onto a tangent plane along a straight line from the antipode of the point of tangency, with the exception that the center of projection, is not projected to any point in the Euclidean plane; but corresponds to a *point at infinity*.

Formally a qubit is represented as: $\Psi = \xi|0\rangle + \eta|1\rangle$ with each ray $\xi,\eta \in C$ in complex Hilbert space and $\|\Psi\|^2 = \xi\overline{\xi} + \eta\overline{\eta} = 1$, where $|0\rangle$ corresponds to the south or 0 pole of the Riemann sphere and $|1\rangle$ corresponds to the opposite, north or ∞ pole of the Riemann complex sphere. The conventional (non-relativistic) qubit maps to the complex plane of the Riemann Bloch sphere in Hilbert space as:

$$\xi\overline{\eta} + \eta\overline{\xi} \to X, \quad \xi\overline{\eta} - \eta\overline{\xi} \to iY, \quad \xi\overline{\xi} - \eta\overline{\eta} \to Z\,. \tag{22}$$

By introducing parity to the spinor representations, the generators **K** change sign because they act as vectors but the generators **J** do not because they act as axial vectors or pseudo-vectors. Thus, under parity, (j,0) and (0, j) interchange accordingly giving $\xi \leftrightarrow \eta$ under parity operations, implying that extending the Lorentz group by parity can no longer be described by the 2-spinor representations; and we must introduce the 4-spinor representation. Following Vlasov and Yeh [114,115], massive spin ½ particles such as an electron, e^- or neutrino, $\nu_e, \nu_\mu, \nu_\tau, \overline{\nu}_e, \overline{\nu}_\mu, \overline{\nu}_\tau$ for example, are described by two Weyl spinors with four complex components:

$$\psi \equiv \begin{pmatrix} \xi \\ \eta \end{pmatrix} = \begin{pmatrix} \varphi R \\ \varphi L \end{pmatrix} \varphi R, \varphi L \in \mathbb{C}^2; \quad \psi = \begin{pmatrix} \psi_0 \\ \psi_1 \\ \psi_2 \\ \psi_3 \end{pmatrix} \tag{23}$$

which can be considered as two qubits, $\psi = c_{00}|00\rangle + c_{01}|01\rangle + c_{10}|10\rangle + c_{11}|11\rangle$. For each $\varphi R, \varphi L$ the first index is like $|\uparrow\rangle$ and $|\downarrow\rangle$; and the second index corresponds to discretized coordinate transformations such as spatial reflection, $P:(t,\vec{x}) \to (t,) - \vec{x}$ [115,116]. The 4 x 4 Dirac matrices, γ^μ

can also be used, $j^{\mu} = \psi^{*}\gamma^{0}\gamma^{\mu}\psi$ which is always positive for $j^{0} = \psi^{*}\psi = \sum_{i}|\psi_{i}|^{2} = \|\varphi R\|^{2} + \|\varphi L\|^{2}$, but j^{0} is not Lorentz invariant. The Lorentz invariant scalar is, $\psi^{*}\gamma^{0}\psi = \varphi^{*}R\varphi L + \varphi^{*}L\varphi R$ [116].

Unitary transformations of a standard qubit correspond to 3D rotations of the Riemann Bloch sphere. Following Vlasov [110,115] for relativistic consideration of a qubit (r-qubit) an additional 4D parameter is added to equation (22): $\xi\overline{\eta} + \eta\overline{\xi} \to X,\ \xi\overline{\eta} - \eta\overline{\xi} \to iY,\ \xi\overline{\xi} - \eta\overline{\eta} \to Z,\ \xi\overline{\xi} + \eta\overline{\eta} \to T$.

Unitary representations preserve transition probabilities between two eigenstates measured in different reference frames; but the irreducible spinor representation of the Lorentz group is not unitary because the Lorentz group is not compact since the Lorentz boost takes on values along an open line from 0 to 1, unlike the rotation group where the angle extends from $\theta = 0$ to 2π. Thus the true symmetry group for particles is not the homogeneous Lorentz group; but a symmetry group with translations in spacetime in addition to Lorentz boosts and rotations. This group is the inhomogeneous Lorentz group, or Poincairé group. The generator of spacetime translation, P_{μ} is given by the transformation: $x^{\mu} \to x'^{\mu} = x^{\mu} + a^{\mu},$ and $P_{\mu} = i\frac{\partial}{\partial x^{\mu}}$.

There are 4 translation generators in the Poincairé group, in addition to 3 generators for Lorentz boosts and 3 for rotations. Totaling 10 generators in the Poincairé group. The rank 2 Poincairé group has only two invariants that commute with all generators; these are the Casimir invariants or operators, C_1 associated with mass invariance and C_2 for spin invariance [114].

Detailed analysis of quantum information processing suggested that the whole basis of quantum information theory itself required reassessment. Now finally, in the last couple of years numerous papers on relativistic computing have appeared [116-119].

We will briefly review and contrast some of these ideas [115-124].

The acquisition of information from a quantum system is at the interface of classical and quantum physics [111]. This type of measurement occurs at the semi-classical limit, wherein quantum information processing has remained stuck at a few qubits hampered by decoherence. Increasing capacity requires another form of data acquisition occurring instead at a 'semi-quantum limit'; thus it is postulated that usual theories of computation need to be merged not just with Relativistic Quantum Field Theory (RQFT) and Topological Quantum Field Theory (TQFT) but must also take an additional step. We know now that both RQFT and TQFT are required; we believe that a relativistic topological quantum field theory, if such is possible, is not the answer. We also know that to perform UQC, information theory needs to be extended not only to the 4D Poincairé group, but also into the HD realm of the 3rd regime of UFM [13,43,125]. In [12] we outline a nascent 'Ontological-Phase Topological Field Theory' (OPTFT) to address the brane dynamics of the unified field.

A TQFT computes topological invariants (topological space remains unchanged when transforms are applied to an object under homeomorphisms). A topological isomorphism is a continuous function between topological spaces that has a continuous inverse function. Homeomorphisms are the isomorphisms in the category of topological spaces, that is, they are the mappings that preserve all the topological properties of a given space. Two spaces with a homeomorphism between them are called homeomorphic, and from a topological viewpoint they are the same space.

Assuming quantum field theory is a necessity for a consistent description of quantum interactions; suggests current concepts in quantum information theory likely require reassessment and will need to be brought in line with a relativistic quantum informational theory before quantum computation can be fully realized. New properties of this transformation also require a change in the usual model of a qubit. We agree with the assessment given by Perez 'Most of the current concepts in quantum information theory may then require a reassessment' [111]. Information needs a material carrier, and the latter must obey the laws of physics. Information is physical [112,113].

Relativistic kinematics is all about information transfer between observers in relative motion. Quantum mechanics texts tell us that observable quantities are represented by Hermitian operators,

$\int_{-\infty}^{\infty} \Psi^* \Psi d\tau \equiv \langle \Psi | \Psi \rangle$ in integral and Dirac notation respectively. Their possible values are the eigenvalues of these operators, and that the probability of detecting eigenvalue, λn corresponding to eigenvector, $\mu\nu$ is $\langle \mu\nu | \Psi \rangle^2$, where Ψ is the pure state of the quantum system observed. If mixed states are included, the probability can be generally written, $\langle \mu\nu | \rho | \mu\nu \rangle$, where ρ is a mathematical expression that encodes information about measurements. *This is nice and neat, but this does not describe what happens in real life. Quantum phenomena do not occur in a Hilbert space; they occur in a laboratory. If you visit a real laboratory, you will never find there Hermitian operators* [111].

Drell pointedly asked *When is a particle?* [126]. A wave function is not defined in spacetime, but in a multidimensional mathematical representation called Hilbert space. It has become necessary to physicalize quantum information processing to an actual real multidimensional space.

Dirac wrote *a measurement always causes the system to jump into an eigenstate of the dynamical variable being measured* [127]. Collapse of the wavefunction 'happens' in our description of the system, not to the system itself. Von Neumann also 'speculated' that the final step involves the consciousness of the observer [128].

Another consequence is a change of the environment in which the quantum system evolves after completion of an intervention. For example, the measuring apparatus can generate a new Hamiltonian which depends on the recorded result. Classical signals may be emitted for controlling the execution of further interventions. These signals are of course limited to the velocity of light (until now). These interventions, as defined above, start by an interaction with a measuring apparatus [111]. Following Peres, the quantum system and the apparatus are initially in a state, $\sum_s c_s |s\rangle \otimes |A\rangle$, and become entangled into a single composite system *C*: $\sum_s c_s |s\rangle \otimes |A\rangle \rightarrow \sum_{s,\lambda} c_s U_{s\lambda} |\lambda\rangle$, where $\{|\lambda\rangle\}$ is a complete basis for the states of *C*. It is the choice of the unitary matrix, $U_{s\lambda}$ that determines which property of the system under study is correlated to the apparatus, and therefore is measured. An essential property of the composite system *C*, which is necessary to produce a meaningful measurement, is that its states form a finite number of orthogonal subspaces which are distinguishable by the observer [111].

Up to now, the quantum evolution is well defined and is in principle reversible. It would remain so if the environment *could be perfectly isolated from the macroscopic degrees of freedom of the apparatus ... This demand is of course self-contradictory, since we have to read the result of the measurement if we wish to make any use of it* [113]. States of the environment that are correlated to subspaces of *C* with different labels, μ can be treated as if they were orthogonal [111].

To become fully relativistic, the conception of intervention needs refinement. The precise location of an intervention is important in a relativistic information process. It is the point from which classical information is sent that can affect the input of other interventions. A simpler case of space-like separated interventions, amenable to complete analysis, is Bohm's version of the EPR paradox with two coordinate systems in relative motion [111]. Such phenomena are often attributed to quantum nonlocality and the possibility of superluminal or rather instantaneous communication. Herbert's proposal on this matter [129] led to the discovery of the no-cloning theorem [130,131]. Note: We will address this issue later; surmounting uncertainty also obviates the no-cloning and quantum non-copying theorems.

Bell's theorem asserts that it is impossible to mimic quantum theory by introducing a set of objective *local hidden variables* so that any classical imitation of quantum mechanics must be nonlocal. But there is no inherent suggestion for the existence of nonlocality in Bell's theorem.

Importantly, RQFT is manifestly local. Peres states 'the obvious fact is that information must be carried by material objects, quantized or not' [111]. Therefore, quantum measurements do not allow any information to be transmitted faster than the characteristic velocity that appears in the Green's functions of the particles emitted in the experiment. In a Lorentz invariant theory, this limit is the velocity of light. Relativistic causality cannot be violated by quantum measurements. The only physical assumption

needed to prove this is that Lorentz transformations of spacetime coordinates are implemented in quantum theory by unitary transformations of operators [111]. This is the same as saying that the Lorentz group is a valid symmetry of the physical system [132].

5.2 The Dynamics of Topological Phase Transitions

To show further insight into operating a DEB device with a UFM based UQC requires additional description of topological phase transitions in the bulk. To climb the dimensional ladder, we start with the 3-space of observation. The central vertices in Fig. 23a are ambiguous and may topologically switch. We can consider this as a nilpotent space-antispace *zitterbewegung*.

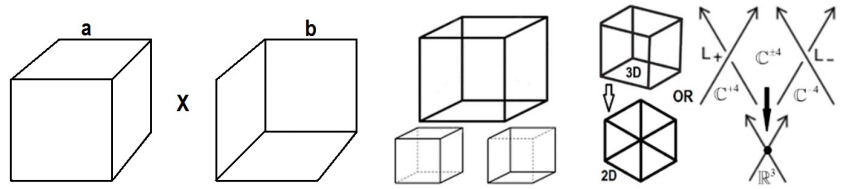

Figure 24. Ambiguous Necker cubes. a) Visual test of stereoscopic Necker construction (cross eyes to see the two states merge, L – R mirror images merge). b) Two topological states of the Necker cube. c) 3D cube to 2D hexagon. d) knot crossing shadow, HD to 3D vertex.

Quaternions have the ability to represent rotations of 3D space. If we represent 3-space, $\mathbb{R}^3$ as the set of pure quaternions of the form $\mathbb{Z} = ai + bj + ck$ with *a, b, c* real numbers, then *g* is a unit quaternion mapping $\rho : \mathbb{R}^3 \to \mathbb{R}^3$ defined by the equation $\rho(\mathbb{Z}) = g\mathbb{Z}g^{-1}$ describes a 3-space rotation by angle θ around axis μ when $g = \cos(\theta/2) + \sin(\theta/2)\mu.$

In this manner, μ is a unit length quaternion giving a direction to a vector in 3-space, a rotation is specified by an angle θ about an axis *U*, which in the case below is in the positive direction [133].

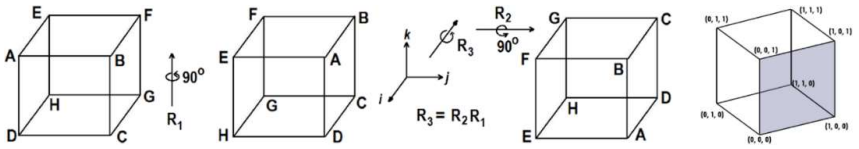

Figure 25. Denoting two 90° rotations R_1 and R_2, we write $R_3 = R_2R_1$ for the rotation obtained by 1st performing R_1 and then R_2. R_3 fixes the corners B and H; Thus, R_3 is a 120° rotation about the diagonal axis. A first step towards physicality might be distinguishing the vertices.

Thus, following Kauffman [133],

$$e^{j(\pi/4)}e^{k(\pi/4)} = \left(\frac{\sqrt{2}}{2} + j\frac{\sqrt{2}}{2}\right)\left(\frac{\sqrt{2}}{2} + k\frac{\sqrt{2}}{2}\right) = \frac{1}{2}(1+j)(1+k) = \frac{1}{2}(1+j+k+jk) =$$

$$\frac{1}{2}(1+i+j+k) = \frac{1}{2} + \frac{\sqrt{3}}{2}\left(\frac{i+j+k}{\sqrt{3}}\right) \quad \therefore \; e^{j(\pi/4)}e^{k(\pi/4)} = e^{\lceil (i+j+k)/\sqrt{3} \rceil [2\pi/3]/2}$$

$$\uparrow \qquad \uparrow$$

diagonal axis 120°.

These quaternion rotations can be considered phase changes under certain conditions; but they do not correspond to the ontological phase we are looking for because Euclidean geometry has no natural

inherent perspective. It appears we need a duo-morphic projection perhaps involving Berry phase because the ambiguous vertices of the Necker cube are not distinguished in Kauffman's quaternion rotation system [133].

If we consider this quantum mechanically, only one *zitterbewegung* element exists at a time, with the other 90º out of phase and thus invisible; we have only used 3 dimensions. If we next embed this quaternionic description in an Octonion manifold we have the topology of fig. 25.

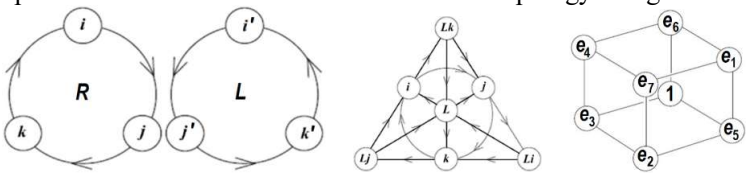

Figure 26. a) L-R space-antispace quaternion mirror symmetry. b) Embedding the quaternion cycles in the Octonionic Fano plane. c) Cubic illustration of the Octonion algebra.

6. Ontological-phase topological field theory (OPTFT)

Topological switching – key to ontological-phase. The 2-state formalism currently forms the basis of QC. Qubits, are 2-state systems. Any QC operation is a unitary operation that rotates the state vector on the Bloch sphere. To move from Hilbert space to ontological-phase space we must begin to define what we mean by topological switching [43,98,134]. We begin with a number of ways of looking at the ambiguous Necker cube [135].

To clarify how projective transformations lose orientable information, rotating a triangle in a plane is used as an illustration [136].

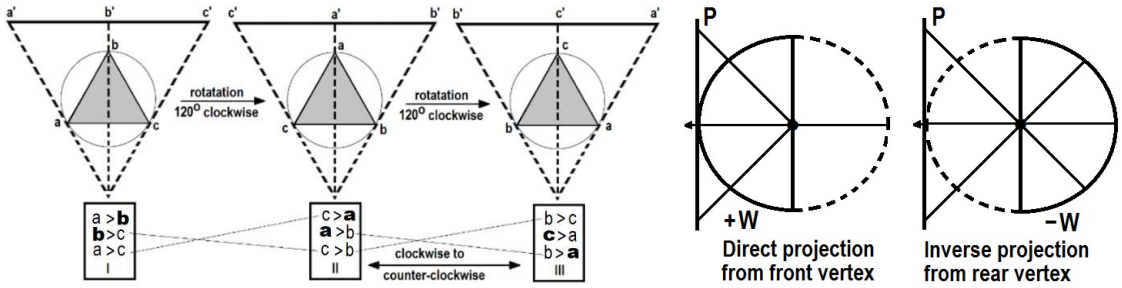

Figure 27. a) Removing ambiguity from a projected rotation, with > denoting order of sequence occurrence – to the left on the projective line. **Bold** letters are the front range of projective mapping. Fig. redrawn from [136]. b) Duo-morphic oriented projections (+W, -W) yield a double covering of the projective plane, P.

The rotation sequences in Fig. 26a are I, II, III for clockwise and I, III, II for counter-clockwise. According to Shaw the direction of rotation reverses if the back and front ranges are interchanged. This is denoted by the connecting lines in the boxes below the rotation triangles. **Bold** letters mark the front range; this system is able to preserve orientation information under projected rotation.

The 3D wire-frame Necker cube can be projected onto a 2D surface, collapsing the cubes six faces into a complex of one to seven coplanar polygons depending on orientation of the cube.

To distinguish front and back ambiguous vertices of the Necker cube is a problem of orientation. Oriented projective geometry introduces a methodology for distinguishing the ambiguous vertices of the Necker cube [136]. Shaw [137] assigns a dual range, +W and -W to represent front and rear ranges of a sphere.

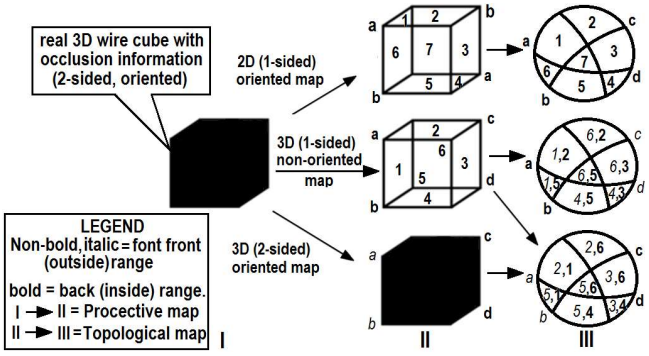

Figure 28. Contrasting nonoriented - oriented projective geometries. Redrawn from [37].

Figure 28 illustrates three different forms of projection.

- $\mathrm{I} \rightarrow$ II-Top $\rightarrow$ III-Top: no occlusion information
- $\mathrm{I} \rightarrow$ II-Middle $\rightarrow$ III-Middle and III-Bottom: occlusion information is specified ambiguously
- $\mathrm{I} \rightarrow$ II-Bottom $\rightarrow$ III-Bottom: occlusion information is specified unambiguously.

The Necker cube, like the Möbius strip is an ambiguous figure because of the problem of projective mapping. In ordinary projective space, the Möbius strip and Necker cube, are one-sided. The spherical model of this geometry represents the fact that the projections of a point on the back of the sphere and of a point on its front both have the same image in the Euclidean (projective) plane. All of the projected points, regardless of the hemisphere to which they belong, cover the projective plane in the usual way without any designation of where they originated. The loss of orientation is due to this failure of the projective mapping to preserve a distinction between front and back range, collapsing both into positive values of the dimension of depth *w*. This loss of orientation is represented by the fact that relationships (e.g., the arrows) invert when the projective angle passes through the points at infinity [136].

To keep the front and back ranges distinguished, traditional computational geometries use the line at infinity as a reference; but this move is not a real solution to the orientation problem in projective geometry because it is tantamount to a return to Euclidean geometry with no inherent natural perspective.

Figures 24 and 25 separate the ambiguous Necker cube into its component perspectives. Although what we are about to illustrate is usually considered a mental construct, we use it here to illustrate what we mean by ontological phase and an ontological phase transformation. Focus on the 'X' halfway between the 2D L-R Necker perspectives; relax one's eyes and allow them to lose focus and cross. Soon, a 3rd image appears between the two printed L-R images fusing the original perspective into one apparent 3D image, confirmed by noticing the labels 'a' and 'b' are now superposed. This stereoscopic condition is the scenario we want to utilize to define ontological-phase.

Masahide & Satoh generalize the class of roll-spun knots for 2-knot theory and show how to calculate the quandle cocycle invariant for any roll-spun knot [138]. For the case $X = S_4 = \mathbb{Z}\left[t, t^{-1}\right] / \left(2, t^2 + t + 1\right)$, the element $w = 1 \cdot t^{-1} \cdot 0 \cdot (t+1)^{-1}$ satisfies $\varphi_w = \mathrm{id}_{S4}$; such that

$$\begin{array}{cccccc} 0 & \xrightarrow{\varphi_1} t+1 & \xrightarrow{\varphi_t^{-1}} 1 & \xrightarrow{\varphi_0} t & \xrightarrow{\varphi_{t+1}^{-1}} 0 \\ 1 & \mapsto 1 & \mapsto 0 & \mapsto 0 & \mapsto 1 \\ t & \mapsto 0 & \mapsto t+1 & \mapsto 1 & \mapsto t \\ t+1 & \mapsto t & \mapsto t & \mapsto t+1 & \mapsto t+1. \end{array} \tag{24}$$

Since $\mathrm{ind}(w) = 0,$ it holds that $w \in G_0(S_4),$ showing that $w^2 = 1$ in $\mathbf{G}_0(S_4)$, and that w is the generator of $G_0(S_4) \cong \mathbb{Z}_2$.

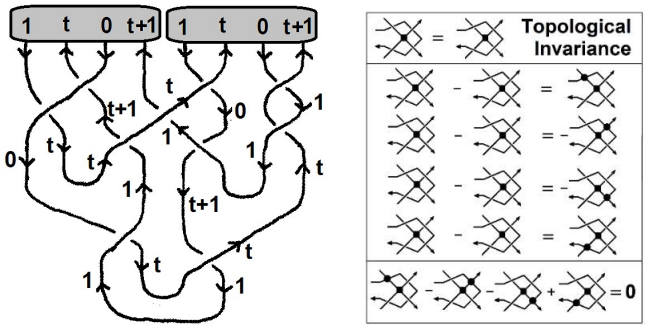

Figure 29. a) Deform-spun knot tangle diagram. Redrawn from [138]. b) Topological Invariance must be included in any phase labeling. Figure redrawn from [139].

The spun knot is explored as a possible component topological move for ontological-phase transitions. When parallel transport creates a deficit angle in brane raising and lowering dynamics, in addition to Reidemeister moves, rotations, reflections and any other topological moves, spun knot components may add another type of phase transition with lattice charge. A Rolling spun knot topology may be infused with topological charge by a phase transitions related to UFM 'force of coherence' which drives evolution throughout the multidimensional brane hierarchy allowing multiple types of moves to occur at multiple levels simultaneously.

An important feature of TQFTs is that they do not presume a fixed topology for space or spacetime. In other words, when dealing with an *n*-dimensional TQFT, one is free to choose any (*n* - 1)-dimensional manifold to represent space at a given time. Moreover, given two such manifolds, say S and S', one is free to choose any *n*D manifold M to represent the portion of spacetime between S and S'. Mathematicians call M a 'cobordism' from S to S'. We write $M : S \to S'$, because we may think of M as the process of time passing from the moment S to the moment S'.

There are various important operations one can perform on cobordisms, but we only describe two. First, we may 'compose' two cobordisms $M : S \to S'$ and $M : S' \to S''$, obtaining a cobordism $M'M : S \to S''$, as illustrated in Fig. 29. The idea here is that the passage of time corresponding to M followed by the passage of time corresponding to M' equals the passage of time corresponding to $M'M$. This is analogous to the familiar idea that waiting t seconds followed by waiting t' seconds is the same as waiting $t + t'$ seconds. The big difference is that in topological quantum field theory we cannot measure time in seconds, because there is no background metric available to let us count the passage of time! We can only keep track of topology change. Just as ordinary addition is associative, composition of cobordisms satisfies the associative law: $(M''M')M = M''(M'M)$. However, composition of cobordisms is not commutative. As we shall see, this is related to the famous noncommutativity of observables in quantum theory [140].

Second, for any (n–1)D manifold S representing space, there is a cobordism $1_S : S \to S$ called the `identity' cobordism, which represents a passage of time without topological change. For example, when S is a circle, the identity cobordism 1_S is a cylinder, as shown in Fig. 30 In general, the identity cobordism 1_S has the property that for any cobordism $M : S' \to S$ we have $1_S M = M$, while for any cobordism $M : S \to S'$ we have $M1_S = \boldsymbol{M}$ [140].

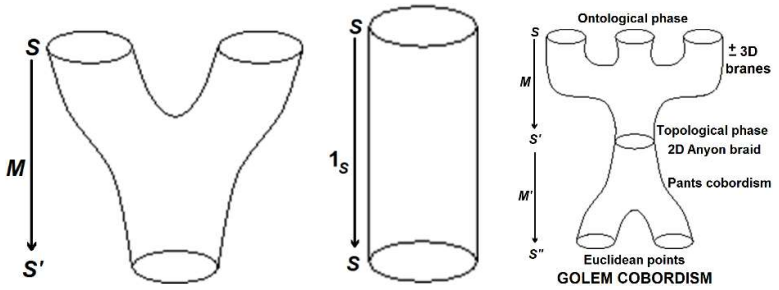

Figure 30. a) Basic cobordism. b) Identity cobordism. c) The Golem, composition of cobordisms designed to handle M-theoretic ontological-phase transitions in the bulk.

For example, Fig. 29b depicts a 2D manifold *M* going from a 1D manifold *S* (a pair of circles) to a 1D manifold S' (single circle). Crudely speaking, *M* represents a process in which two separate spaces collide to form a single one! Baez says: *This may seem outré, but currently physicists are quite willing to speculate about processes in which the topology of space changes with the passage of time* [140].

These properties say an identity cobordism is analogous to waiting 0 seconds: if you wait 0 seconds and then wait *t* more seconds, or wait *t* seconds and then wait 0 more seconds, this is the same as waiting *t* seconds. These operations just formalize the notion of *the passage of time* in a context where the topology of spacetime is arbitrary with no background metric. Atiyah's axioms relate this notion to quantum theory as follows. First, a TQFT must assign a Hilbert space *Z*(*S*) to each (n – 1)D manifold *S*. Vectors in this Hilbert space represent possible states of the universe given that space is the manifold *S*. Second, the TQFT must assign a linear operator $Z(M): Z(S) \to Z(S')$ to each *n*D cobordism $M: S \to S'$. This operator describes how states change given that the portion of spacetime between S and S' is the manifold *M*. In other words, if space is initially the manifold S and the state of the universe is ψ, after the passage of time corresponding to *M* the state of the universe is $Z(M)\psi$ [140].

TQFTs must satisfy a list of properties. Let's mention two. First, a TQFT must preserve composition. That is, given cobordisms $M: S \to S'$ and $M': S' \to S''$, we must have $Z(M'M) = Z(M')Z(M)$, where the right-hand side denotes the composite of the operators $Z(M)$ and $Z(M')$. Second, it must preserve identities. That is, given any manifold S representing space, we must have $Z(1_S) = 1_{Z(S)}$, where the right-hand side denotes the identity operator on the Hilbert space *Z*(*S*) [140].

Both these axioms are eminently reasonable if one ponders them a bit. The first says that the passage of time corresponding to the cobordism *M* followed by the passage of time corresponding to M' has the same effect on a state as the combined passage of time corresponding to $M'M$. The second says that a passage of time in which no topology change occurs has no effect at all on the state of the universe. This seems paradoxical at first, since it seems we regularly observe things happening even in the absence of topology change. However, this paradox is easily resolved: a TQFT describes a world quite unlike ours, one without local degrees of freedom. In such a world, nothing local happens, so the state of the universe can only change when the topology of space itself changes [141].

The most interesting thing about the TQFT axioms is their common formal character. Loosely speaking, they all say that a TQFT maps structures in differential topology (study of manifolds) to corresponding structures in quantum theory. In coming up with these axioms, Atiyah took advantage of a powerful analogy between differential topology and quantum theory, summarized in Table 2 [140].

This analogy between differential topology and quantum theory the sort of clue we should pursue for a deeper understanding of quantum gravity. At first glance, general relativity and quantum theory look very different mathematically: one deals with space and spacetime, the other with Hilbert spaces and operators. Combining them has always seemed a bit like mixing oil and water. But topological quantum field theory suggests that perhaps they are not so different after all! Even better, it suggests a concrete

program of synthesizing the two, which many mathematical physicists are currently pursuing. Sometimes this goes by the name of `quantum topology' [142,143].

DIFFERENTIAL TOPOLOGY	QUANTUM THEORY
(n – 1)-dimensional manifold (space)	Hilbert space (states)
cobordism between (n – 1)-dimensional manifolds (spacetime)	operator (process)
composition of cobordisms	composition of operators
identity cobordism	identity operator

Table 2. Analogy between differential topology and quantum theory.

Quantum topology is very technical, as anything involving mathematical physicists inevitably becomes. But if we stand back a moment, it should be perfectly obvious that differential topology and quantum theory must merge if we are to understand background-free quantum field theories. In physics that ignores general relativity, we treat space as a background on which states of the world are displayed. Similarly, we treat spacetime as a background on which the process of change occurs. But these are idealizations which we must overcome in a background-free theory. In fact, the concepts of *space* and *state* are two aspects of a unified whole; likewise for concepts of *spacetime* and *process*. It is a challenge, not just for mathematical physicists, but also for philosophers, to understand this more deeply [140].

We begin to explore various types of crossover links and moves to start cataloguing the variety of moves that maybe applicable to ontological-phase transitions.

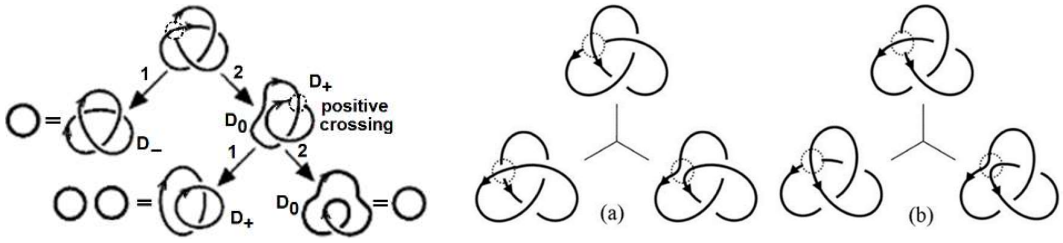

Figure 31. a) Crossings for octonion trefoil knots**.** b) Reduction schemes for L- and R-handed trefoil knots. b-a) Top: L-handed trefoil knot; bottom: writhe γ_- and a Hopf link H_-, with crossing −1. b-b) Top: R-handed trefoil knot; bottom: writhe γ_+ and a Hopf link H_+, with crossing +1. The two knots are mirror images of one another. Figure adapted from [144].

Thus, a true octonion contains three trefoil knots, whereas a split octonion may be specified by mixing a pair of quaternion trefoil lines. To define a tripled Fano plane requires three copies of Furey's particle zoo. It describes a set of 21 = 3 x 7 (left cyclic) modules over a noncommutative ring on eight elements. The ring is given by the upper triangular 2 x 2 matrices over the field with two elements. Similarly, for right cyclic modules [145,146].

The quaternions, *H* are a 4D algebra with basis $1, i, j, k$. To describe the product, it is easy to note: 1 is the multiplicative identity, i, j, k are square roots of -1, we have $ij = k$, $ji = -k$ and all identities obtained from these by cyclic permutations of (i, j, k). We can summarize the last rule as a diagram.

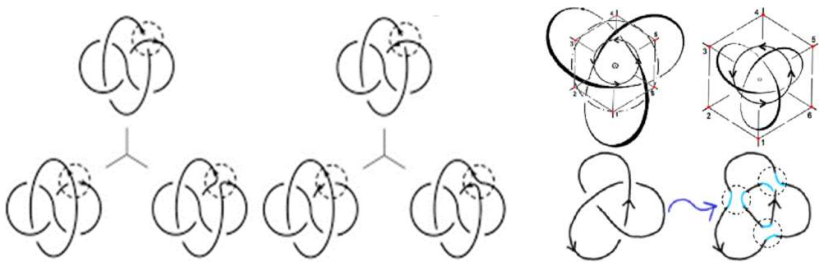

Figure 32. a) Reduction schemes for Whitehead links W_+ and W_-. (a-Top: Whitehead link W_+ with crossing +1; bottom: Hopf link H_- and the L-handed trefoil knot T^L. b) Whitehead link W_- with crossing −1; (b-bottom: Hopf link H_+, and a figure-eight knot F^8. Figure adapted from [144]. c) Top: Raising and lowering dynamics, c) Bottom: Additional topological moves.

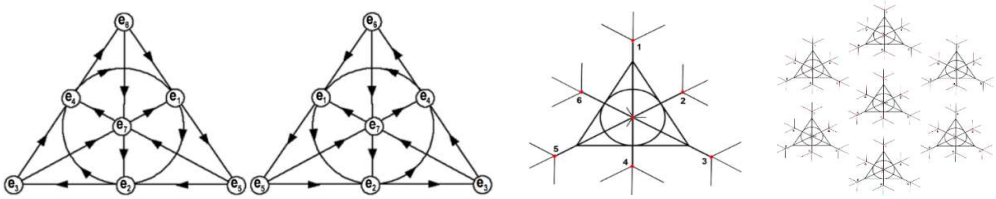

Figure 33. a) The Fano plane and its mirror image showing clockwise and counterclockwise rule for Octonion-Quaternion cyclicality. b) Fano plane with Fano snowflake antennae able to involute into hexagon/cube (Fig. 33 c-d) c) 3-cube vertices as Fano groups, another metaphor for LCU tessellation.

In multiplying two elements going clockwise around the circle we get the next one: for example, $ij = k$, but when we multiply two going around counterclockwise, we get *minus* the next one: for example, $ji = -k$. We can use the same sort of picture to remember how to multiply octonions: The Fano plane is the finite projective plane of order 2, having the smallest possible number of points and lines, 7 each, with 3 points on every line and 3 lines through every point. The Fano plane has 7 points and 7 lines. The 'lines' are the sides of the triangle, its altitudes, and the circle containing all the midpoints of the sides. Each pair of distinct points lies on a unique line. Each line contains three points, and each of these triples has a cyclic ordering shown by the arrows. If e_i, e_j, e_k are cyclically ordered in this way then $e_i e_j = e_k$, $e_j e_i = -e_k$.

Together with these rules: 1 is the multiplicative identity, $e_1, \ldots, e_7$ are square roots of -1, the Fano plane completely describes the algebra structure of the octonions. Index-doubling corresponds to rotating the picture a third of a turn. Interestingly, The Fano plane is the projective plane over the 2-element field $\mathbb{Z}_2$. In other words, it consists of lines through the origin in the vector space $\mathbb{Z}_2^3$. Since every such line contains a single nonzero element, we can also think of the Fano plane as consisting of the seven nonzero elements of $\mathbb{Z}_2^3$. If we think of the origin in $\mathbb{Z}_2^3$ as corresponding to $1 \in \mathrm{O}$, we get the following picture of the octonions:

Note that planes through the origin of this 3D vector space (Fig. 32a) give subalgebras of O isomorphic to the quaternions, lines through the origin give subalgebras isomorphic to the complex numbers, and the origin itself gives a subalgebra isomorphic to the real numbers [140].

Now we finally arrive at the fundamental geometric topology for describing ontological-phase topological field theory. When the formalism is next written it will be created by utilizing both topology

and complex quaternion/octonions Clifford algebra which is especially suited to handle the manifold embedding [147].

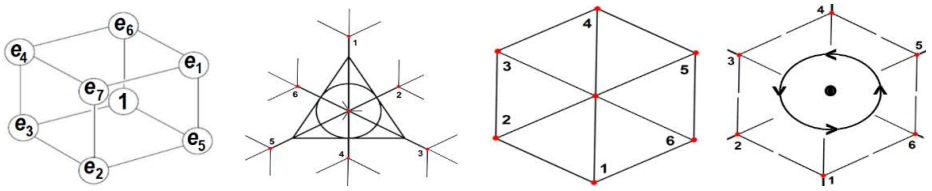

Figure 34. a) The octonions for $1 \in \mathrm{O}$ **.** b) Antennas (snowflakes) on a Fano plane represent vertices on the circumference of an involuted hexagon or cube c-d). The center rotates unconnected so position 1 or 2 can create the front/rear vertices of a Necker cube. c) Antennas 1-6 combine to form the outer vertices of a cube/hexagon depending on what dimensional phase the state is in. d) Rotations, as in Fig. 33a.

The Fano snowflake configuration in Fig. 33, 34b involutes to form a 2D hexagon or vertices of a Euclidean Necker 3-cube. We expect to require a dual set of twin Fano-Snowflakes as would be derived from Fig. 33b to account for all the parameters necessary for the antispace image of mirror image of the mirror image to be causally free of the Euclidean 3-space QED quantum state [12].

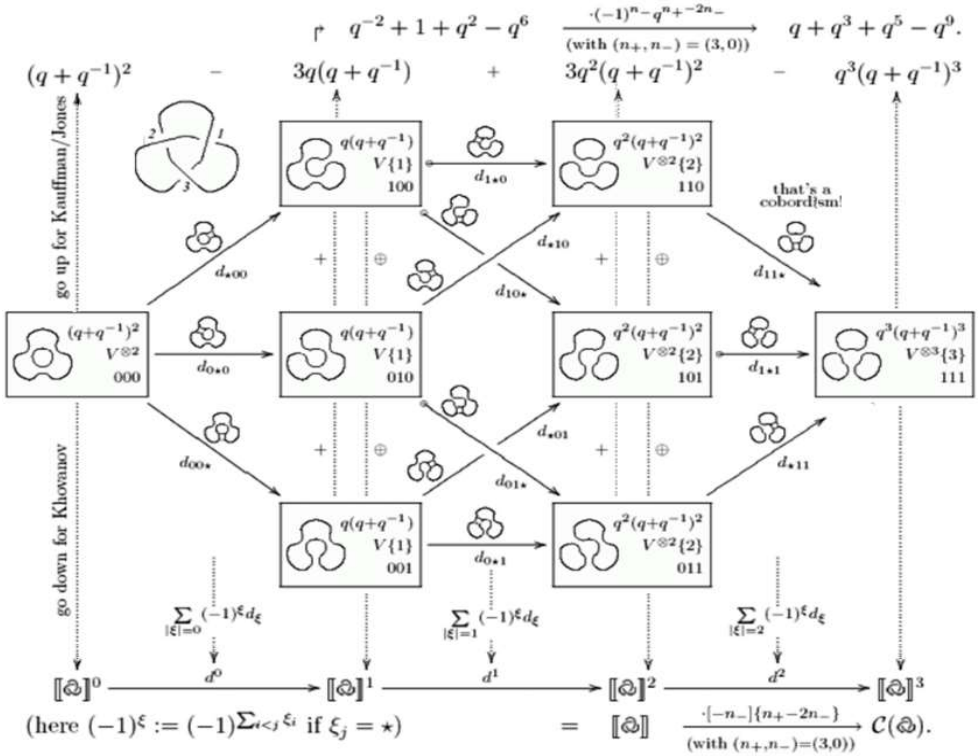

Figure 35. Construction to improve Khovanov's seminal work on the categorification of the Jones polynomial. Figure adapted from [148,149].

Some of the complexity for categorizing the Jones polynomial is shown in Figs.34 and 35 as it might apply to modeling ontological-phase.

A 3D topology approach, a new type of crossing (called virtual) is allowed, regarded as a *projection* of the knot theory in thickened surfaces Sg × R. Regarded from this point of view, virtual crossings appear as artifacts of the diagram projection from Sg to R^2 [150].

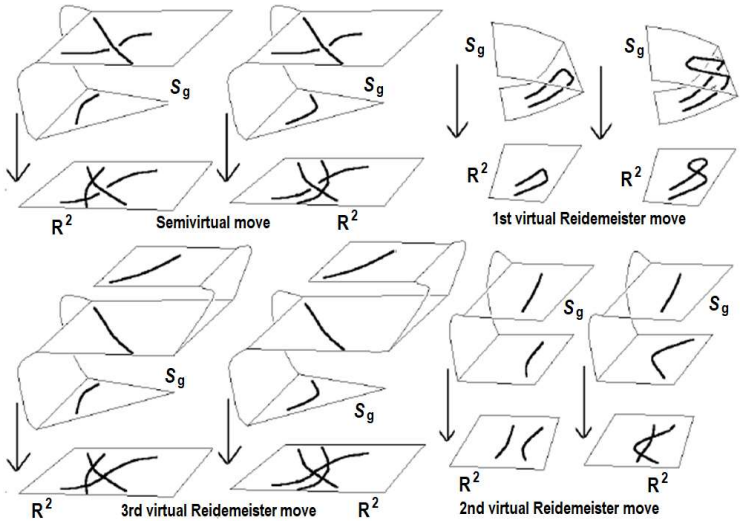

Figure 36. Generalized Reidemeister moves and topological surfaces. Fig. adapted from [150].

7. Ballistic conduction of vacuum energy with cyclical evanescent modes

Understanding ballistic conduction along a mean-free path is key to the utility of DEB technology. The purpose of the applied field, the driving force, is to manipulate the Dirac polarized vacuum with a Sagnac Effect incursive oscillator to surmount the uncertainty principle, only be discovered by experiment, that coherent emission is a naturally occurring factor inherent in the holophote propagation of the UF. This inherent synchronization backbone is like getting half the device for free - a gift of the universe. The emission cycle is hidden from utility by the uncertainty principle. The applied field must cyclically on the one hand, destructively interfere with the annihilation-creation modes and constructively interfere for summation of UF propagation for dioxygen dication subduction. To restate, the duality in LCU rotation creates a tuned phase alignment in parallel transport cycles along the Mean Free Path (MFP), with periodic ballistic alignment opening LSXD channels that are LCU exciplex pumping mechanisms that summate and collect UF topological charge along the coherence length of the array. The domain wall of the LCU cavity-QED is a static-dynamic Casimir hysteresis loop emission dynamic cycle with a beat frequency in the duality of the LCU structure, i.e. the semi-quantum finite radius manifold of uncertainty throat, and the nonlocal holographic instantaneity. It is important for the hysteresis noeon flux dynamic to have an exciplex substrate, for if the ground state cycled into the process, the uncertainty principle would block the OCHRE-OCRET DEB process.

Figure 37 models generalized exciplex hysteresis loops, mapped over an LCU Dirac vacuum array of programmable space-antispace coherence length as a variable emission power pumping factor.

The uncertainty principle has led to the erroneous conclusion that the Planck-scale QM stochastic foam is an absolute basement of reality, the result of empirical well-tested measurement. DEB operation does not take any form of measurement, it leaves Heisenberg potentia untouched, so in that since the Uncertainty Principle is nonexistent. What we are doing through a system of applied resonances is to interfere with UF flux into 3-space singularities (matter). It is a hidden evanescence driving the evolution of quantum systems nonlocally. If one drops a stone in a pool, one obtains ripples; dropping a series of stones with a beat frequency and a coherence length between them, produces modes of destructive and constructive interference.

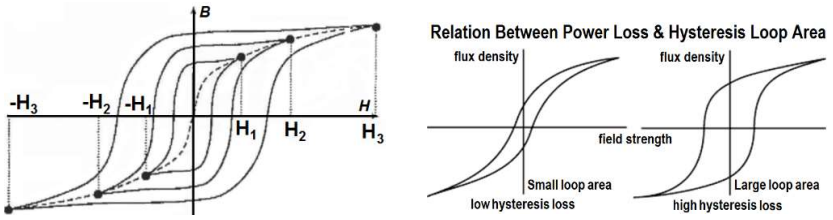

Figure 37. a) The charge characteristics of nested Hysteresis loops can be used as a method for modeling the cyclic cavity dynamics of fermionic space-antispace parameters. Our postulate is that the Dirac polarized vacuum can demonstrate hysteresis properties. b) We model our spacetime MOU QED cavity as a hysteresis loop of UFM charge. The cavity opens and closes; timing is crucial.

Instead of the usual consideration of the Bohr atom, imagine an atom in 3-space as a configuration of rosebuds *x,y,z* (Fig. 16). Then consider the rose in bloom in the HD M-theoretic brane topological bulk. Next, think of the Bohr rosebud as a superposition shadow or resultant of several roses in bloom along the *x,y,x,w* directions in the bulk, $\aleph = x, y, z, w.$ there is also a mirror symmetric copy, thus $\pm\aleph$, forming a complex 8-space. But the symmetry is more complex than this; it takes the form of a dual trefoil, this forming a 12-space. The 3rd lip of the trefoil forms a triune nilpotency with the other 2 lips. The system of rosebuds is best described by a space – antispace nilpotent quaternion-octonion algebra in spherical coordinates with correspondence to trigonometric functions of the Pythagorean theorem so phase angles can be more easily followed. The space antispace quaternion pair would be mapped onto a sphere. Extending the model, the q-spheres would comprise the center of an Octonions Fano plane (Figs. 26,33). Quaternions and Octonions have been suggested to be algebras that correlate with the natural world. If this is true, we may theorize that the structure of the Fano tetrahedron should offer much-needed restrictions to the transport of UF noeon energy through the Calabi-Yau rose petal florets.

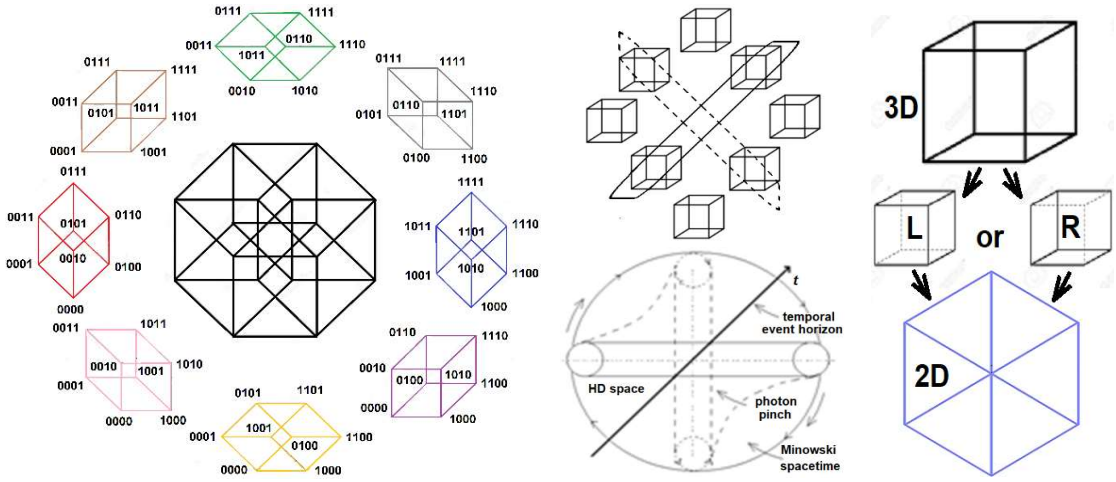

Figure 38. a) Exploded 4D hypercube, 64 overlapping vertices (4) or 16 subsets (16 x 4 = 64). b-top) Exciplex configuration of LCU array. One of four orthogonal configurations, with mirror symmetry another four. In terms of developing the required noetic transform, each 3-cube represents an ambiguous Necker cube able to perform topological raising and lowering moves. The four cubes illustrated have interplaying vertex points, dotted – 0101:1011 and 0100:1010; solid – 0110:1101 and 0010:1001. b-bottom) Conceptualized view of the HD quadrupole photon-vacuum complex for *quadrupole* ⇔ *dipole* interactions as elements of the UF at the event horizon of Minkowski spacetime. c) Dimensional reduction.

Quaternion space-antispace mirror symmetry notation, R) $\mathrm{H} = \{i, j, k\}$; L) $\hat{\mathrm{H}} = \{\hat{i}, \hat{j}, \hat{k}\}$ is said to describe the most fundamental physical object (fermion), that of the electron [17,67,68]. To embed the object within the Octonion Fano plane (HD space) is as follows. Firstly, the element L is added. $L^2 = -1,\ La = -aL,$ with $a \in \mathrm{H}$. Thus, $(La)(Lb) = ba,\ (La)b = L(ba),\ a(Lb) = L(ba).$ To integrate within the Octonion Fano plane (Figs. 26,33) we have, $(Lj)L = j,\ i(Lk) = L(ki),\ Li = Lj,$ $(Lj)i = L(ij) = Lki,\ (Lk)(Lj) = jk = i,$ with octonion inverses not shown. While the quaternionic $\pm x, y, z$ elements represent mirror symmetric nilpotent vertices, the octonionic topology (Figs. 26,33) renders the quaternion as wrapped on a sphere.

We are concerned with the boundary conditions in the region outside the event horizon, where r ≥ M/2 which are of conceptual interest even though here applied to a black hole because it might reflect scale invariant principles as authors such as Susskind propose.

The general scalar equation in spherical coordinates of wave motion in spacetime which has spherical symmetry [61,62]

$$\nabla^2\Phi - \frac{1}{c^2}\partial^2\frac{\Phi}{\partial t^2} = 0 \tag{25}$$

where Φ is the wave amplitude. The equation has two solutions

$$\Phi_{out} = \frac{1}{r}\Phi_{\max}\exp(i\omega t - ikr);\ \ \Phi_{in} = \frac{1}{r}\Phi_{\max}\exp(i\omega t + ikr) \tag{26}$$

which for the programming of spacetime can be applied to the propagation of Cramer's advanced retarded waves from an emission locus at $\pm x, t = 0, 0$ by Eqs. (26, 27) and Fig. 14.

$$F_{1-Ret} = F_0 e^{-ikx}e^{-2\pi ift},\ F_{2-Ret} = F_0 e^{ikx}e^{-2\pi ift},\ F_{3-Adv} = F_0 e^{-ikx}e^{2\pi ift},\ F_{4-Adv} = F_0 e^{ikx}e^{2\pi ift} \tag{27}$$

The development of laser theory occurred over several decades before a device was finally proposed. Prominent physicists at the time strongly claimed lasers were impossible as they would be a violation of the uncertainty principle. Copernicus waited until he was on his deathbed, and Galileo was nearly executed for similar promulgations. One must be allowed to theorize. Lasers provide a source of highly correlated energy at near 0 entropy, very effective for cooling close to absolute 0. In addition, laser traps are considered to have 0 temperature walls, generated with oscillations able to reach the quantum ground state. Recent generations of experiments allowed cryogenic temperatures of macroscopic objects. The efficiency of cycles per background (antispace) absorption can be tremendously increased using exciplex states, having a particular property of exhibiting a transitory (hysteresis) bound excited state

Elsewhere, we have derived an alternative to the energy of cosmological inflation [13]. Not re-claiming an Einstein static, Narlikar steady or quasi-steady state, but a continuous-state cosmology; where the energy given to expansion/inflation is internalized in each spatial LCU as if each fiducial was in gravitational freefall. Fortunately, a case can be made for this scenario to make correspondence with Mach's principles of inertia. Of note is that our derivation led to an alternative formulation of string tension which profoundly also led to a unique string background [12,13]. What do we get from this? Something profound relating to the nature of reality. Reality itself is like a 1st quantization (collapse) of the wave function of the universe, with virtual Planck-scale lower bound asymptotically only reaching the Larmor radius of the hydrogen atom (hidden by uncertainty) and an upper bound of the cosmological constant. Both oscillating ± 0. As an aside this makes dark matter/energy simply a weak causal connection of the rest of the multiverse. So, what we have is like a big drain, drawn by gravity from the bulk from the Hubble radius to the Planck scale. The synchronization backbone mediated by the UF is the energy stream that must be latched onto for DEB technologies. We have proposed that the UF is mediated by an ontological (energyless topological information transfer) dubbed the noeon. The other three force field are phenomenological mediated by quanta. Perhaps the noeon is small-scale ordering

the semi-quantum manifold of uncertainty; and it has a big brother, a large-scale conformal topological field, a realiton. Setting heresy aside for the time being; the point is that an inherent synchronization backbone of the UF is essential to DEB technology. Without it, there is no DEB technology.

Generally, Ballistic conduction or Ballistic transport occurs when the mean free path of the electron is significantly longer than the dimension of the medium through which the electron travels. Hence there is no chance of electrons collisions, and thus no energy dissipated during conduction. In contrast, Superconductivity is the result of a quantum mechanical effect that avoids the collision and scattering. In the superconductive state, all the mobile electrons cooperate together to form a coherent state (Cooper pair) as whole. If the coherent state is sufficiently lower in energy than the usual normal state, it is hardly destroyed by the collisions or scatterings. The difference, although both are electron transport that are not affected by the collisions and scatterings but ballistic conduction differs from superconductivity due to the absence of the Meissner effect in the material. A ballistic conductor would stop conducting if the driving force is turned off, whereas in a superconductor current would continue to flow after the driving supply is disconnected. Also, charge carriers in Ballistic transport are electrons which act as Fermions. In Superconductor charge carrier are Cooper pair and it behave as Bosons [151-158].

On scales short compared to the Mean-Free Path (MFP) conduction is ballistic. In general, a MFP will exhibit ballistic transport when the length, L of the active part of a device (or in our case vacuum LCU cellular automata array) is $L \leq \lambda_{MFP}$ which in this form is simply the scattering length for the carrier, i.e. electrons or as we hope to demonstrate topological switching of the Unified Field, U_F brane topology by Parallel transport (and topological switching) around the LCU array.

.

7.1 Ballistic transport/conduction evanescence along mean free-path (MFP)

To illustrate concepts of MFP consider a particle as a solid sphere of diameter, α. How far can a particle travel at speed v in a random distribution of n spheres per unit volume before colliding with another particle when moving in a cylinder of radius, α (Fig. 39a)? Shaded sphere No. 1 travels at speed v sweeping out the volume of the cylinder drawn in solid lines. Spheres Nos. 2 and 3 are stationary. Collisions will be unavoidable with No. 3 and a likely grazing collision with No. 2. If the centers of the molecules lie within the dashed cylinder, which has radius a, sphere No. 1 will collide with them.

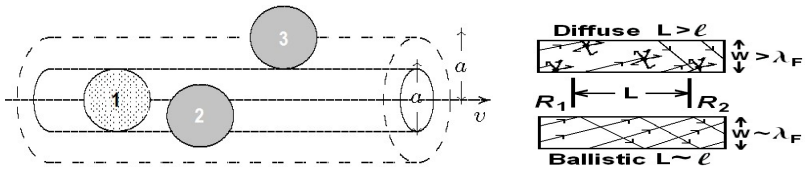

Figure 39. a) Collision of moving particles with random stationary particles. b) Diffuse and ballistic conduction.

Now suppose molecule No. 1 travels length d through a gas. The number of molecules lying within radial distance a of the path, and with which collisions will occur, is $N = \pi a^2 dn$ where n is the number density of molecules. Therefore, the molecule will make one collision with the other molecules when it has travelled a typical distance λ so that $N = 1 = \pi a^2 \lambda n$, that is $\lambda = 1/\sigma n$ where $\sigma = \pi a^2$. In a coherent region, conductance involves adding amplitudes from all trajectories.

In ballistic conduction, transport of charge carriers, has negligible electrical resistivity caused by scattering, such that electrons simply obey Newton's second law of motion at non-relativistic speeds. In general, resistivity exists because an electron moving in a medium, is scattered by any freely-moving species of the medium. For any particle, a MFP is described as the average length that the electron can travel ballistically before a collision changing its momentum. The MFP can be increased by reducing the number of impurities in a crystal or by lowering its temperature. Ballistic transport is observed when

the MFP of the electron is longer than the dimension of the medium the electron travels. An electron alters its motion only by collision with the *walls*.

The Landauer-Büttiker formalism holds as long as the carriers are coherent (length of the active channel is less than the phase-breaking MFP). Transmission functions can be calculated from Schrödinger's equation. Even in a case of a perfect ballistic transport, there is a fundamental ballistic conductance saturating the current of the device with a resistance of approximately 12.9 kΩ per mode [159-161]. For example, ballistic transport observed in a metal nanowire: is simply because the wire is of the size of a nanometer (10^{-9} meters) and the MFP can be longer than in a metal [162].

Normally, transport of electrons (or holes) is dominated by scattering events, which relax the carrier momentum in an effort to bring the conducting material to equilibrium. Thus, ballistic transport in a material is determined by how ballistically conductive that material is. Ballistic conduction differs from superconductivity due to the absence of the Meissner effect in the material. A ballistic conductor would stop conducting if the driving force is turned off, whereas in a superconductor current would continue to flow after the driving supply is disconnected.

Ballistic transport of electrons is a starting point for the understanding of Topological Switching of the *Cone of Enlightenment*. There are some similarities to the principles governing the MFP of Ballistic Conduction in 4-Space to that of the Ontological energyless phase transitions in brane dynamics of Einstein's UF in M-Theoretic brane bouquet in the Bulk (Fig. 16). The dynamics of the propagation within the regime of the Unified Field is different in that there is an inherent periodic MFP inherent in the cyclicality of the topological phase transitions that can be resonantly coupled to an applied harmonic oscillator to produce evanescence with a programmable coherence length. Regarding the LCU tessellation of space, each close-packed LCU cluster has within it a mean-free path accessible by vacuum programming.

As the length scale of a wire is reduced to the mean free path of electrons, the electron transport mechanism changes from diffusive to ballistic, and effects of spin-orbit interaction [163]. Transport properties of CNs are interesting because of their unique topological structure.

Re: Time/frequency-domain reflectance, makes use of rapid boundary transients, structures under rapid transient (not as in) cyclical conditions in phase-change mediation of ballistic topology
Me, the key to maximizing ballistic effects is to use the correct physical boundary conditions.

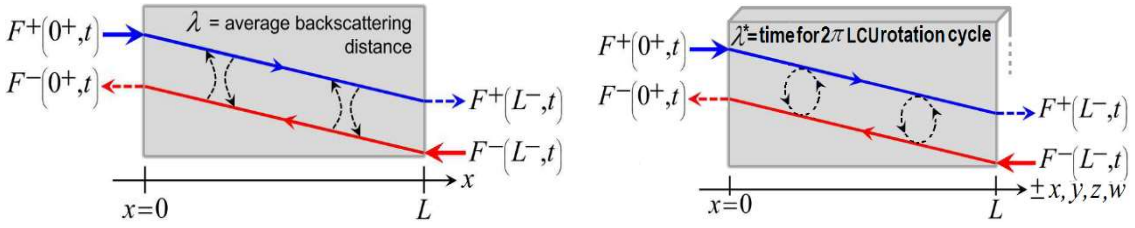

Figure 40. a) 1D transmission in graphene along x. Thermal conductor of length L. The MFP for backscattering λ controls the scattering between forward/backward fluxes. By specifying the injected phonon fluxes (solid arrows), the McKelvey-Shockley flux equations describe the evolution of the fluxes inside the material. b) UFM to 2D. Figure adapted/modified from [151].

Consider 1D transport on x, with y and z directions extending to infinity. This technique categorizes phonons into two components, those that are forward moving ($vx > 0$) and backward moving ($vx < 0$). In Fig. 40b we begin climbing the XD ladder from 1D to 2D. In Fig. 41 this process is extended further to 4D. We hint at the topological phase transitions; 1D lines (current quantum Hall effects in 1D anyons) become 2-spheres, then in Fig. 41, the brane components are topologically switched by *moves* to 4D.

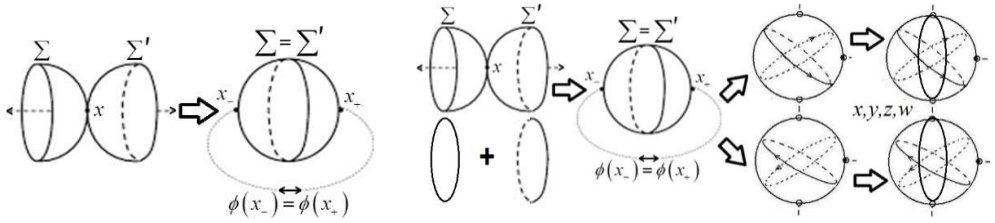

Figure 41. a) Topological phase transition boost 1D to 2-sphere and additional mirror symmetric phase doublings (not shown). b) Topological phase transitions (boosts) 1D to 4D. An evolution of Fig.40.

7.2. Coherent control of standing matter-waves

Ultimately controlling standing de Broglie waves depends on applying the noetic field equation, $F_{(N)} = \aleph / \rho$ (Figs. 38,42) [13] to program parameters for ballistic programming of cellular automata.

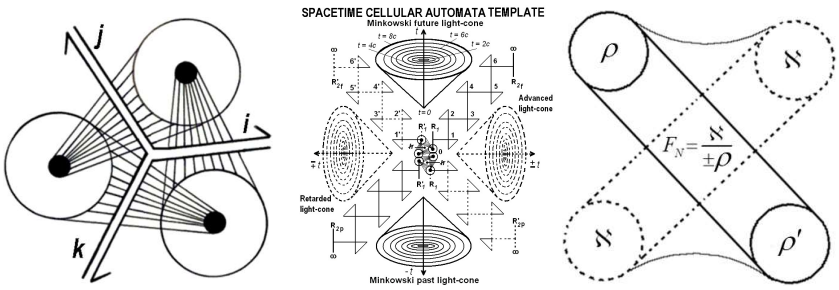

Figure 42. Conceptualized schema of the underlying spacetime structure utilized as a template for modulating the matter-wave resonance hierarchy mimicked in the programmable cellular automata vacuum. a) One element of a 12 unit close-packed LCU array (Fig. 5) b) Exciplex geometry of the UFM noetic field equation (derived in [13], where $F_{(N)}$ is the noetic force, $\aleph$ noeon energy and ρ the radius of coherent action. Detailed in [12,13].

Figure 42 above conceptually summarizes everything required to program a vacuum cellular automata array. It represents an exploded conformal scale-invariant view of the continuous-state wave-particle seesaw leapfrog dynamics inherent in the topology of spacetime shown as a template within a brane topology hierarchy amenable to application of resonance. This nanoscale programmable automata substrate also the leading edge or wave envelope would not merely be a Huygens wave front but be programmed with an annihilation-creation vector spin structure which would asymptotically increase the effectiveness of ballistic programming e by optimizing the periodicity of the mean free path. Also, with sufficiently versatile programming this 'surface' would not create a percussive back-reaction but annihilate or damp the phases of the incoming shock waves to attenuation by destructive rather than constructive interference techniques.

7.3. Energy increase from lattice-gas properties

In terms of a SUSY spacetime lattice represented by close-packed least units (LCUs) functioning as a Riemann 3-sphere Ising model spin lattice, with total energy, $E_T\{s_i\}$ a function of spin hysteresis loop

$$E_T\{s_i\} = \sum_i e_i(s_i) = E_0 - \sum_i h_i s_i \tag{28}$$

where $e_i(s_i)$ is the energy of an isolated individual least unit, E_0 the ground state and h_i the energy from spin orientation from the external field that allows coherent control of the Ising spin lattice [12,13].

The external field is the unitary action driving the evolution of the spacetime lattice structure as a putative self-organized complex system.

The Pythagorean Theorem $a^2+b^2+c^2=d^2$ gives the length, *d* of the diagonal of a 3D cube, *a,b,c*. By adding additional terms to the equation, it describes the diagonal of an ND hypercube. This is illustrated in Fig. 38 above. The locking together of the Calabi-Yau components in the resultant localized cube creates the quantum uncertainty principle which can be surmounted if the Calabi-Yau *copies* are accessed by the UFM resonance procedure [12,13].

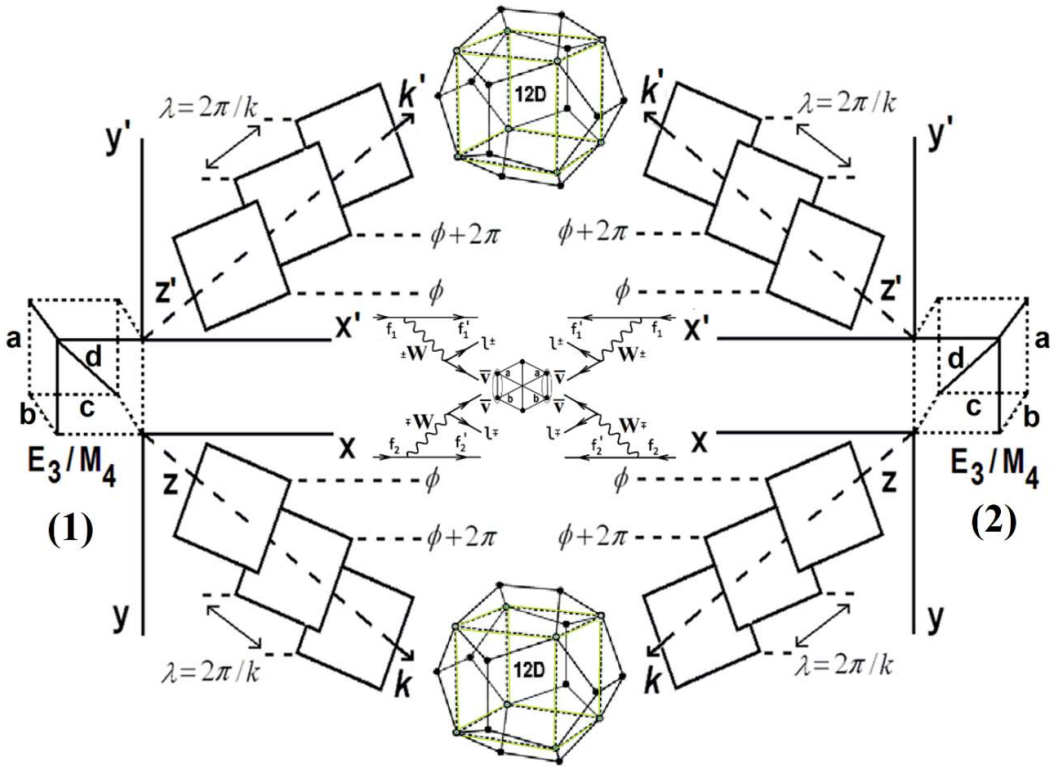

Figure 43. Calabi-Yau future-past mirror symmetry potentia dual 3-tori illustrated as tiered surfaces of constant phase, in this case to represent cyclic components evenly spaced orthogonal standing reality waves with the E_3/M_4 cubic (3-space) resultant line element points in *t*, localized left, x_1 and right, x_2. We do not know how to draw this yet; the center represents the 12D LSXD superspace *causally-free* copy of the local quantum state in 3-space. The center is more clearly seen in expanded form in Fig. X.

A surface of constant phase, $k\cdot r-\omega t=k_x x+k_y y+k_z z-\omega t=$ *constant* is a wavefront [164]. For a surface of constant phase if any wave equation has a time harmonic (sinusoidal) solution of the form $Ae^{i\phi}$ where *A* is the amplitude and the phase, ϕ a function of position with (*x,y,z*) constant and phase difference 2π separated by wavelength, $\lambda=2\pi/k$. The direction cosines of the planes of constant phase are proportional to *k* and move in the direction of *k* equal to the phase velocity where

$$\mu=\frac{\omega}{k}=\frac{\omega}{\sqrt{k_x^2+k_y^2}+k_z^2}. \tag{29}$$

Where $\lambda=2\pi/k=2\pi\hbar/p=h/p$ is equivalent to de Broglie matter waves, $E=\hbar\omega$, $\mathbf{p}=\hbar k$ [65].

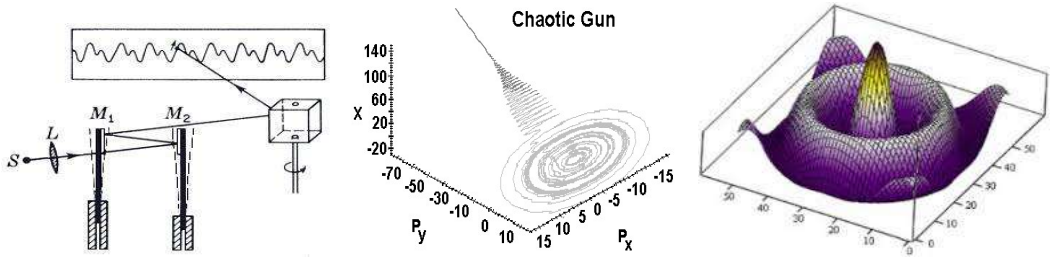

Figure 44. a) Modeled symbolically after a Lissajous apparatus: vibrating mirrors, M_1 -M_2 are dynamic-static Casimir-Polder vacuum domain walls, the 3-cube represents the confabulation of M-theoretic brane topology, the screen is directed energy nodes, L is the manifold of uncertainty (MOU) and S the external field driver. b) Simplistic summation of UFM coherence for DEB operation. c) First 4D TBS spectral line in hydrogen emerging from the 4D spherical potential well for $\alpha = \pm 1$

When coherence cyclically appears, superradiating from the synchronization backcloth (Fig. 45b) summation becomes evanescent for dioxygen dication subduction when the phase period is aligned with the correct mode of topological charge, such that the dioxygen species *path to 3-space*, is interfered with causing the moment of subduction. The 12D LCU brane panoply for the oscillation of the Casimir-Polder-like conditions of each 3-point has sufficient degrees of freedom to reverse he de Broglie-Bohm matter-wave cycle, such that the normal 3-space matter component gets stuck (subducted) momentarily in antispace. This phase manipulation is contrived by the reversal of topological charge.

8. Experimental protocols for accessing XD-LSXD

A putative protocol for utilizing YM-KK equivalence as a path for demonstrating additional dimensionality (XD) beyond the Standard Model (SM) is outlined in preliminary form [12,13]. For example, Riemannian KK manifolds, M with horizontal and vertical subspaces in the tangent bundle (M = X x G) defined by the YM connection are orthogonal with respect to the KK metric, where X is a 4D spacetime and G an arbitrary gauge Lie group; and for the corresponding YM theory, M is a trivial principle G-bundle [34]. This suggests putative orthogonal extensions of dimensionality beyond the 4D utilized by the SM requiring a fundamental change in the meaning of the concept of dimensionality [17]. A novel protocol has been found for empirically testing the model; which if successful could have far reaching consequences for validating M-Theory and provide tabletop-low energy Unified Field Mechanical (UFM) 'cross section' alternatives for 'viewing' putative SUSY partners (or alternative brane topologies) in a trans-dimensional 'slice' rather than the TeV, PeV supercollider techniques utilized/proposed to produce standard cross section particle sprays in the highly successful 100 year history of high energy collision physics.

8.1 TBS Access Requires Violation of the Quantum Uncertainty Principle

Demonstrating new TBS spectral lines requires experimentally surmounting the quantum uncertainty principle. A new Noetic Transform will tell us whether one or two additional doublings of a Rowland's type space anti-space model are required for up to five additional spectral lines which completes the radius of the MOU. Yang-Mills Kaluza-Klein equivalence provides an empirical path extending standard model particle physics. Einstein realized (1905) that Maxwell's equations obey a special relativity principle – Physical law is the same for all observers in uniform relative motion, $x^{\mu} = \left(x^0, x^1, x^2, x^3\right) = \left(t, x, y, z\right)$. Then, his General Relativity required two indices: $g_{\mu\nu}(x)$ with line element $ds^2 = g_{\mu\nu}(x)dx^{\mu}dx^{\nu}$. In 1919, Kaluza made his attempt to combine electromagnetism and general relativity by postulating a 5th dimension with the additional HD coordinate,

$x^M = \left(x^0, x^1, x^2, x^3, x^4\right) = \left(t, x, y, z, \theta\right)$, with line element: $d\hat{s}^2 = \hat{g}_{MN}(x)dx^M dx^N$ where he then made a 4D + 1D split. Klein assumed the 5th dimension had circular topology so that the coordinate, θ is periodic: $0 \le \theta \le 2\pi$. The KK 5th dimension was assumed to be curled up at the Planck scale because it was unobserved – As mentioned above this is not the only interpretation for *hidden* XD!

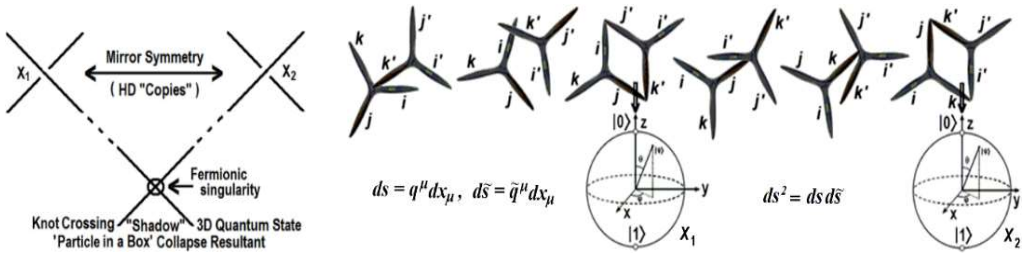

Figure 45. a) Bottom, uncertainty principle arises by a 3-space *knot shadow* of XD topological M-brane degrees of freedom. b) SM line element, locus of semi-classical Riemann Bloch 2-spheres, X_1, X_2, as *basement of reality*; Top, 1st space-antispace mirror symmetric UFM step of quaternionic vertices cycling from 5D QM chaos to topological order as faces of 3-cube.

Figure 45 shows how a localized knot shadow hides XD behind the uncertainty principle. In Fig. 45b we see the beginning of separation of the standard 3-space line element into an extended KK cyclicality from order to chaos at the semi-quantum limit. The inherent *beat frequency* is revealed by rf-modulation of the Dirac polarized vacuum. When the stochastic background coheres into the square, a channel opens into ballistic conduction and DEB energy emanates causing dioxygen dication subduction.

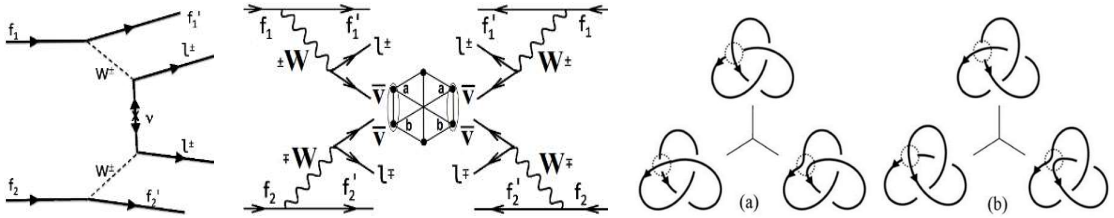

Figure 46. a) Fundamental diagram changing lepton number transitions by two units, generalized for Majorana modes (MJM). b) Dual MJM cyclic modes for fusion of a-b Berry phase cycles (center) in graphene. c) Reduction schemes for L & R-handed trefoil knots.

8.2 Dication

Historically, dications were regarded as curiosities observed incidentally in mass spectrometric studies. Small polyatomic dications are remarkable species; usually thermodynamically unstable with respect to dissociation into two monocations, but significantly kinetic stability may result if large barriers impede dissociation. This is illustrated by the methyleneoxonium dication $CH_2OH_2^{++}$ discussed above. This species is less stable than its dissociation products $CH_2OH^{++}H^+$ (by 105 kJ mol^{-1}), but a barrier of 250 kJ mol^{-1} makes the ion experimentally accessible. In many cases, deprotonation of a dication is best viewed as a two-stage process. Initially, the departing unit is a hydrogen atom rather than a proton, and later an electron transfer takes place to form the products: $AH^{++} \rightarrow A^{++} - H \rightarrow A^{+} \cdots H^{+} \rightarrow A^{++}H^{+}$. The first step, a homolytic cleavage, is responsible for the large barrier. Hence, a dication is truly a tiger in a cage.

Recently reactions of Dioxygen dications O_2^{2+} with various small neutral biological molecules like methane, ethyne and ethene has been studied. A center-of-mass collision technique was used to create a bond-forming electron transfer reaction to strip an atom from the neutral by the O_2^{2+} reactant.

We propose a novel, as yet highly speculative, M-theoretic interference technique to produce dioxygen dications O_2^{2+} in a space-antispace coincidence of the topology of the brane bulk in tandem with a Dirac spinor coupling reaction between the dioxygen dication O_2^{2+} and periodic positive holes in the covariant Dirac polarized vacuum. This is a complex process utilizing Unified Field Mechanics, still in its infancy.

Bond-dissociation energy (BDE or D_0) is one measure of the strength of a chemical bond. The reactivity of O_2^{2+} with CO_2, OCS and CS_2 has recently been investigated at center-of-mass collision energies of 7.0, 7.9 and 8.5 eV, respectively. The position-sensitive coincidence technique we employ shows the reactivity in the three collision systems is dominated by double- and single-electron transfer. Analysis of the observed electron transfer reactivity indicates that the two-electron transfer is concerted and the translational energy does not couple efficiently to the electronic co-ordinates. In the O_2^{2+} + OCS collision system we observe a channel forming a new chemical bond, generating $SO^+ + CO^+ + O$. The angular scattering in this channel indicates that this reaction proceeds via complexation, then fragmentation of the complex to form $SO_2^+ + CO^+$. The primary SO_2 + product then dissociates to $SO^+ + O$. *Ab initio* calculations support the presence of a collision complex in the pathway to $SO^+ + CO^+ + O$. The single electron transfer reactions are direct and the energy releases we extract for the subsequent dissociation of the primary products (e.g. $O_2^+ + CO_2^+$) show that the internal vibrational energy of the O_2^{2+} reactant does not participate in the reaction.

The reactions of O_2^{2+} with CH_4, C_2H_2 and C_2H_4 have been investigated for the first time, using a position sensitive coincidence technique, at center-of-mass collision energies close to 4eV. The experiments show these interactions yield a wide variety of products which involve the formation of new chemical bonds. The mechanisms of these bond-forming reactions have been investigated by examining the correlations between the velocities of the reactant and product ions which are revealed by the coincidence data. Many of the bond-forming reactions occur via the stripping of an atom (or group of atoms) from the neutral by the O_2^{2+} reactant, while other reactions clearly involve the initial formation of a collision complex which then fragments to form the detected products [165].

9. Summary of experimental protocols

If experimentation proves viable, string theory becomes experimental, an explosion of new technology occurs and a new class of UQC based biophysical research platform for studying fundamental properties of the spacetime vacuum as it relates to long-range coherence in living systems, especially Cartesian dualism and the Eccles Psychon. We briefly outline eight of fourteen protocols here, the Main experimental protocol and seven derivatives to test the LSXD continuous-state Long-Range Coherence hypotheses:

9.1. Basic Experiment - Fundamental test that the concatenation of new OPTFT *UF* principles is theoretically sound. A laser oscillated rf-pulsed vacuum Sagnac resonance hierarchy is set up to interfere with the periodic (continuous-state) structure of the inherent 'beat frequency' of a covariant Dirac polarized spacetime vacuum exciplex to detect the new coherence principle associated with a cyclical holophote entry of the *UF* into 4-space. This experiment *pokes a hole in spacetime* in order to bring the energy of the *UF* into a detector, essentially discovering XD beyond the 4D SM. The remaining protocols are variations of the parameters of this experiment (and basis of all technologies).

9.2. Bulk Quantum Computing - Utilizing protocol (1) Bulk Scalable UQC can be achieved by superseding the quantum uncertainty principle. (see [6,66,73,74] for details) Programming and data I/O are performed without decoherence by utilizing the inherent mirror symmetry properties that act like a 'synchronization backbone' [13] whereby 'LSXD copies' of the local 3-space quantum state are causally free (measurable without decoherence) at specific resonance nodes in the continuous-state conformal Calabi-Yau symmetry cycle hierarchy.

9.3. Protein Conformation - (similar to discussion in [166]). Utilizing more macroscopic aspects of protocols (1 & 2) dual Hadamard quantum logic gates are set as a Cavity-QED spacetime cellular automata [12,167] experiment to facilitate conformational propagation in the prion protein from normal cellular form, PrP_C to pathological, PrPSc form by noeon bombardment with the UF *force of coherence*.

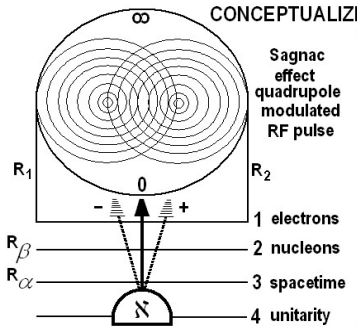

Harmonic Oscillator Parameters	
classical	$X = A\cos(\omega t)$
quantum	$\frac{\hbar^2}{2m}\frac{d^2\psi}{dx^2} + \left(E - \frac{kx^2}{2}\right)\psi = 0$
annihilation creation	$x(t) = x_0\left[a\exp(-i\omega t) + a^{\dagger}\exp(i\omega t)\right]$
future-past retarded-advanced	$F_1 = F_0 e^{-ikx}e^{-2\pi ift}$, $F_2 = F_0 e^{ikx}e^{-2\pi ift}$, $F_3 = F_0 e^{-ikx}e^{2\pi ift}$, $F_4 = F_0 e^{ikx}e^{2\pi ift}$
incursive	$\frac{dx(t+\Delta t)}{dt} - v(t) = 0$, $\frac{dv(t+\Delta t)}{dt} + \omega^2$

Figure 47. a) Conceptualized cavity-QED multi-level Sagnac effect interferometer designed to 'punch' a hole in spacetime to emit the 'eternity wave, ℵ'. b) Components of the applied harmonic oscillator - classical, quantum, relativistic, transactional and incursive required to achieve coherent control of the cumulative resonance coupling hierarchy in order to produce harmonic nodes of destructive and constructive interference in the spacetime backcloth.

9.4. **Manipulating special case of the Lorentz Transformation** [35,36]. Aspects of a spacetime exciplex model [13] in terms of restrictions imposed by Cramer's Transactional Interpretation [15] on mirror symmetry can be used for the putative detection of virtual tachyon-tardyon interactions in *zitterbewegung* [7].

Hypersphere Volumes

Dimension	Volume	Volume at $r = 1$
2	πr^2	3.14159
3	4/3 πr^3	4.18879
4	½ $\pi^2 r^4$	4.93480
5	8/15 $\pi^2 r^5$	5.26379
6	1/6 $\pi^3 r^6$	5.16771

Table 3. Hypersphere volumes which can be used to calculate new TBS spectral lines.

9.5. Extended Quantum Theory - Test of causal properties of de Broglie- Bohm-Vigier quantum theory by utility of the *UF* holophote effect (protocol 1 parameters) as a 'super quantum potential' to summate by constructive interference the density of de Broglie matter waves [12,13].
9.6. Coherent Control of Quantum Phase - Additional test of the de Broglie- Bohm interpretation for existence of a nonlocal 'pilot wave - quantum potential' for manipulating the phase 'space quantization' in the double slit experiment by controlling which slit quanta passes through. Application to quantum measurement and transistor lithography refinement.
9.7. Manipulating Spacetime LCU Structure - (similar to protocol 6) Test of conformal scale-invariant properties of a putative Dirac conformal polarized vacuum, possible *continuous-state* property related to an arrow of time [12,13,168,169] (Also similar to basic experiment, but more advanced).
9.8. Testing for and Manipulating Tight Bound States (TBS) - (similar to protocol 4) Vigier [66,73] has proposed TBS below the 1st Bohr orbit in the Hydrogen atom. Utilizing tenets of the original hadronic form of string theory [13] such as a variable string tension, T_S where the Planck constant, $\hbar$ is replaced with a version of the original Stoney ƛ [13], where $\hbar$ is an asymptote never reached, instead oscillating from virtual Planck to the Larmor radius of the hydrogen atom, i.e. the so-called Planck scale is a restriction imposed by the limitations of the Copenhagen Interpretation and is not a fundamental physical barrier. LSXD exist putatively behind the barrier of uncertainty and the oscillation of the Planck

constant is part of the exciplex gating mechanism [13]. Utilizing ontological-phase topological field theory (OPTFT) at the moment of spin-spin coupling or spin-orbit coupling an rf-pulse is kicked at various nodes harmonically set to coincide with putative phases in the cycle between local and LSXD cavity TBS properties [13,66,73,74].

9.9. Test for the noetic Unique String Vacuum - Until now the structure of matter has been explored by building ever bigger supercolliders like the CERN LHC. If the LSXD access model in terms of a Dirac covariant polarized energy dependent vacuum proves correct utilizing the inherent conformal scale-invariant mirror symmetry properties of de Broglie matter waves will allow examining various cross sections in the structure of matter in symmetry interactions during cyclic continuous-state future-past annihilation-creation modes of matter in the LCU tessellated spacetime metric without the need for supercolliders. There are a number of very specific postulated cosmological properties required in order to perform these experiments [13,43,125].

10. Why an ontological-phase topological field - A form of topological M-theory

A topological quantum field theory (TQFT) is a quantum field theory which computes topological invariants (property of topological space invariant under homeomorphisms. (continuous between topological spaces) That is, a property of spaces is a topological property if whenever a space *X* possesses that property every space homeomorphic to *X* possesses that property [170-174].

To advance beyond the quantum condition (locality and unitarity) and surmount uncertainty in order to technologically utilize XD-LSXD, we outline a nascent Ontological-Phase Topological Field Theory (OPTFT) [8,12,34], to address the brane dynamics of the unified field. A TQFT computes topological invariants (property of a topological space which remains unchanged when transformations are applied to the object under homeomorphisms). A topological isomorphism is a continuous function between topological spaces that has a continuous inverse function. Homeomorphisms are the isomorphisms in the category of topological spaces, that is, they are the mappings that preserve all the topological properties of a given space. Two spaces with a homeomorphism between them are called homeomorphic, and from a topological viewpoint they are the same space. Assuming quantum field theory is a necessity for consistent descriptions of quantum interactions; suggests current concepts in quantum information theory require reassessment and will need to be brought in line with a relativistic quantum informational theory before quantum computation can be fully realized. New properties of this transformation also require a change in the usual model of a qubit. We agree with the assessment given by Perez *Most of the current concepts in quantum information theory may then require a reassessment* [111]. Information needs a material carrier, and the latter must obey the laws of physics. Information is physical [112,113].

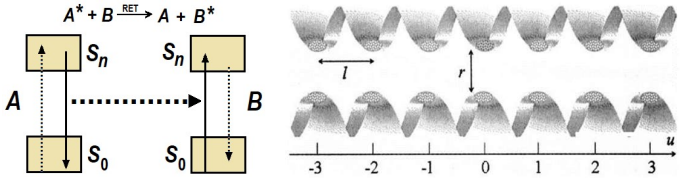

Figure 48. a) Single step Resonance Energy Transfer (RET) complex showing excitation and decay of the donor, *A* and acceptor, *B* RET energetics. Shaded boxes are ground (bottom) and excited (top) QED cavity and topological states *S*. b) Graphical depiction of parallel 1D linear-lattice arrays, with the lattice constant, *l* and *r* displacement of upper donor array from the lower acceptor array. Optically active molecules, labeled with integer coordinates, are denoted by pale ellipses - ground state or a dark ellipse - excited state. Figs. redrawn from [175,176].

$$W_{\mathrm{F}} = \frac{9\kappa^2 c^4}{8\pi\tau_{A^*}\eta^4 R^6}\int F_A(\omega)\frac{d\omega}{\omega^4} \tag{30}$$

Andrews also claims the lattice arrangements form hexagons applicable to RET-OCHRET spontaneous emission [176]. This coincides with UFM M-theory postulates related to the hexagonal trefoil topology discussed above. We additionally relate the Casimir-Polder effect to RET, OCRET – The force between two boundary conditions in a volume with a field (here the noetic field) The energy of the field depends on the frequency which in turn depends on the boundary conditions. Changing the position of the boundaries changes the frequency and energy of the field which can be a potential energy per area of the boundaries which leads to a force depending on the boundary conditions. We adapt this effect in the physical basis of mental energy.

Casimir outlined the influence of retardation on London-van der Waals forces between neutral atoms. Instantaneous dipoles account for interactions between electric double layers separated by large distances. The interaction energy of a neutral atom by analogy with a perfectly conducting wall and is given by the atomic dipole with its antispace image. Retardation effects are expected when the distance from the wall becomes large, according to Cavity-Quantum Electrodynamics (C-QED). The asymptotic expression of R contains Planck's constant and the static polarizability of the atom as the only quantities. Casimir confined the neutral atom within a perfectly conducting plane wherein the eigenstates of the electromagnetic field are described by Maxwell's equations and treated as if the atom were a quantum particle in a box. The box in our case of dynamic-static complementarity is a system or domain of fundamental LCUs (dualistic form of sphere packing tiling the spacetime backcloth – semi-quantum throat (Fig. 13) to LSXD brane topology) that are the continuously changing boundary conditions of the systems dynamics in fermion-quasiparticle-boson (FQB) translation. The total energy interaction between the wall and the atom is given by [177], $\Delta_t E = \Delta_d E + \Delta_e E$.

XD-LSXD are of sufficient interest that experiments (called gravities rainbow) at CERN are being developed to search for them. However, our UFM protocols to find them are table top and low energy, which if successful will put an end to the need for supercolliders. We are formulating an Ontological-Phase Topological Field Theory (OPTFT) to address the putative parameters that will be used to implement DEB technologies. Our view of UFM fortunately makes correspondence to HD extensions of Wheeler-Feynman-Absorber Cramer-Transactional De Broglie-Bohm-Vigier causal interpretations of quantum theory as well as dual 3-tori Calabi-Yau brane mirror symmetry (thus OPTFT).

We relate Dirac hole theory to Casimir-Polder/Bohm interactions. As well known, there are both positive and negative energy solutions to the Dirac equation. Traditionally considered problematic because it required a positron. However, if we consider M-Theoretic Topological Charge in terms of annihilation-creation modes in Bohm's guidance model, as illustrated in Figs. 14,16,20,23,26a, as an inherent harmonic oscillator of the UF propagation, the realization that M-theory can be technologically harnessed arises.

Note that Dirac's idea of a polarized vacuum is absolutely correct in the context of solid state physics, where the valence band in a solid can be regarded as a sea of electrons. Holes in this sea indeed occur, and are extremely important for understanding the effects of semiconductors, though they are never referred to as positrons. Unlike in particle physics, there is an underlying positive charge – the charge of the ionic lattice – that cancels (nilpotent) out the electric charge of the sea.

10.1 Current Thinking in String/M-Theoretic Topological Brane Dynamics

String Theory arose nearly a century ago from the seminal work of Kaluza-Klein proposing a cyclical compactified 5D model to unify electromagnetism and gravitation. Current thinking in String/M-Theory is based on Super Minkowski Spacetimes (SMS) where the simplest possible SMS, called the Superpoint, from which a so-called *brane scan* classifies all known string/brane cocycles into a complete fundamental content of string/M-Theory extended to the 10/11D SMS of String/M-Theory. This brane scan process has led to what is commonly called a *brane bouquet*, comprised of the variety of interpretations of dual Calabi-Yau mirror symmetric brane configurations [178,179].

We have been addressing this model incrementally elsewhere [8,12,34]. A full delineation of our unique derivation of M-Theoretic UFM Theory is beyond the scope of this paper; we will confine our final putative description of DEB wild fire attenuation technology to dual semi-quantum OCRET and

UF OCHRE parameters required to produce directed nonlocal vacuum energy in a manner locally suppressing dioxygen's ability to release its electrons by coupling the dioxygen dication O_2^{2+} to topological holes the Dirac vacuum. The three known quantum fields are mediated phenomenologically by exchange quanta. In contrast, the UF is mediated ontologically, as an energyless topological exchange of information. The OCHRE-OCRET model is based on a plethora of current thinking as it evolution point [180-184].

Susceptible to being perturbed. Van der Waals forces quickly vanish at longer distances between interacting molecules. Van der Waals forces are of the same origin as the Casimir effect, arising from quantum interactions with the zero-point field [185]. The resulting van der Waals forces can be attractive or repulsive [186]. An example of parametric oscillation is *pumping* on a playground swing. A person on a moving swing can increase the amplitude of the swing's oscillations without any external drive force (pushes) being applied, by changing the moment of inertia of the swing by rocking back and forth (pumping) or alternately standing and squatting, in rhythm with the swing's oscillations. The varying of the parameters drives the system.

The Casimir-Polder interaction between a single neutral atom and a nearby surface, arising from the (quantum and thermal) fluctuations of the electromagnetic field, is a cornerstone of cavity quantum electrodynamics (cQED), and theoretically well established. Recently, Bose-Einstein condensates (BECs) of ultracold atoms have been used to test the predictions of cQED. The purpose of the present thesis is to upgrade single-atom cQED with the many-body theory needed to describe trapped atomic BECs. Tools and methods are developed in a second-quantized picture that treats atom and photon fields on the same footing. We formulate a diagrammatic expansion using correlation functions for both the electromagnetic field and the atomic system. The formalism is applied to investigate, for BECs trapped near surfaces, dispersion interactions of the van der Waals-Casimir-Polder type, and the Bosonic stimulation in spontaneous decay of excited atomic states.

What this means is that when constructive resonance occurs, information of state is ontologically transferred. Spin-spin or spin-orbit coupling can only transfer information under proper commutativity conditions. When q-uncertainty is in a topological phase state (exclusion principle) only destructive interference may occur. When sufficient mirror symmetric phase is applied, such that the *n*th state is causally free of the local c-QED state, the ontological phase transition may then summate (transfer information) as a resonance of constructive interference.

The at present putative ontological phase transition is a LSXD M-theoretic form on the well-known 5D K-K cyclicality. It is the inherent cyclicality of the M-theoretic brane topology that allows both periodic commutative violation of the uncertainty principle and the ontological transfer of information relative to the quantum state. Interaction free measurement entails a quantum Zeno effect because it cannot fully escape or cheat uncertainty and not bypass the semiclassical limit of the standard model in 4D. But measurement at the semi-quantum limit may under stringent phase periodicity perform an ontological interaction of $P \equiv 1$.

Traditionally electron standing-waves oscillate about the atomic nucleus. Here we attempt to expand the wave nature of matter itself as static waves centered on the locus of least spacetime units as it is annihilated and recreated in the arrow of time relative to the observer. This requires a conversion of the de Broglie wave equation, $mvr = n(h/2\pi)$ to a static form amenable to the parameters of continuous-state cosmology [12]. For Hyperspherical Representation the magnitudes of the radial coordinates of a two-state wavefunction, $\psi(\vec{r}_1, \vec{r}_2)$ in hyperspherical representation are replaced by the hyper-spherical radius, *R* and the hyperspherical angle, α such that $R \equiv \left(r_1^2 + r_2^2\right)^{1/2}$ and $\alpha \equiv \arctan r_2/r_1$ in order that the symmetries may be more clearly shown. The hyperspherical radius, *R* represents the size of the 2-state system and the hyperspherical angle, α is a measure of the radial correlation of the two-state system [12]. It is critical to note that when $\alpha = \pi/4,\ r_1 = r_2$; and when $\alpha = 0$ or $\pi/2$ one of the states is at a greater distance from the least-unit vertex than the other.

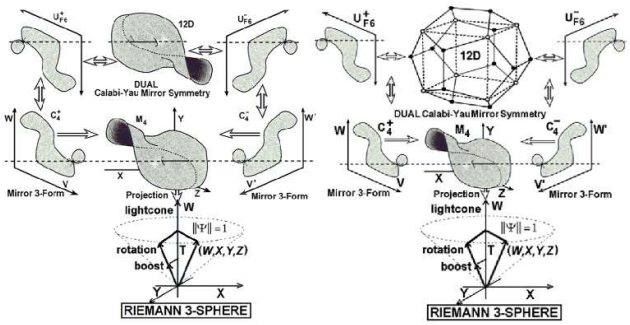

Figure 49. Completing Fig. 45 8D to 12D illustrating full extended rendition of additional parameters for a relativistic XD quantum state and instantaneous LSXD in continuous-state dual Calabi-Yau mirror symmetric UFM cosmology as far as currently understood. Replacing also the Bloch 2-sphere qubit representation (Fig. 45) with the new extended r-qubit Riemann 3-sphere resultant representation that has sufficient parameters to surmount the uncertainty principle. The figure can be seen as an alternative rendition of Fig. 43.

11. OCHRE-OCRET modules in DEB design systems

At this point it seems time to send Alice down the rabbit hole and fall short here at the end, leaving OCHRE-OCRET details for a part II document discussing actual prototyping; and briefly hint at where we see development going.

A computer is a system with many parts; the duality of localized OCRET (Optically Controlled Resonance Energy Transfer**)** in tandem with nonlocal OCHRE (Oscillation Coupled Helicoid Resonance Emission) are the application modules for DEB wildfire suppression technology. We introduce the two main elements necessary for development of DEB fire suppression technology – Duality between
A) Nonlocal coupled oscillator of OCHRE class systems in tandem with
B) localized OCRET class systems

In a molecular system of energy donors and acceptors, resonance energy transfer is the primary mechanism by means of which electronic energy is redistributed between molecules, following the excitation of a donor. Given a suitable geometric configuration it is possible to completely inhibit this energy transfer in such a way that it can only be activated by application of an off-resonant laser beam: this is the principle of optically controlled resonance energy transfer, the basis for an all-optical switch. Optically controlled energy transfer between a single donor and acceptor molecule, identifying the symmetry and structural constraints and analyzing in detail the dependence on molecular energy level positioning has been investigated, see [175,176] and references therein. Spatially correlated donor and acceptor arrays with linear, square, and hexagonally structured arrangements are then assessed as potential configurations.

Now we try to say the same thing stated in the preceding paragraph in terms of UFM M-theory: Instead of a molecular system, the energy donors and acceptors are LCU domains in space-spacetime, resonance energy transfer occurs by a gearing of the external oscillating driving field spin coupled to the UFM synchronization backbone. Because of the wheeler-Feynman-Cramer standing wave mechanism, donor-acceptor energy transfer modalities are programmable. That hexagonally structured arrangements are prime configuration, as we discussed above, is gift in that the dynamics of the bulk have this inherent configuration.

Given the known fact that *given a suitable geometric configuration it is possible to completely inhibit energy transfer in such a way that it can only be activated by application of an off-resonant laser beam* provides sufficient prescient insight for developing the DEB fire prevention theory that will subduct the dioxygen dication by periodic adduction to the oscillating static-dynamic Casimir-polder cavity walls, an OCHRE-OCRET Energy Transfer mechanism that together periodically confine the dioxygen dication to C-QED bumps and holes in the Dirac covariant polarized vacuum in resonance with the beat

frequency of LCU K-K cyclicality. When the ontological phase transition path is *open*, ballistic conduction (with superradiance) may be directed to evanesce by OCRET-OCHRE duality at an energy directly corresponding to the coherence length of ballistic LCU alignment of commutative modes. The ballistic alignment modes must be periodic because the manifold of uncertainty is a regime of reality in the same respect as the existence and limits of the classical regime and the imminent utility of the regime of Einstein's unified field, the 3rd regime of natural science where ontological phase interactions occur.

Acknowledgements
Like Newton, we have stood on the *shoulders of Giants*; more than can be mentioned! Vigier's shoulders were broad and high; his premise of tight-bound states (TBS) in the hydrogen atom (below the lowest Bohr orbit), initially was myopically thought logically untenable. Twelve years later we finally realized the profundity TBS provided: key to designing low energy tabletop (sans supercollider) experimental protocols for surmounting quantum uncertainty. Seven years more, we have not quite mustered to perform these experiments; but prepare. But have in that interim, as hopefully evident here, developed deep (as yet philosophical) and radical insight into the nature of unified field theory (UFT).

One of us is, in some ways a similitude of Georges Lemaitre of the prior century who was both a physicist and catholic priest. Albeit unpopular at present, physical science cannot ignore much longer finding the place of the Observer and the fact of our existence in an anthropic multiverse. Human capacity to learn has steadily evolved from medieval myth and superstition → the Greek advance of logic and reason → Galileo instituted the current age of empiricism → now the final tool completing the evolution of epistemology is that of the utility of transcendence as a tool in scientific theory formation, which Plato termed 2,000 years ago as Noetic Insight as follows: Noetic insight is beyond the self, arising from the entelechies of the cosmos. No matter how great one's intellect, breath of one's knowledge base or depth of wisdom noetic insight arises from the entelechies of the cosmos.

CERN rectors' statement that discovery of XD by Gravities Rainbow, is evidence of a multiverse existing beyond the observational limits of the putative Big Bang – evidence of an Anthropic Landscape. Realized as yet by few, UFT provides an additional investigative tool completing the tools of epistemology. In that respect, acknowledgement is given to אלוהים האב and his ministering ombudsman.

In 88 words of summation: Assume a Bulk Universal QC sits on a workbench in an R&D facility, the new set of UFM noetic transforms allowing empirical access to the topological interactions in the brane bulk is embodied in several QC algorithms able to process realistic brane-world r-qubits (there would be no Bulk UQC without this). All that remains to prototype DEB a device, and it is deemed that this scenario would be inherently obvious, is another set of programs to suppress (by vacuum subduction-adduction) dioxygen dication, the electronics and the DEB transmitter.

References

[1] Yang C N 2009 – Stoney Brook masters series interview (https://www.youtube.com/watch?v=6d3hZ8jnqXg)
[2] (https://en.wikipedia.org/wiki/List_of_wildfires)
[3] (http://wepreventfires.com/2018/06/12/california-wildfire-facts/)
[4] Lyons L 2013 Discovering the significance of 5σ (arXiv:13101284v1 [physicsdata-an])
[5] Chantler C T et al 2012 Testing three-body quantum electrodynamics with trapped Ti^{20+} ions: evidence for a *z*-dependent divergence between experiment and calculation *Phys Rev Let* **109** 15 3001
[6] Amoroso R L and Di Biase F 2013 Empirical protocols for mediating long-range coherence in biological systems *J Consc Explor Res* **4** 9 955-976
[7] Amoroso R L and Rauscher E A 2010 *Empirical protocol* for measuring virtual tachyon tardon interactions in a Dirac vacuum *AIP Conf Proceed* **1316** 99
[8] Amoroso R L 2018 Einstein/Newton duality: An ontological-phase topological field theory XX Intl Meeting Physical Interpretations Relativity Theory (PIRT) 3–6 July 2017 Moscow Russian Federation *J Phys Conf Series* **1051** open access (https://iopscienceioporg/article/101088/

1742-6596/1051/1/012003)
[9] Amoroso R L and Rauscher E A 2011 Speculation on a unified field theory (UFT) grand unification theories (GUT) and supersymmetry and superstring theories in *Orbiting the Moons of Pluto* 238-266 London World Scientific (http://vixra.org/pdf/1802.0434v1.pdf)
[10] Amoroso R L 2018 Buckaroo Banzai across the 8th dimension A strategic assault on the dimensional barrier *Proceedings ANPA 39* http://anpa.onl/wp-content/uploads/2018/04/Amoroso-ANPA18-Topology.pdf
[11] Amoroso R L 2018 Millennial science the imminent age of discovery's conscious technologies *Essays on Consciousness Towards a New Paradigm* I Fredriksson (ed) Balboa Press
[12] Amoroso R L 2017 *Universal Quantum Computing: Surmounting Uncertainty Supervening Decoherence* Hackensack World Scientific
[13] Amoroso R L and Rauscher E A 2009 *The Holographic Anthropic Multiverse Formalizing the Complex Geometry of Reality* London World Scientific.
[14] Rauscher E A and Amoroso R L 2011 *Orbiting the Moons of Pluto: Complex Solutions to the Einstein Maxwell Schrödinger and Dirac Equations* Singapore World Scientific
[15] Cramer J G 1986 Transactional interpretation of quantum mechanics *Rev Mod Phys* **58** 3 647
[16] Bohm D 1952 A suggested interpretation of the quantum theory in terms of hidden variables I *Phys Rev* **85** 2 166; A suggested interpretation of the quantum theory in terms of hidden variables II *Phys Rev* **85** 2 180
[17] Rowlands P 2015 How many dimensions are there? In R L Amoroso LH Kauffman and P Rowlands (eds) *Unified Field Mechanics: Natural Science Beyond the Veil of Spacetime* Hackensack World Scientific
[18] Yuan L Lin Q Xiao M and Fan S 2018 Synthetic dimension in photonics (arXiv:180711468v1 [physicsoptics])
[19] Bradshaw D S and Andrews D L 2008 Optically controlled resonance energy transfer: Mechanism and configuration for all-optical switching *J chem phys* **128** 144506
[20] Lehnert B 1998 Electromagnetic theory with space-charges in vacuo in G Hunter S Jeffers and J-P Vigier (eds) *Causality and Locality in Modern Physics Dordrecht* Kluwer Academic
[21] Proca A 1936 *Compt Rend* **202** 1420
[22] Roy S and Lehnert B 1998 *Extended Electromagnetic Theory Space Charge in Vacuo and the Rest Mass of the Photon* Singapore World Scientific
[23] Schwinger J 1992 Casimir energy for dielectrics *Proc Nat Acad Sci* **89** 4091-3
[24] Schwinger J 1993 Casimir light the source *Proc Nat Acad Sci* **90** 2105-6
[25] Schwinger J 1994 Casimir energy for dielectrics: spherical geometry *Proc Nat Acad Math Psych* **41** 64-67
[26] Dirac P A M 1952 *Nature London* **169** 702
[27] Cufaro N Petroni C and Vigier J-P 1983 Dirac's ether in relativistic quantum mechanics *Found Phys* **13** 253-286
[28] Jeong C Kim R Luisier M Datta S and Lundstrom M 2010 *J Appl Phys* **107** 023707
[29] Schempp W 1998 Quantum holography and magnetic resonance tomography: An ensemble quantum computing approach *Taiwanese J Math* **2** 3 257-285
[30] Aoun B and Tarifi M 2004 Quantum cellular automata (https://arxiv org/ftp/quant-ph/papers/0401/0401123.pdf)
[31] Choi K-K and Mait J N (eds) 2015 *The International Year of Light* **4** 1 US Army Res Laboratory (https://www.arl.army.mil/www/pages/172/docs/research_at_arl_IntYearofLight.pdf)
[32] Chabab M El Moumni H Iraoui S Masmar K and Zhizeh S 2018 Joule-Thomson expansion of RN-AdS black holes in f(R) gravity (arXiv:1804 10042v2 [gr-qc])
[33] Alia A F Faizald M and Khalile M M 2015 Absence of black holes at LHC due to gravity's rainbow *Phys Let B* **743** 295; (arXiv:1410.4765v2 [hep-th])
[34] Amoroso R L 2016 Yang-Mills Kaluza-Klein equivalence An empirical path extending the standard model of particle physics (http://vixra.org/pdf/1511.0257v1.pdf) address given at:

(http://www.ntu.edu.sg/ias/PastEvents/2015/Yang-Mills60/Pages/default.aspx); (https://www.youtube.com/watch?v=ecu86GY7Xt8)
[35] Amoroso R L and Di Biase F 2013 Crossing the psycho-physical bridge Elucidating the objective character of experience J Cons Exp Res **4** 9
[36] Amoroso R L 2010 Simple resonance hierarchy for surmounting quantum uncertainty in R L Amoroso P Rowlands and S Jeffers (eds) *AIP Conference Proceedings-American Institute of Physics* **1316** 1 185
[37] Duff M J 2001 The world in eleven dimensions A tribute to Oskar Klein (http://arxiv.org/pdf/hep-th/0111237)
[38] Klein O 1926 Quantum theory and five-dimensional relativity theory *Zeit Phys* **37** 895
[39] Klein O 1926 The atomicity of electricity as a quantum theory law *Nature* **118** 516
[40] Amoroso R L 2016 Unified field mechanics & its applications Special Issue (6 articles) *Sci God J* **7** 2 59-163
[41] Amoroso R L 2015 Introduction to unified field mechanics Formalizing the protocol (http://vixra.org /pdf/1511.0175v1.pdf)
[42] Fischbach G D 1992 Mind and Brain September *Scientific American*
[43] Amoroso R L 2015 Unified field mechanics A brief introduction (http://vixra.org/pdf/ 1511.0176v1.pdf)
[44] Tinkham M 1996 *Introduction to Superconductivity* Second Ed New York NY McGraw-Hill
[45] Annett J 2004 *Superconductivity Superfluids and Condensates* NY Oxford Univ Press
[46] Shytov A Kong J F Falkovich G and Leonid Levitov 2018 Particle collisions and negative nonlocal response of ballistic electrons (arXiv:1806.09538v2 [cond-mat.mes-hall])
[47] Randall L and Sundrum R 1999 An alternative to compactification *Phys Rev Let* **83** 4690-4693 ([hep-th/9906064])
[48] Randall L 2005 *Warped Passages* New York Harper-Collins
[49] El Kabbash M Miele E Fumani A K Wolf M S Bozzola A et al 2019 Cooperative energy transfer controls the spontaneous emission rate beyond field enhancement limits (arXiv 1901.03457)
[50] Wilkowski D Chalony M Kaiser R and Kastberg A 2009 Low and high intensity velocity selective coherent population trapping in a two-level system (arXiv:0907.5296v1 [physics.atom-ph])
[51] Phillips W D 1998 Nobel lecture Laser cooling and trapping of neutral atoms *Rev Mod Phys* **70** 721
[52] Shuman E S Barry J F and DeMille D 2010 Laser cooling of a diatomic molecule *Nature* **467** 820-823
[53] Hendricks R J Phillips E S Segal D M and Thompson R C 2008 Laser cooling in the Penning trap an analytical model for cooling rates in the presence of an axializing field *IOP J Physics B Atomic Molecular and Optical Physics* **41** 3 (arXiv:0709.3817v1 [quant-ph])
[54] Powell H F de Echaniz S R Phillips E S Segal D M and Thompson R C 2003 Improvement of laser cooling of ions in a Penning Trap by use of the axialisation technique (arXiv:quant-ph/0211016v2)
[55] Horak P Hechenblaikner G Gheri K M Stecher H and Ritsch H 1988 Cavity-induced atom cooling in the strong coupling regime *Phys Rev Lett* **79** 4974–4977
[56] Sommer C Joly N Y Ritsch H and Genes C 2019 Laser refrigeration using exciplex resonances in gas filled hollow-core fibres (arXiv:1902.01216v1 [quant-ph])
[57] Zibrov A S Lukin M D Nikonov D E Hollberg L Scully M O Velichansky V L and Robinson H G 1995 *Phys Rev Lett* **75** 1499
[58] Anderson B P and Kasevich M A 1998 *Science* **282** 1686
[59] Peters A Chung K Y and Chu S 2001 *Metrologia* **38** 25
[60] Alzetta G Gozzini A Moi L and Orriols G 1976 *Nuovo Cimento B* **36** 5
[61] Kim O Deb P and Beige A 2017 Cavity-mediated collective laser-cooling of a non-interacting atomic gas in an asymmetric trap to very low temperatures (arXiv:1506 02910v5 [quant-ph])
[62] Blaum K Dilling J Nortershauser W 2013 Precision atomic physics techniques for nuclear physics

with radioactive beams *Phys Scripta* **T152** 014017 (arXiv:1210.4045 [physics.atom-ph])
[63] Amoroso R L 2015 Multiverse space-antispace dual Calabi-Yau exciplex *zitterbewegung* particle creation in R L Amoroso L H Kauffman and P Rowlands (eds) *Unified Field Mechanics Natural Science Beyond the Veil of Spacetime* Hackensack World Scientific
[64] Fournier J and P G Langford M L Mousselmal M Robbe J M and Gandara G 1992 An experimental and theoretical study of the doubly charged ion Oz+ *J Chem Phys* **96** 5 3594-3602
[65] Larsson M Baltzer P Svensson S Wannberg B Martensson N de Brito A N Correia N Keane M P Carlsson-Gothe M and Karlsson L 1990 X-ray photoelectron, Auger electron and ion fragment spectra of O_2 and potential curves of O_2^{2+} *J Phys B Atomic Mol Opt Phys* **23** 7
[66] Amoroso R L and Vigier J-P 2013 Evidencing tight bound states in the hydrogen atom Empirical manipulation of large-scale XD in violation of QED *The Physics of Reality Space Time Matter Cosmos - Proc 8th Symp Honoring Math Physicist Jean-Pierre Vigier* (eds) R L Amoroso et al London World Sci; (http://vixra.org/pdf/1305.0053v2.pdf)
[67] Rowlands P 2013 Space and antispace in R L Amoroso L H Kauffman and P Rowlands (eds) *The Physics of Reality Space Time Matter Cosmos* World Scientific 29-37
[68] Rowlands P 2014 A dual space as the basis of quantum mechanics and other aspects of physics in J C Amson and L H Kauffman (eds) *Scientific Essays in Honor of H Pierre Noyes on the Occasion of His 90th Birthday* World Scientific 318-338
[69] Rauscher E A Rowlands P and Amoroso R L 2015 Dirac equations in nilpotent quaternionic space-antispace and eight dimensional (8D) complex Minkowski space *Unified Field Mechanics* 66-87 (https://www.worldscientific.com/doi/abs/10.1142/9789814719063_0006)
[70] Rowlands P 2014 *The Foundations of Physical Law* Singapore World Scientific
[71] Bailin D and Love A 1987 Kaluza-Klein theory *Rep Prog Phys* **50** 1087-1170
[72] Becker K Becker M and Schwartz J H 2007 *String Theory and M-theory A Modern Introduction* Cambridge Cambridge Univ Press
[73] Amoroso R L 2013 Shut the front door Obviating the challenge of large-scale extra dimensions and psychophysical bridging in R L Amoroso L H Kauffman and P Rowlands (eds) *The Physics of Reality Space Time Matter Cosmos* Singapore World Scientific
[74] Amoroso R L 2010 Simple resonance hierarchy for surmounting quantum uncertainty in R L Amoroso P Rowlands and S Jeffers (eds) *AIP Conf Proc* **1316** 1 185-193
[75] O'Raifeartaigh L 1997 *The Dawning of Gauge Theory Princeton* Princeton Univ Press Princeton
[76] Chivukula RS Dicus DA and He HJ 2002 Unitarity of compactified five-dimensional Yang–Mills theory *Phys Let B* **525** 1 175-182
[77] Reifler F and Morris R 2007 Conditions for exact equivalence of Kaluza-Klein and Yang-Mills theories (arXiv:0707.3790 [gr-qc])
[78] Witten E 1997 Solutions of four-dimensional field theories via M-theory *Nuclear Physics B* **500** 1-3 3-42
[79] Banks T 2003 A critique of pure string theory Heterodox opinions of diverse dimensions (arXiv: hep-th/0306074)
[80] Martin SP 2011 A supersymmetry primer (arXiv:hep-ph/9709356v6)
[81] Gogberashvili M 1999 Four dimensionality in non-compact Kaluza-Klein model (ArXiv:hep ph/9904383v1)
[82] Overduin J M and Wesson P S 1997 Kaluza-Klein gravity *Physics Reports* **283** 303-378
[83] Witten E 1981 Search for a realistic Kaluza-Klein theory *Nuclear Physics B* **186** 412-428
[84] Kaluza T 1921 Zum Unitätsproblem in der Physik Sitzungsber *Preuss Akad Wiss Berlin Math Phys* 966-972
[85] Sundrum R 2005 SSI lecture notes part 2 (http://www.slac.stanford.edu/econf/ C0507252/ lecnotes/Sundrum2/sundrum2.pdf)
[86] Wheeler J A and Feynman R P 1945 Interaction with the absorber as the mechanism of radiation *Rev Mod Phys* **17** 2–3 157–181
[87] Rauscher EA 2002 Non-Abelian gauge groups for real and complex Maxwell's equations in

RL Amoroso G Hunter S Jeffers and M Kafatos (eds) *Gravitation and Cosmology From the Hubble Radius to the Planck Scale* Dordrecht Kluwer
[88] Cole E A B 1977 *Il Nuovo Cimento* **40** 2 171-180
[89] Hansen R O and Newman ET 1975 *Gen Rel and Grav* **6** 216
[90] Frankel T 2012 *The Geometry of Physics An Introduction 3rd ed* Cambridge Univ Press
[91] Spiegel E O'Donnell C J 1997 Incidence algebras *Pure Applied Maths* **206** Marcel Dekker
[92] Janovska´ D and Opfer G 2013 Linear equations and the Kronecker product in coquaternions *Mitt Math Ges Hamburg* **33** 181–196
[93] Kauffman L H 2016 Iterants braiding and the Dirac Equation in R L Amoroso G Albertini L H Kauffman and P Rowlands (eds) *Unified Field Mechanics II*, Xth Vigier Symposium, London World Sci
[94] Kauffman L H 2019 Iterants and the Dirac equation in R L Amoroso D M Dubois L H Kauffman and P Rowlands (eds) *Advances In Fundamental Physics Prelude to Paradigm Shift* XI Vigier Symposium IOP Journal of Physics Conference Series London
[95] Schrödinger E 1930 Über die kräftefreie bewegung in der relativistischen quantenmechanik *Sitz Preuss Akad Wiss Phys-Math Kl* **24** 418 28
[96] Berry M V 1984 *Proc R Soc Lond A* **392** 45 57
[97] Sung JC 1993 *Pixels of Space-Time* Woburn Scientific Publications
[98] Kotigua R P and Toffoli T 1998 Potential for computing in micromagnetics via topological conservation laws *Physica D* **120** 1-2 139-161
[99] Langer J C and Singer D A 2013 The trefoil *Milan J Math* **99** 9999 1-23
[100] Chang H (ed) 1975 *Magnetic Bubble Technology* IEEE Press New York
[101] O'Dell T H 1973 The dynamics of magnetic bubble domain arrays *Philos Mag* **27** 596-606
[102] Nielson MA and Chuang IL 2000 *Quantum Computation and Quantum Information* Cambridge Cambridge Univ Press
[103] Feynman RP 1982 Simulating physics with computers *Int J Theor Phys* **21** 467-488
[104] Feynman RP 1986 Quantum-mechanical computers *Foundations Phys* **16** 507-531
[105] Deutsch D 1985 Quantum theory the Church-Turing principle and the universal quantum computer *Proceedings of Royal Society of London A* **400** 97-117
[106] Deutsch D 1989 Quantum computational networks *Proc Roy Soc Lon A* **425** 73-90
[107] Schumacher B 1995 Quantum coding *Physical Review A* **51** 2738-2747
[108] Bennett C 1995 Quantum information and computation *Physics Today* **48** 10 24-30
[109] 't Hooft G 2007 *Lie Groups in Physics* (http://www.staff.science.uu.nl/~hooft101/ lectures/lieg07.pdf)
[110] Vlasov AY 1999 Quantum theory of computation and relativistic physics *PhysComp96 Workshop* Boston MA 22-24 Nov 1996 (arXiv: quant-ph/ 9701027v4)
[111] Peres A and Terno DR 2004 Quantum information and relativity theory *Rev Mod Phys* **76** 93 (arXiv:quant-ph/0212023v2); Introduction to relativistic quantum information 2006 arXiv:quant-ph/0508049v2)
[112] Shannon C E 1948 *Bell Syst Tech J* **27** 379 623
[113] Landauer R 1991 Information is physical *Physics Today* **44** 5 23
[114] Yeh N-C 2007 (http://www.its.caltech.edu/~yehgroup/ NTU_2007SummerLectures/ NTU2007_Supplement_3.pdf)
[115] Vlasov AY 1996 Quantum theory of computation and relativistic physics in T Toffoli M Biafore and J Leao (eds) *Physcomp96 Cambridge New England Complex Systems Institute* and additional material from private communication
[116] Jafarizadeh_ M A and Mahdian M 2011 Quantifying entanglement of two relativistic particles using optimal entanglement witness *Quant Inf Proces* **10** 4 501-518
[117] Amoroso R L 2016 A unified field mechanical approach to the arrow of time utilizing large size extra dimensions in preparation
[118] Felicetti S Sabın C Fuentes I Lamata L Romero G and Solano E 2015 Relativistic motion

with superconducting qubits (arXiv1503.06653v2 [quant-ph])
[119] Xu H Huang L Lai YC and Grebogi C 2015 Superpersistent currents and whispering gallery modes in relativistic quantum chaotic systems *Sci Rep* **11** 5 8965
[120] Bargmann V and Wigner EP 1948 Group theoretical discussion of relativistic wave equations *Proc National Academy of Sciences United States America* **34** 5 211-23
[121] Dvoeglazov VV 2010 The Bargmann-Wigner formalism for higher spins (up to 2) (arXiv1011.1696v1 [math-ph])
[122] Banerjee S Fransson J Black-Schaffer AM Ågren H and Balatsky A V 2015 Bosonic Dirac materials in two dimensions (arXiv:1511.05282v2 [cond-mat.mes-hall])
[123] Wang J Deng S Liu Z and Liu Z 2015 The rare two-dimensional materials with Dirac cones *Natl Sci Rev* **2** 1 22-39; (http://arxiv.org/ftp/arxiv/papers/1410/1410.5895.pdf)
[124] Pletikosic I Kralj M Pervan P Brako R Coraux J N'Diaye A T Busse C and Michely T 2009 Dirac cones and minigaps for graphene on Ir (111 arXiv:0807.2770v2 [cond-mat.mtrl-sci]
[125] Amoroso R L Kauffman L H and Rowlands P 2013 *The Physics of Reality Space Time Matter Cosmos* Hackensack World Scientific
[126] Drell S 1978 *Am J Phys* **46** 597; *Physics Today* **31** 6 23
[127] Dirac P A M 1947 The *Principles of Quantum Mechanics* Oxford University Press 36
[128] von Neumann J 1955 *Mathematical Foundations of Quantum Mechanics* R T Beyer (trans) Princeton Princeton Univ Press 418
[129] Herbert N 1981 *Found Phys* **12** 1171
[130] Wootters W K and Zurek W H 1982 A single quantum cannot be cloned *Nature* **299** 5886 802-803
[131] Dieks D G B J 1982 Communication by EPR devices *Physics Letters A* **92** 6 271-272
[132] Weinberg S 1995 *The Quantum Theory of Fields Vol 1* Cambridge Cambridge Univ Press
[133] Kauffman LH 2016 From Hamilton's quaternions to Graves and Cayley's Octonions (https://www.researchgate.net/publication/299575683)
[134] Stern A 1992 *Matrix logic and the Mind a Probe Into a Unified Theory of Mind and Matter* Amsterdam Northern-Holland; Stern A 2000 *Quantum Theoretic Machines* New York Elsevier Science
[135] Necker LA 1832 Observations on some remarkable optical phænomena seen in Switzerland and on an optical phænomenon which occurs on viewing a figure of a crystal or geometrical solid 329-337 1 5 *Philosoph Magazine* **3**
[136] Stolfi J 1991 *Oriented Projective Geometry* Boston Academic Press
[137] Shaw R E and Mace W M 2005 The value of oriented geometry for ecological psychology and moving image art in J D Anderson and B F Anderson (eds) *Moving Image Theory* Carbondale S Il Univ Press
[138] Iwakiri M and Satoh S 2011) Quandle cocycle invariants of roll-spun knots (http://www. kurims.kyoto-u.ac.jp/~kyodo/kokyuroku/contents/pdf/1766-04.pdf)
[139] Petit J-P 2012) Twin universe astrophysics (http://www.jp-petit.org/science/f300/f3800/ f3802.htm)
[140] Baez J C and Dolan J 1995 Higher dimensional algebra and topological quantum field theory *J Math Phys* **36** 6073 ([arXiv:q-alg/9503002])
[141] Nayak C Simon S H Stern A Freedman M and Sarma D S 2008 Non-Abelian anyons and topological quantum computation (arXiv:0707.1889v2 [cond-mat.str-el])
[142] Atiya M 1988 New invariants of three and four dimensional manifolds *Proc Symp Pure Math American Math Soc* **48** 285-299
[143] Atiyah M 1989 Topological quantum field theories *Inst Hautes Etudes Sci Publ Math* **68** 175-186
[144] Liu X and Ricca R L 2012 The Jones polynomial for fluid knots from helicity *J Phys A Math Theor* **45** 205501
[145] Furey C 2012 Unified theory of ideals *Physical Review D* **86** 2 025024

[146] (http://pseudomonad.blogspot.com/2011/02/theory-update-51.html)
[147] Schray J and Manogue C A 1994 Octonionic representations of Clifford algebras and triality (arXiv:hep th/9407179v1)
[148] Bar-Natan D 2002 On Khovanov's categorification of the Jones polynomial *Algebraic and Geometric Topology* 2-16 337-370 (http://www.math.toronto.edu/drorbn/papers/Categorification/ (arXiv:math.QA/9908171) (arXiv:math.QA/0103190)
[149] Bar-Natan D 2001 A categorification quickie New techniques in topological quantum field theory (https://www.math.toronto.edu/drorbn/Talks/Calgary-010824/index.html)
[150] Kauffman L H and Manturov V O 2005 Virtual knots and links (arXiv:math/0502014v3 [math.GT])
[151] Maassen J and Lundstrom M 2015 A Simple Boltzmann transport equation for ballistic to diffusive transient heat transport (arXiv:1501.05209v1)
[152] Jeong C Kim R Luisier M Datta S and Lundstrom M 2010 *J Appl Phys* **107** 023707
[153] Wilson and R B Cahill D G 2014 *Nature Comm* **5** 5075
[154] Minnich A J Johnson J A Schmidt A J Esfarjani K Dresselhaus M SNelson and K A Chen G 2011 *Phys Rev Lett* **107** 095901
[155] Sellan D P Turney J E McGaughey A J H and Amon C H 2010 *J Appl Phys* **108** 113 524
[156] Bae M-H Li Z Aksamija Z Martin P N Xiong F Ong Z-Y Knezevic I and Pop E 2013 *Nature Comm* **4** 1734
[157] Esfarjani K Chen G and Stokes H T 2011 *Phys Rev B* **84** 085204
[158] Yang F and Dames C 2013 *Phys Rev B* **87** 035437
[159] Datta S 1997 Electronic Transport in Mesoscopic Systems in H Ahmad A Broers M Pepper New York Cambridge University Press 57–111
[160] Pastawski H M 1999 Classical and quantum transport from generalized Landauer-Büttiker equationsand *Physical Review B* **44** 12 6329–6339
[161] Pastawski H M 1992 Classical and quantum transport from generalized Landauer-Buttiker equations II Time-dependent resonant tunnelingand *Phys Rev B* **46** 7 4053–4070
[162] Takayanagi K Yukihito K and Hideaki O 2001 Suspended gold nanowires ballistic transport of electrons *JSAP International* **3** 9
[163] Ando T Matsumura H and Takeshi N T 2002 Theory of ballistic transport in carbon nanotubes *Physica B Condensed Matter* **323** 1–4 44-50
[164] Peebles P J E 1992 *Quantum Mechanics* Princeton Princeton Univ Press
[165] Parkes M A Lockyear J F and Price S D 2014 Bond-forming reactions between the molecular oxygen dication and small organic molecules Intl J Mass Spectrometry 365–366 68–74
[166] Chu M-Y J and Amoroso R L 2008 Empirical mediation of the primary mechanism initiating protein conformation in prion propagation in D Dubois (ed) *Partial Proceedings of CASYS07 IJCAS* **22** Univ Liege Belgium (http://vixra.org/pdf/1305.0090v1.pdf)
[167] Osoroma DS 2013 A programmable cellular automata polarized Dirac vacuum 71-80 in R L Amoroso et al *The Physics of Reality Space Time Matter Cosmos* 504-509 NY World Sci
[168] Amoroso RL 2000 The parameters of temporal correspondence in a continuous-state conscious universe in R Buccheri and M Saniga (eds) *Studies in the Structure of Time From Physics to Psycho(patho)logy* Dordrecht Kluwer Academic
[169] Amoroso RL 2013 Time? in R L Amoroso et al *The Physics of Reality Space Time Matter Cosmos* 504-509 New York World Scientific
[170] Atiyah M 1988 New invariants of three and four dimensional manifolds *Proc Symp Pure Math Am Math Soc* **48** 285–299
[171] Atiyah M 1988 Topological quantum field theories *Pubs Math de l'IHÉS* **68** 68 175–186
[172] Gukov S Kapustin A 2013 Topological quantum field theory nonlocal operators and gapped phases of gauge theories *JHEP* (arXiv1307.4793)
[173] Witten E 1988 Topological quantum field theory *Comm in Math Phys* **117** 3 353–386
[174] Lurie J 2009 *On the Classification of topological field theories*

(http://www-math.mit.edu/~lurie/papers/cobordism.pdf)
[175] Andrews D L and Demidov A A 1999 *Resonance Energy Transfer* NY J Wiley and sons
[176] David S Bradshaw and David L Andrewsathe 2008 Optically controlled resonance energy transfer Mechanism and configuration for all-optical switching *J Chem phys* **128** 144 506
[177] Casimir H and Polder D 1948 The influence of retardation on the London-van der Waals forces *Phys Rev* **73** 4 360-372
[178] Huerta J 2019 How space-times emerge from the superpoint *LMS/EPSRC Durham Symposium on Higher Structures* in M-Theory (arXiv:190302822v1 [hep-th])
[179] Kitaev A Y 1997 Fault-tolerant quantum computation by anyons (arXiv:quant-ph/9707021v1)
[180] Milton K 2000 Dimensional and dynamical aspects of the Casimir effect Understanding the reality and significance of vacuum energy (arXiv:hep-th/0009173v1)
[181] Stevens H H 1989 Size of a least unit in M Kafatos (ed) Bell's Theorem Quantum Theory and Conceptions of the Universe Dordrecht Kluwer Academic
[182] Ashkin A 1970 Acceleration and trapping of particles by radiation pressure *Phys Rev Lett* **24** 4 156–159
[183] Ashkin A Dziedzic J M Bjorkholm J E and Chu S 1986 Observation of a single-beam gradient force optical trap for dielectric particles *Opt Lett* **11** 5 288–290
[184] Garrett R H Grisham C M 2016 *Biochemistr***y** sixth (ed) Univ Virginia 12–13
[185] Klimchitskaya G L Mostepanenko V M 2015 Casimir and van der Waals forces Advances and problems (https://arxiv.org/ftp/arxiv/papers/1507/1507.02393.pdf)
[186] van Oss C J Absolom D R Neumann A W 1980 Applications of net repulsive van der Waals forces between different particles macro-molecules or biological cells in *Liquids Colloids and Surfaces* **1** 1 45–56